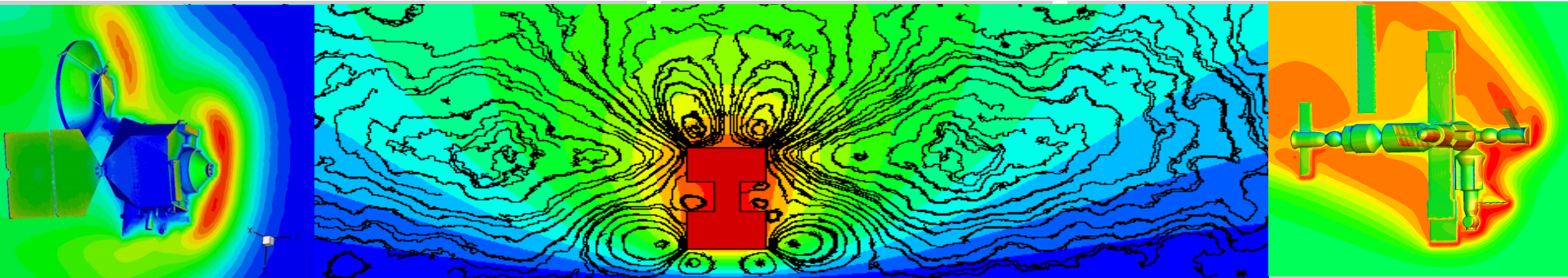


*Exceptional service in the national interest*



## Molecular-Level Simulations of Hydrodynamic Instabilities in Gases

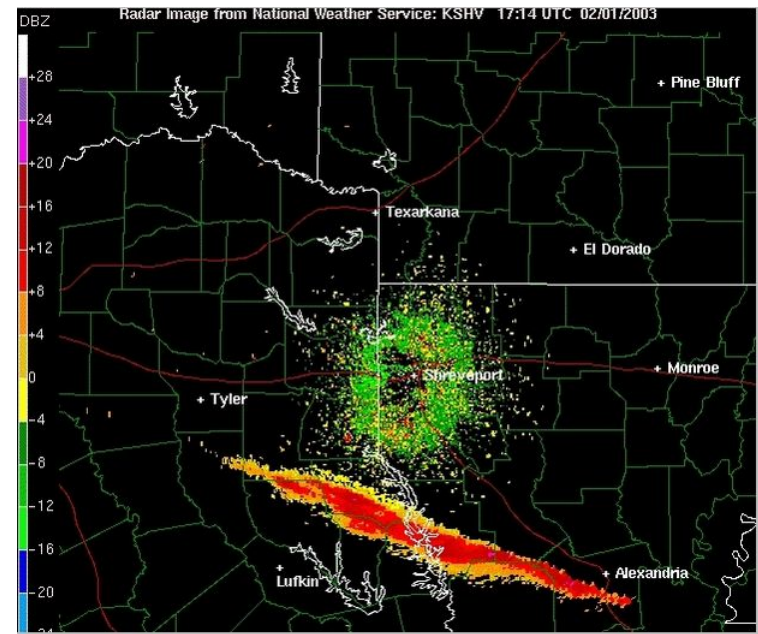
*Michael A. Gallis*

Engineering Sciences Center  
Sandia National Laboratories  
Albuquerque, New Mexico, USA

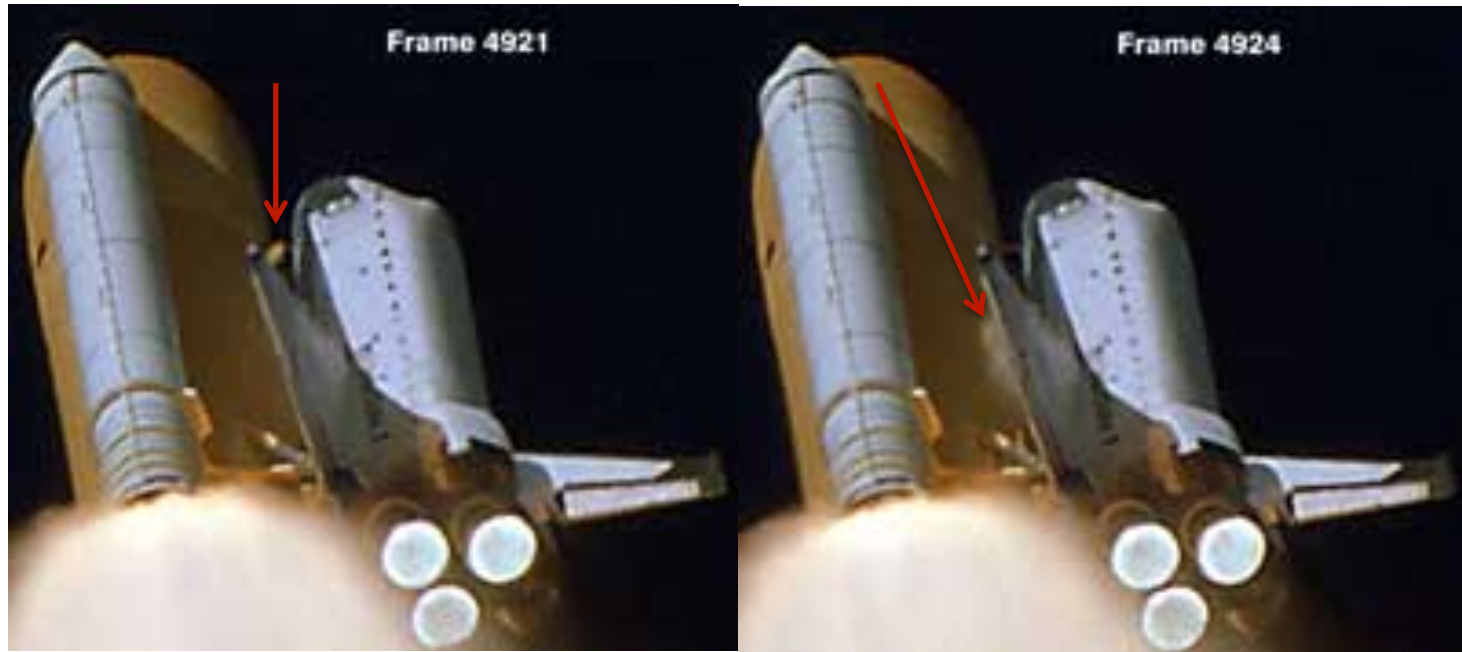
# The Columbia Accident



On February 1<sup>st</sup> 2003 STS-107 with Shuttle orbiter Columbia disintegrated over western Texas, minutes before it was scheduled to land.

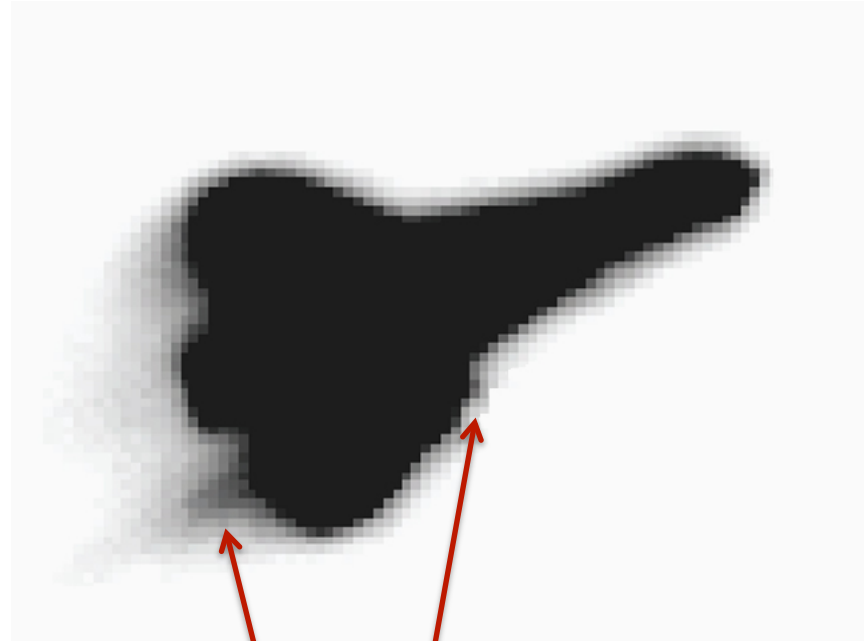
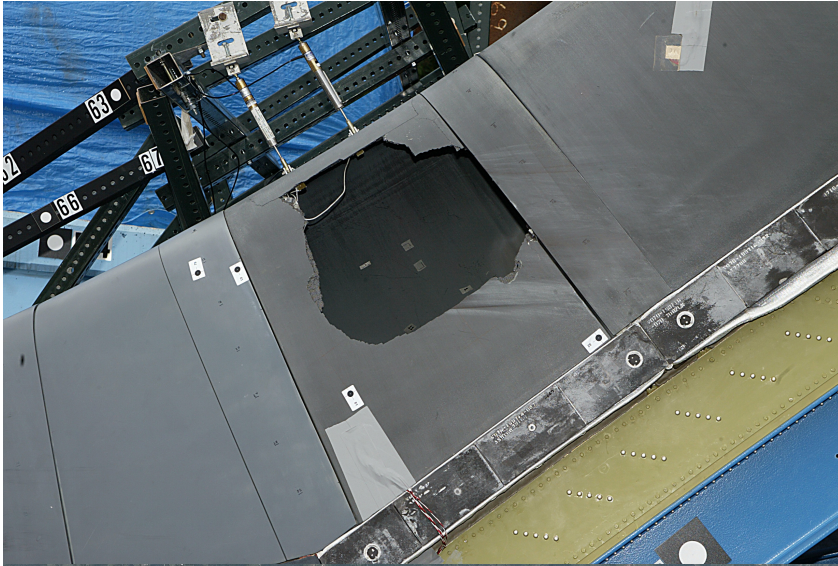


# Foam impact during launch



During the ascent phase a piece of foam insulation broke off from the shuttle's propellant tank damaging (?) the shuttle's left wing.

# Damage Scenario Investigated



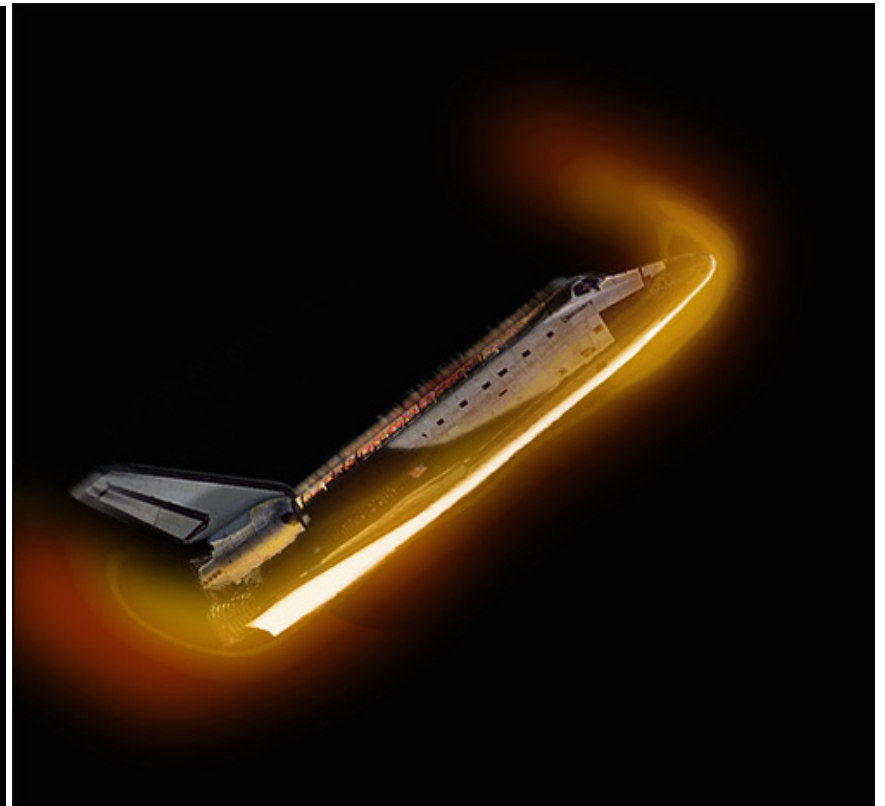
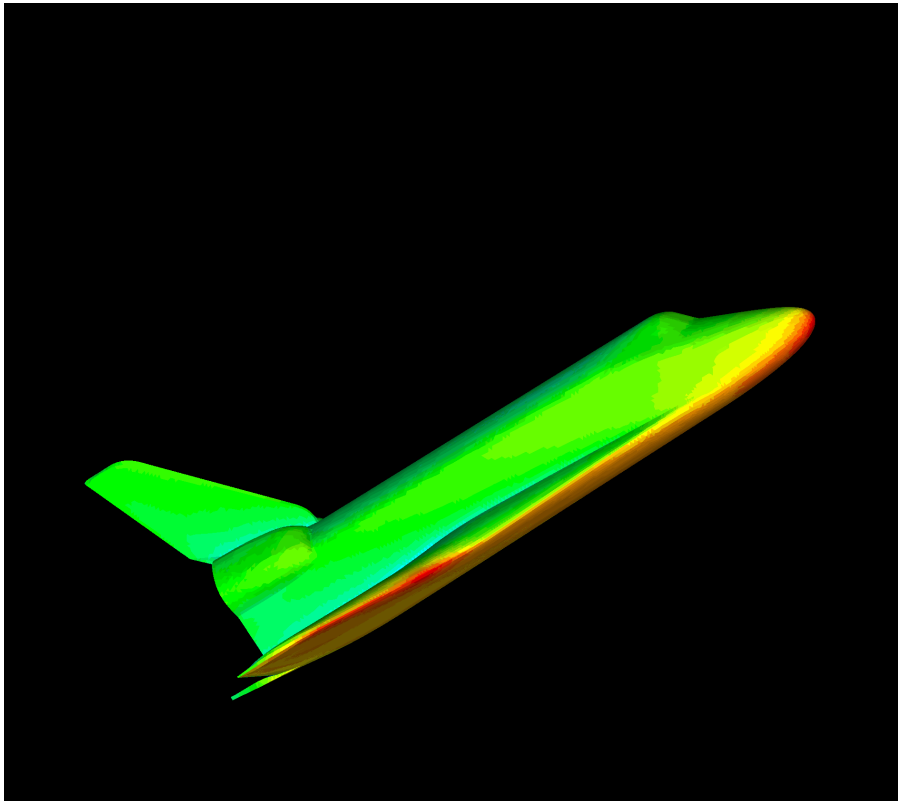
The resulting hole allowed overheated gases to burn through the wing cavity, compromise its structural integrity, leading to a loss of the vehicle during descent

# Numerical Simulations Supporting the Investigation

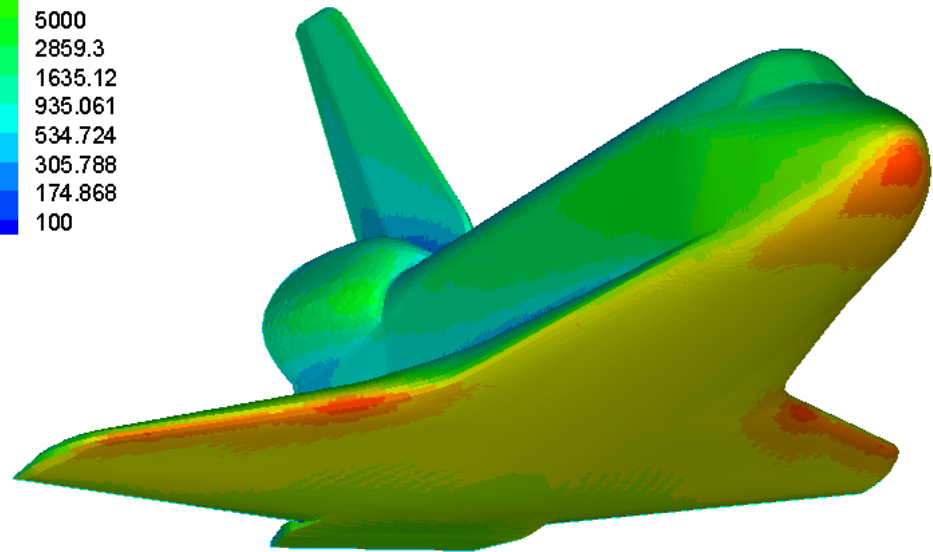
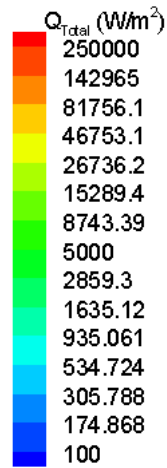
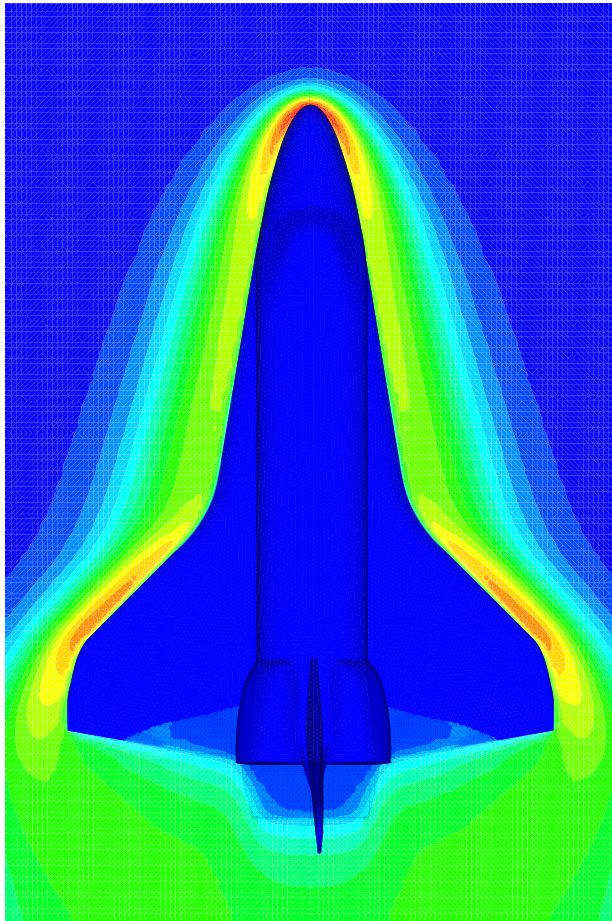
## Simulation conditions

Altitude = 350,000-300,000 ft

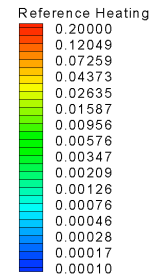
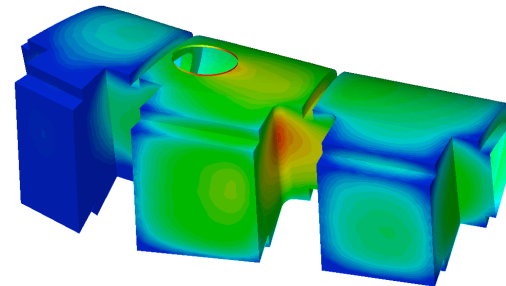
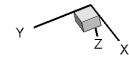
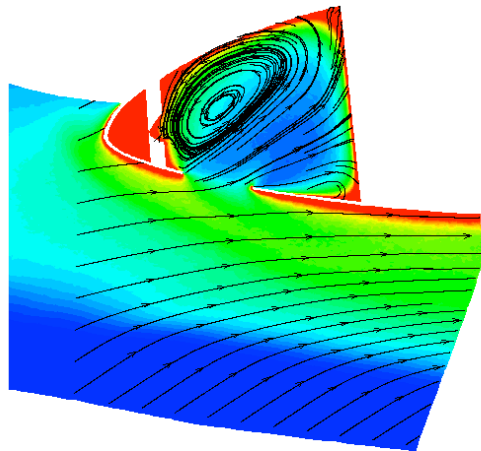
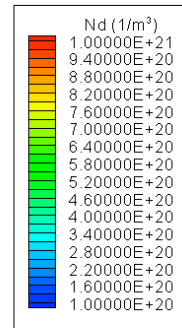
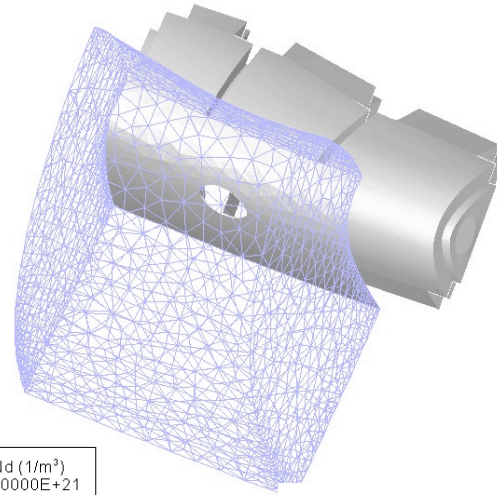
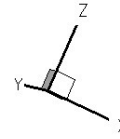
Mach Number = 27



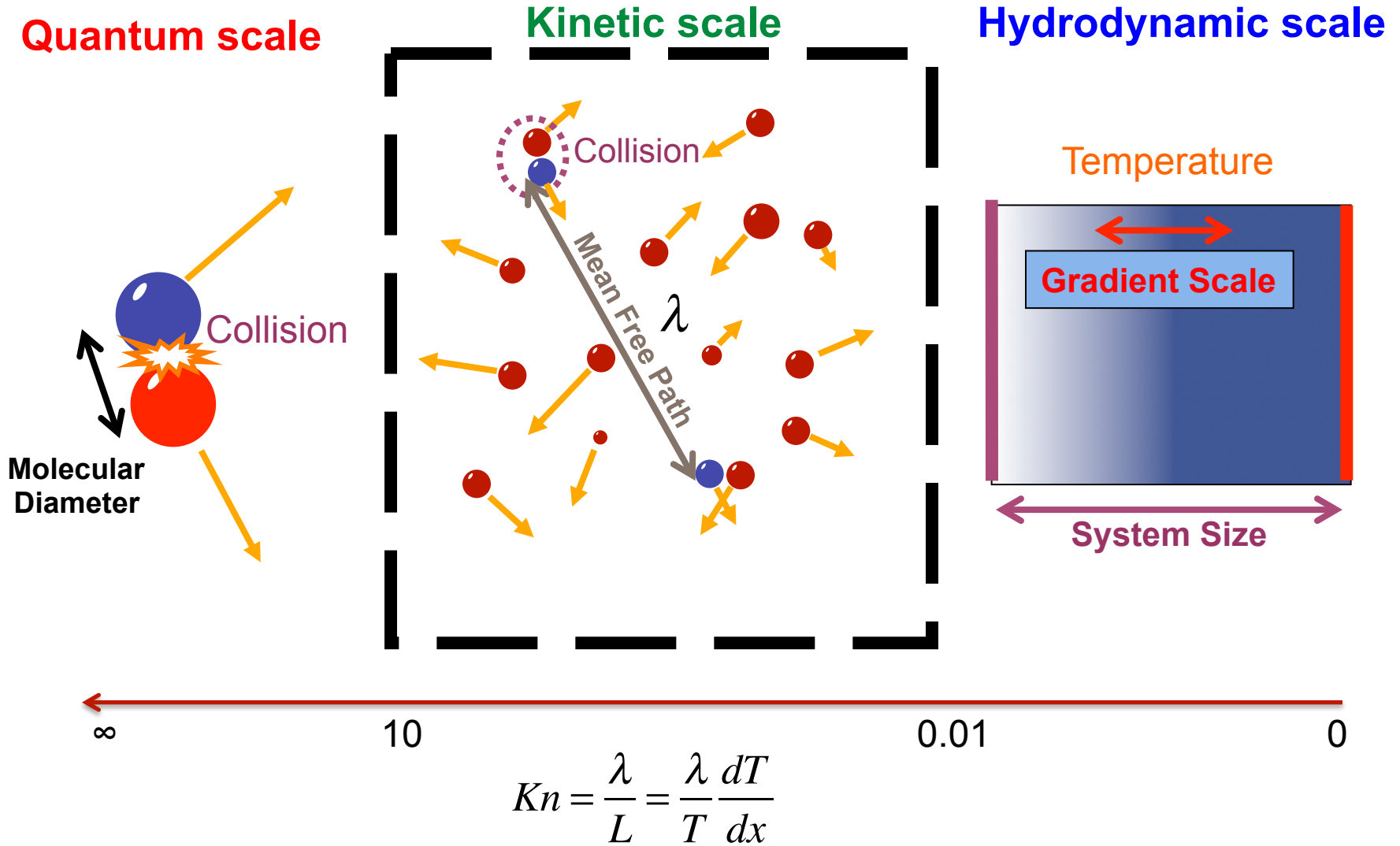
# Temperature and Heating Profile



# Flow Inside the Wing Cavity



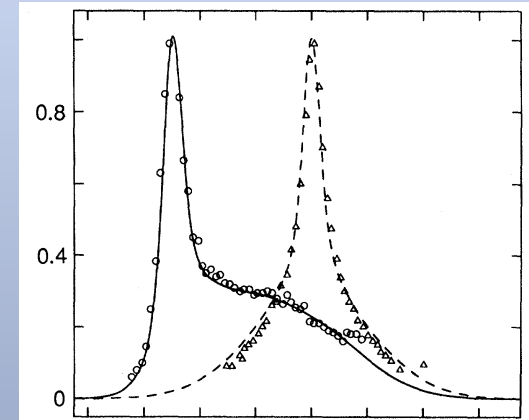
# Length Scales for Dilute Gases



# Non-equilibrium effects

## Non-equilibrium effects:

- Non-Maxwell, Chapman-Enskog velocity distribution functions
  - Non-linear transport properties
  - Non-Boltzmann internal energy, no energy equipartition
  - Non-Arrhenius chemical reactions
  - Non-continuous temperature and velocity profiles (Knudsen layers close to walls)
- 
- Can be caused by:
    - Reduced collisionality (low density)
    - Strong gradients even in near-continuum conditions



Non-equilibrium velocity distribution functions in the front a Mach 25 normal shock of helium  
Pham-Van-Diep, *et al.* , *Science*, 1989

# Boltzmann Equation and the Direct Simulation Monte Carlo Method (DSMC)

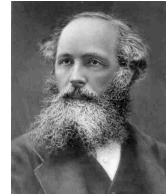


Ludwig Boltzmann

$$\frac{\partial f}{\partial t} + \mathbf{v} \cdot \frac{\partial f}{\partial \mathbf{x}} + \frac{\mathbf{F}}{m} \cdot \frac{\partial f}{\partial \mathbf{v}} = \int_{-\infty}^{\infty} \int_0^{4\pi} (f^* f_1^* - ff_1) |\mathbf{v} - \mathbf{v}_1| \sigma d\Omega d\mathbf{v}_1$$

molecular motion and force-induced acceleration

pairwise molecular collisions (molecular chaos)



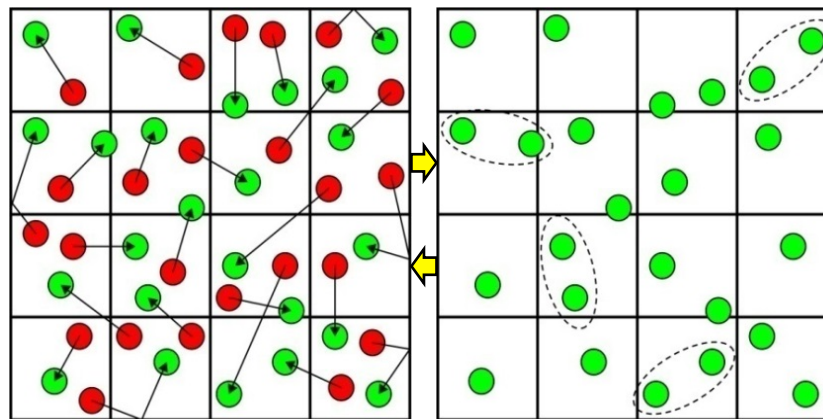
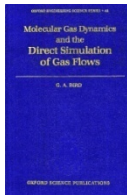
James Clerk Maxwell

$f(\mathbf{r}, \mathbf{c}, t) d^3 r d^3 c \rightarrow$  Expected number of molecules at time  $t$  in at  $\mathbf{r} + d^3 r, \mathbf{c} + d^3 c$

$$n(\mathbf{r}, t) = \int f(\mathbf{r}, \mathbf{c}, t) d^3 c$$



Graeme Bird (1963, 1994)



molecules move

molecules collide

DSMC is a **physical, statistical, molecular-level** simulation method

# Direct Simulation Monte Carlo

## How DSMC works

DSMC molecule-simulators **statistically** represent a large number of real molecules ( $O(10^{10})$ - $O(10^{15})$ )

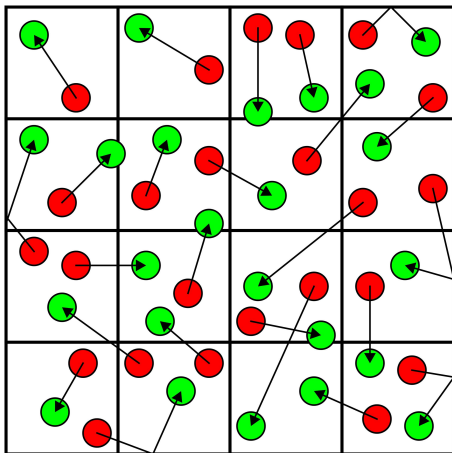
Computational molecules move ballistically, collide statistically, and interact statistically with surfaces **like real molecules**

Molecular movement, surface-interaction, and collision are implemented **sequentially** in the algorithm

Cell-based molecular statistics (“moments”) are sampled and averaged over many time steps for steady flow

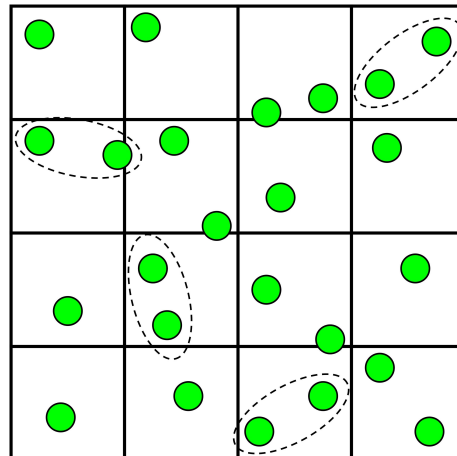
## DSMC is inherently a transient method

Steady state is the ensemble average of unsteady state moves



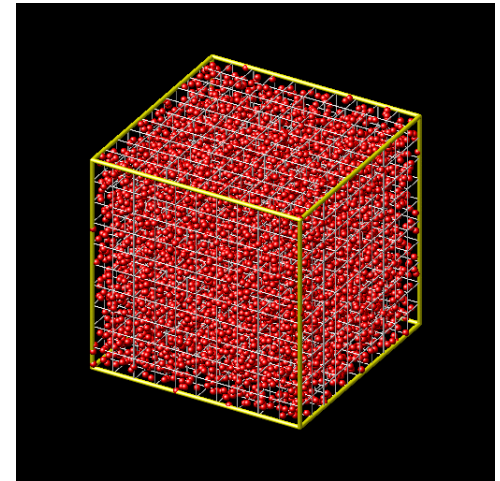
Deterministic ballistic move

+



Stochastic binary collisions

=



# DSMC vs. Boltzmann Equation

- Instead of solving Newton's laws of motion (Molecular Dynamics), DSMC replaces explicit intermolecular forces with stochastic collisions
- It has been shown that DSMC is **equivalent** to solving the Boltzmann equation (Nambu 1980, Babovsky 1989, Wagner 1992)
- DSMC has been shown to reproduce **exact** known solutions (Chapman-Enskog, Moment Hierarchy) of the Boltzmann equation (Gallis et al. 2004, 2006) for **non-equilibrium** flows
- In fact, DSMC is **superior** to solving the Boltzmann equation
  - DSMC can **model complicated processes** (e.g., polyatomic molecules, chemically reacting flows, ionized flows) for which **Boltzmann-type transport equations are not even known** (Struchtrup 2005)
  - DSMC **includes fluctuations**, which have been shown to be physically realistic (Garcia 1990) but which are **absent from the Boltzmann equation**

**The objective of DSMC is to simulate complicated gas flows using only collision mechanics of simulated molecules in the regime described by the Boltzmann equation**

# Navier-Stokes vs. Boltzmann Equation

- The Navier-Stokes equations for gases can be derived from the Boltzmann equation assuming:
  - Near-equilibrium conditions
  - Local Thermodynamic Equilibrium (LTE)
  - Continuum medium
- Conservation equations (mass, momentum, energy) can be derived as **averages of molecular properties**
- Transport is given by **averaging molecular fluxes**. Under LTE Newton's, Fourier's and Fick's laws are obtained



George Stokes



Claude Navier

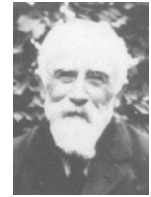
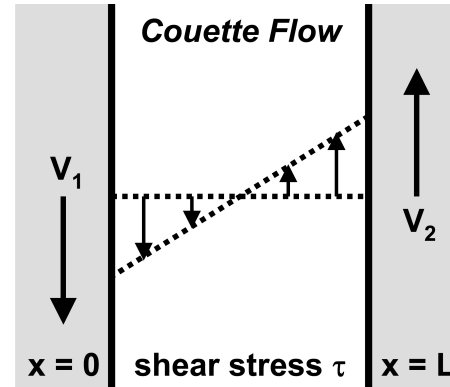
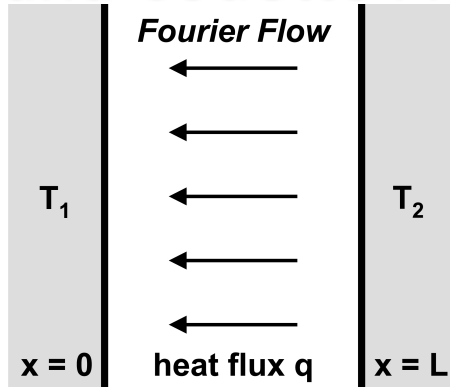
# Quantifying Non-Equilibrium

## Fourier and Couette Flow



Joseph  
Fourier

$$q = -K \frac{\partial T}{\partial x}$$



Maurice  
Couette

$$\tau = \mu \frac{\partial v}{\partial x}$$

### Investigate transport in gas between parallel plates

- Fourier flow: heat conduction in stationary gas
- Couette flow: momentum transport in isothermal shear flow

### Apply DSMC to Fourier flow and Couette flow

- Heat flux, shear stress: one-dimensional, steady

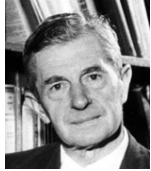
### Compare DSMC to analytical "normal solutions"

- Normal: outside Knudsen layers
- Solutions: Chapman-Enskog (CE), Moment-Hierarchy (MH)

### Verify DSMC accuracy at arbitrary heat flux, shear stress

- Thermal conductivity, viscosity; velocity distribution

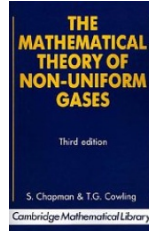
# Near-Equilibrium: Chapman-Enskog (CE) Theory



Sydney  
Chapman



David  
Enskog



$$f = f^{(0)}(1 + \Phi^{(1)} + \Psi^{(1)}) \quad f^{(0)} = (n/\pi^{3/2}c_m^3)\exp[-\tilde{c}^2]$$

$$c_m = \sqrt{2k_B T/m} \quad \tilde{c} = \mathbf{c}/c_m \quad \mathbf{c} = \mathbf{v} - \mathbf{u}$$

$$\Phi^{(1)} = -(8/5)\tilde{A}[\tilde{c}]\tilde{c} \cdot \tilde{\mathbf{q}} \quad \Psi^{(1)} = -2\tilde{B}[\tilde{c}](\tilde{\mathbf{c}} \circ \tilde{\mathbf{c}} : \tilde{\boldsymbol{\tau}})$$

$$K = -(5/4)k_B c_m^2 a_1 \quad \mu = (1/2)mc_m^2 b_1$$

$$\tilde{A}[\tilde{c}] = \sum_{k=1}^{\infty} (a_k/a_1) S_{3/2}^{(k)}[\tilde{c}^2] \quad \tilde{B}[\tilde{c}] = \sum_{k=1}^{\infty} (b_k/b_1) S_{5/2}^{(k-1)}[\tilde{c}^2]$$

$$C_p = (5/2)(k_B/m) \quad Pr = (2/3)(\mu_{\infty}/\mu_1)(K_1/K_{\infty})$$

- Chapman and Enskog analyzed Boltzmann collision term
  - Perturbation expansion using Sonine polynomials
  - Near equilibrium, appropriate in continuum limit
- Determined velocity distribution and transport properties
  - Thermal conductivity  $K$ , viscosity  $\mu$ , mass self-diffusivity  $D$
  - Prandtl number  $Pr$  from “infinite-to-first” ratios  $K_{\infty}/K_1$ ,  $\mu_{\infty}/\mu_1$
  - Distribution “shape”: Sonine polynomial coeffs  $a_k/a_1$ ,  $b_k/b_1$
  - Values for all Inverse-Power-Law (IPL) interactions
    - Maxwell and hard-sphere are special cases

# Extracting CE Parameters from DSMC

$$\begin{aligned}
 q &= K_{eff} \left( \frac{\partial T}{\partial x} \right) & \frac{a_k}{a_1} &= \sum_{i=1}^k \left( \frac{(-1)^{i-1} k! (5/2)!}{(k-i)! i! (i+(3/2))!} \right) \left( \frac{\langle \tilde{c}^{2i} \tilde{c}_x \rangle}{\langle \tilde{c}^2 \tilde{c}_x \rangle} \right) & \tilde{c} &= \frac{\mathbf{v} - \mathbf{V}}{c_m} \\
 \tau &= \mu_{eff} \left( \frac{\partial V}{\partial x} \right) & \frac{b_k}{b_1} &= \sum_{i=1}^k \left( \frac{(-1)^{i-1} (k-1)! (5/2)!}{(k-i)! (i-1)! (i+(3/2))!} \right) \left( \frac{\langle \tilde{c}^{2(i-1)} \tilde{c}_x \tilde{c}_y \rangle}{\langle \tilde{c}_x \tilde{c}_y \rangle} \right) & c_m &= \sqrt{\frac{2k_B T}{m}}
 \end{aligned}$$

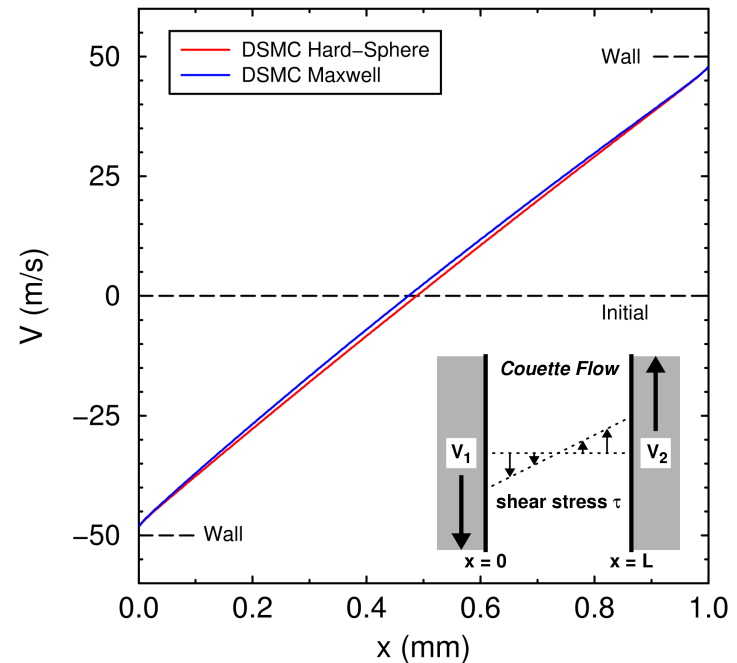
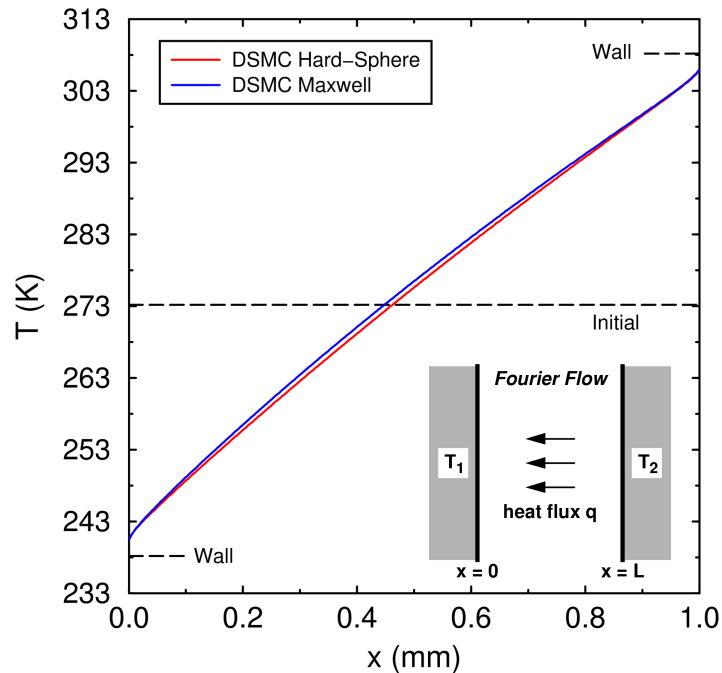
## DSMC moments of velocity distribution function

- Temperature  $T$ , velocity  $V$
- Heat flux  $q$ , shear stress  $\tau$
- Higher-order moments

## DSMC values for VSS molecules (variable-soft-sphere)

- Thermal conductivity and viscosity:  $K_{eff}$  and  $\mu_{eff}$
- Sonine-polynomial coefficients:  $a_k/a_1$  and  $b_k/b_1$
- Applicable for arbitrary  $Kn_L$ ,  $Kn_q$ ,  $Kn_\tau$

# Temperature and Velocity Profiles

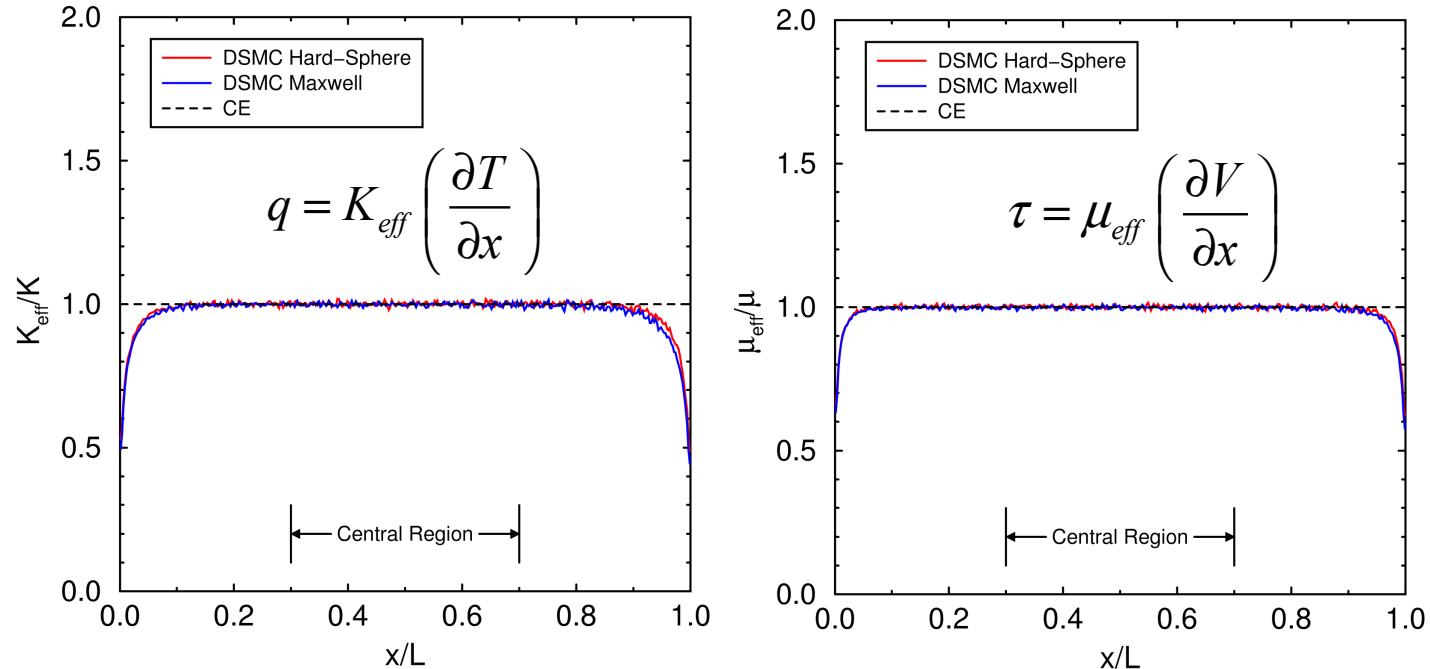


Low heat flux and shear stress:  $Kn_q = 0.006$ ,  $Kn_\tau = 0.003$

- Argon-like: initial  $T = 273.15$  K,  $p = 266.644$  Pa,  $\lambda = 24$   $\mu$ m
- Walls:  $L = 1$  mm =  $42\lambda$ ,  $\Delta T = 70$  K,  $\Delta V = 100$  m/s
- $N_c = 120$ ,  $\Delta t = 7$  ns,  $\Delta x = 2.5$  mm,  $\sim 10^9$  samples/cell, 32 runs

Small velocity slips, temperature jumps, Knudsen layers

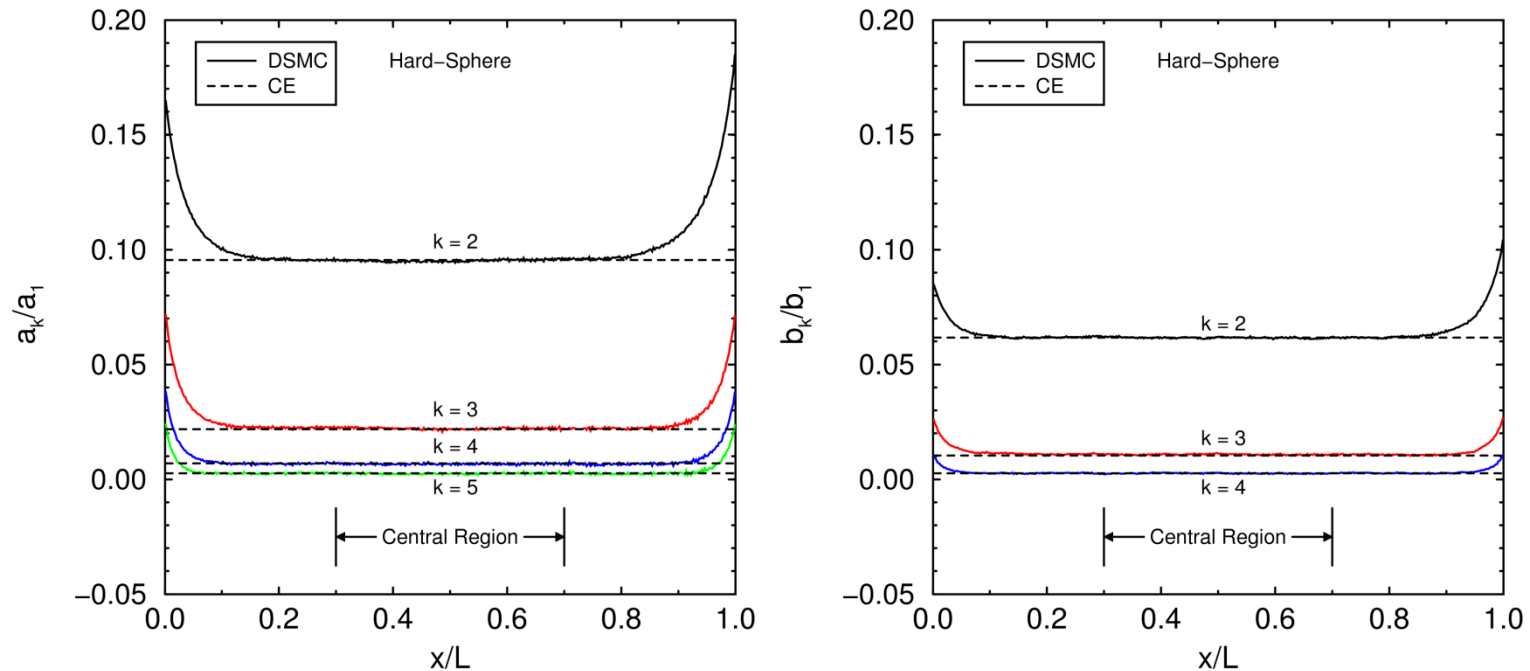
# DSMC Reproduces Infinite-Approximation Chapman-Enskog Transport Coefficients



Thermal conductivity (left) and viscosity (right) away from walls

- Maxwell and hard-sphere results bound most gases
- Agreement with Chapman-Enskog theory verifies DSMC

# DSMC Reproduces Infinite-Approximation Chapman-Enskog Velocity Distribution



## Sonine polynomial coefficients for temperature (left) & velocity (right) gradients

- Hard-sphere values are shown, other interactions have similar agreement
- Higher-order ( $k > 5$ ) coefficients (not shown) also have similar agreement

Gallis M. A., Torczynski J. R., Rader D. J., "Molecular Gas Dynamics Observations of Chapman-Enskog Behavior and Departures Therefrom in Nonequilibrium Gases", *Physical Review E*, 69, 042201, 2004.

# Moment-Hierarchy Method

$$M_{k_1 k_2 k_3} = \int \tilde{c}_x^{k_1} \tilde{c}_y^{k_2} \tilde{c}_z^{k_3} \tilde{f}[\tilde{\mathbf{c}}] d\tilde{\mathbf{c}} = \left\langle \tilde{c}_x^{k_1} \tilde{c}_y^{k_2} \tilde{c}_z^{k_3} \right\rangle$$

$$J_{k_1 k_2 k_3} = \text{Bilinear} \left[ \left\{ M_{k_1 k_2 k_3} \right\} \right]$$

$$K_{\text{eff}} / K = F_K[\text{Kn}_\tau] = 1 - c_K \text{Kn}_\tau^2 + O[\text{Kn}_\tau^4]$$

$$a_k / a_1 = (-1)^{k-1} \sum_{j=1}^{k-1} A_{kj} \text{Kn}_q^{2j}$$

$$J_{k_1 k_2 k_3} = \int \tilde{c}_x^{k_1} \tilde{c}_y^{k_2} \tilde{c}_z^{k_3} J[\tilde{\mathbf{c}} | \tilde{f}, \tilde{f}] d\tilde{\mathbf{c}}$$

$$M_{k_1 k_2 k_3}[\text{Kn}_q, \text{Kn}_\tau] = \sum_{j=0}^{k_1+k_2+k_3-2} \mu_{k_1 k_2 k_3}^{(j)} [\text{Kn}_\tau] \text{Kn}_q^j$$

$$\mu_{\text{eff}} / \mu = F_\mu[\text{Kn}_\tau] = 1 - c_\mu \text{Kn}_\tau^2 + O[\text{Kn}_\tau^4]$$

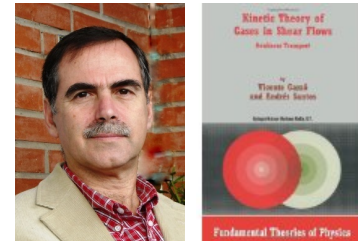
$$b_k / b_1 = (-1)^{k-1} \sum_{j=1}^{k-1} B_{kj} \text{Kn}_q^{2j}$$

## Moment-Hierarchy (MH) normal solution

- Solve Boltzmann eqn. recursively for Maxwell molecules
- MH solution extends CE solution to finite  $\text{Kn}_q$  and  $\text{Kn}_\tau$
- Collision-term moments bilinear in distribution moments

## Compare MH and DSMC for Maxwell molecules

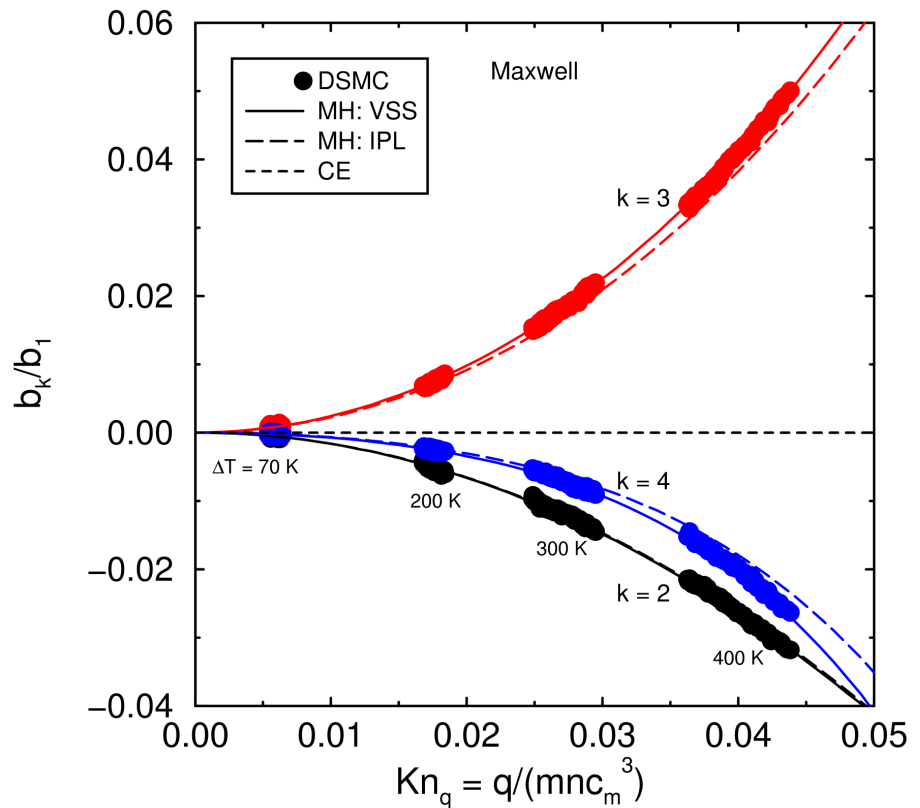
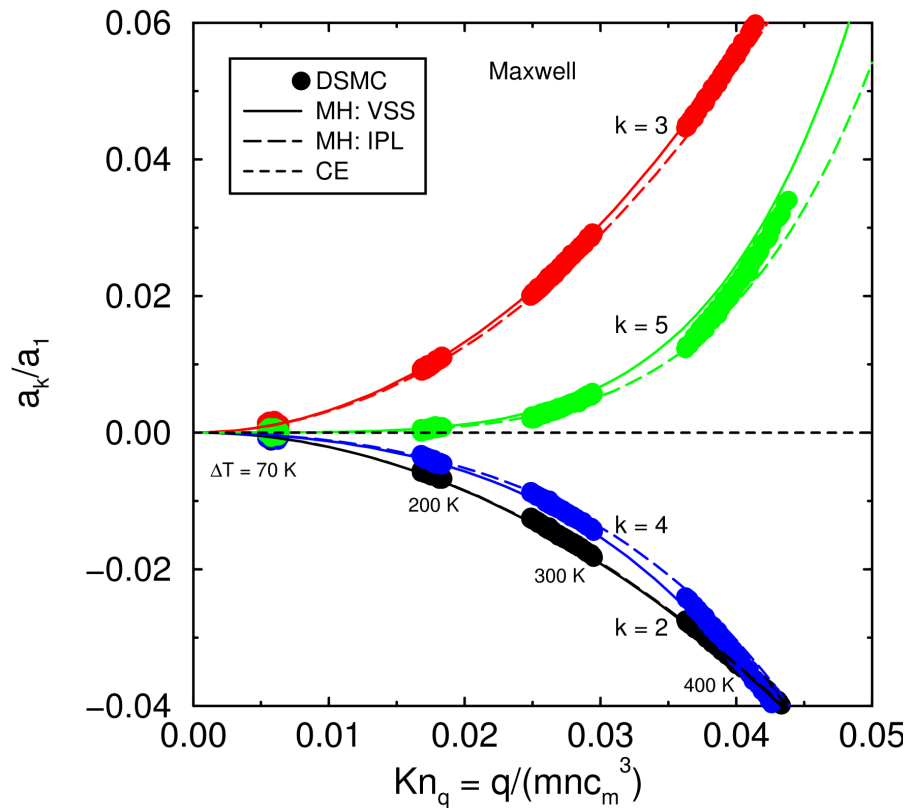
- Dependence of  $K$ ,  $m$ ,  $a_k/a_1$ ,  $b_k/b_1$  on  $\text{Kn}_q$  and  $\text{Kn}_\tau$



Andres Santos

Gallis M. A., Torczynski J. R., Rader D. J., Tij M., Santos A., “Normal Solutions of the Boltzmann Equation for Highly Nonequilibrium Fourier and Couette Flow”, *Phys. Fluids*, 18, 017104, 2006.

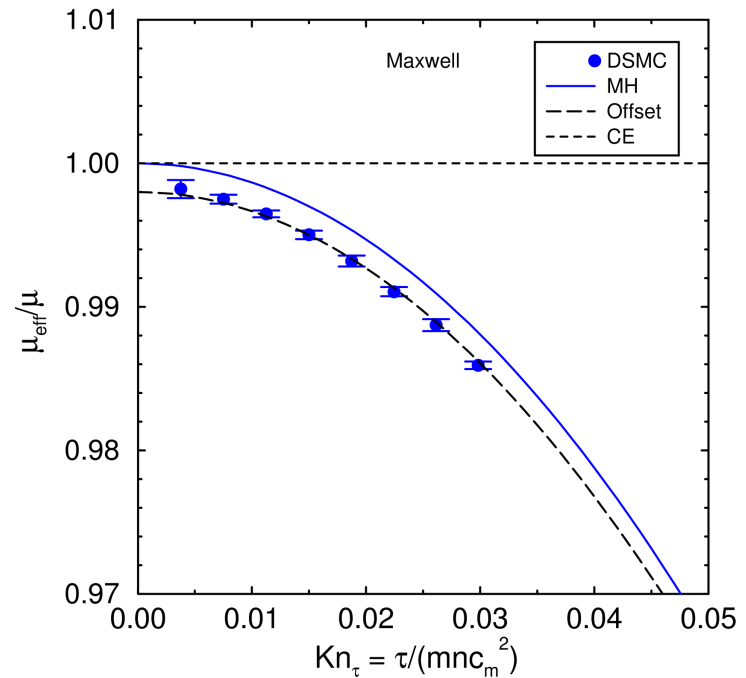
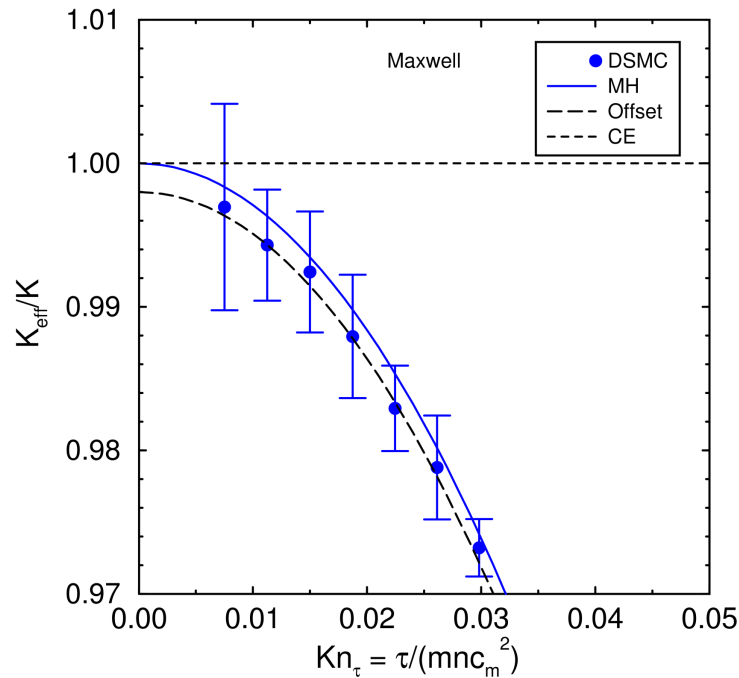
# Maxwell Normalized Sonine Coefficients



## DSMC and MH Maxwell normal solutions for $a_k/a_1$ and $b_k/b_1$

- Four DSMC simulations:  $\Delta T = 70, 200, 300, 400$  K
- MH: VSS-Maxwell (solid) and IPL-Maxwell (dashed) differ
- DSMC and MH VSS-Maxwell normal solutions agree

# Maxwell Normal Transport Coefficients



## DSMC and MH Maxwell normal solutions for $K$ and $m$

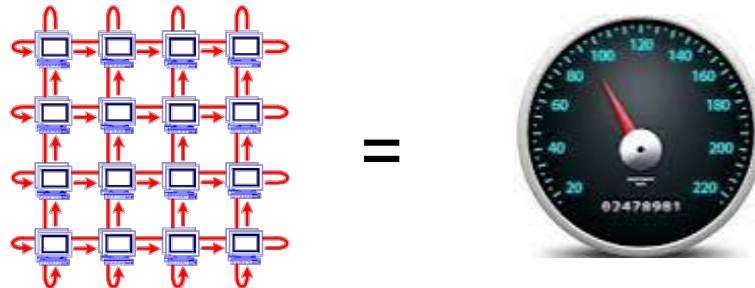
- Finite  $Kn_\tau$  (shear stress), low  $Kn_q$  (heat flux)
- Eight DSMC simulations:  $\Delta V = 100, \dots, 800$  m/s
- Thermal conductivity from viscous heating, larger errors
- Offset MH by DSMC discretization error

Agree to within DSMC discretization error

# Parallel Efficiency: The Unfair Advantage

- The advantages of DSMC come at a cost
- DSMC is **computationally efficient** but **computationally intense**
- Its successful application to real problems depends heavily on its parallel performance
- **1000x speedup** required for some problems of interest
- Monte Carlo methods usually have good parallel performance
  - The workload depends mainly on the molecules within a cell
  - Relatively less need to communicate information between cells
  - Trivial to parallelize in velocity space

The necessary speedup can be achieved without any loss of accuracy or convergence characteristics through parallel computing



# Top 5 Supercomputers (2014)

Rank	Site	System	Cores	Rmax (TFlop/s)	Rpeak (TFlop/s)
1	National Supercomputer Center in Wuxi, China	<b>Sunway TaihuLight</b> - Sunway MPP, Sunway SQ26010 260C 1.45 GHz, Sunway, NRCPC	10,649,600	93,014.4	125,435.9
2	National Super Computer Center in Guangzhou	<b>Tianhe-2 (MilkyWay-2)</b> - TH-IVB-FEP Cluster, Intel Xeon E5-2692 12C 2.200GHz, TH Express-2, Intel Xeon Phi 31S1P	3,120,000	33,862.7	54,902.4
3	DOE/SC/Oak Ridge National Laboratory	<b>Titan</b> - Cray XK7 , Opteron 6274 16C 2.200GHz, Cray Gemini interconnect, NVIDIA K20x	560,640	17,590.0	27,112.5
4	DOE/NNSA/LLNL	<b>Sequoia</b> - BlueGene/Q, Power BQC 16C 1.60 GHz, Custom	1,572,864	17,173.2	20,132.7
5	RIKEN Advanced Institute for Computational Science (AICS)	<b>K computer</b> , SPARC64 VIIIfx 2.0GHz, Tofu interconnect	705,024	10,510.0	11,280.4

**24h hr run on Sequoia = 4,310 years CPU time**

# Programming for Next Generation and Exascale Machines

**Goal is to decouple the science code from the hardware details**

## Envisaged Next Generation Platforms:

- Millions of nodes likely
- Reduced memory per node
- Parallelism within node:
  - Multi-core: 16 and growing
  - Many-core: Intel Xeon Phi, 240 threads
  - GPUs: NVIDIA/AMD, 1000 warps
- **Example:** LLNL BG/Q: 96K nodes, 16 cores/node + 4 MPI tasks/core

## Necessary elements

- Adaptive gridding
- In-situ visualization
- Efficient communications
- Load balancing

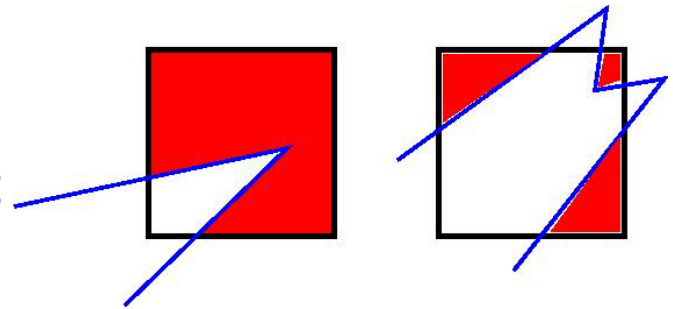


# Developing an Exascale DSMC Code

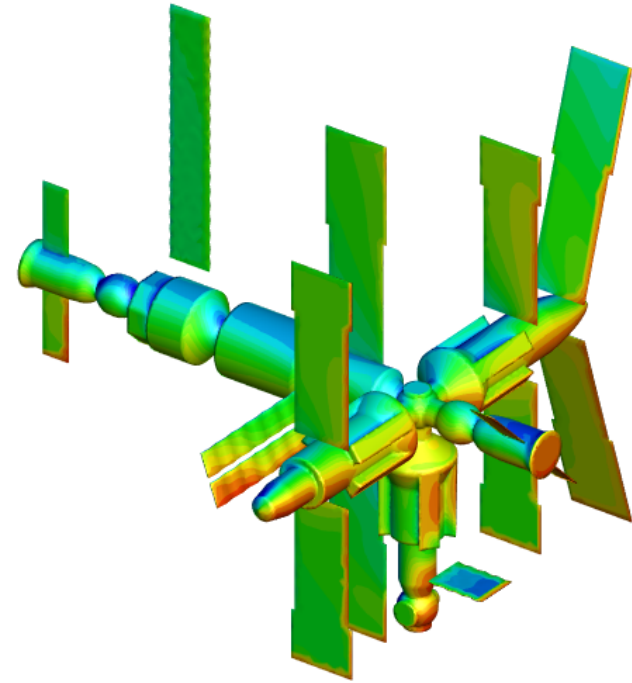
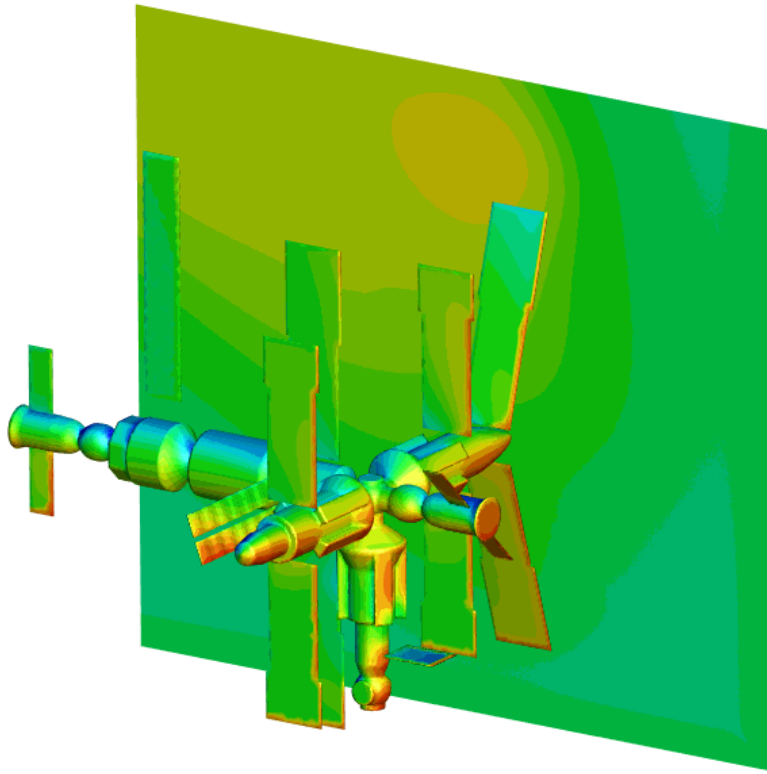
**SPARTA** = Stochastic **PA**rallel **R**arefied-gas **T**ime-accurate **A**nalyzer

## General features

- 2D or 3D, serial or parallel
- Cartesian, hierarchical grid
  - Oct-tree (up to 16 levels in 64-bit cell ID)
  - Multilevel, general NxMxL instead of 2x2x2
- Triangulated surfaces cut/split the grid cells
  - 3D via Schwartzentruber algorithm
  - 2D via Weiler/Atherton algorithm
  - Formulated so can use as kernel in 3D algorithm
- C++, but really object-oriented C
  - Designed to be easy to extend
  - New collision/chemistry models, boundary conditions, etc.
- Code available at <http://sparta.sandia.gov>



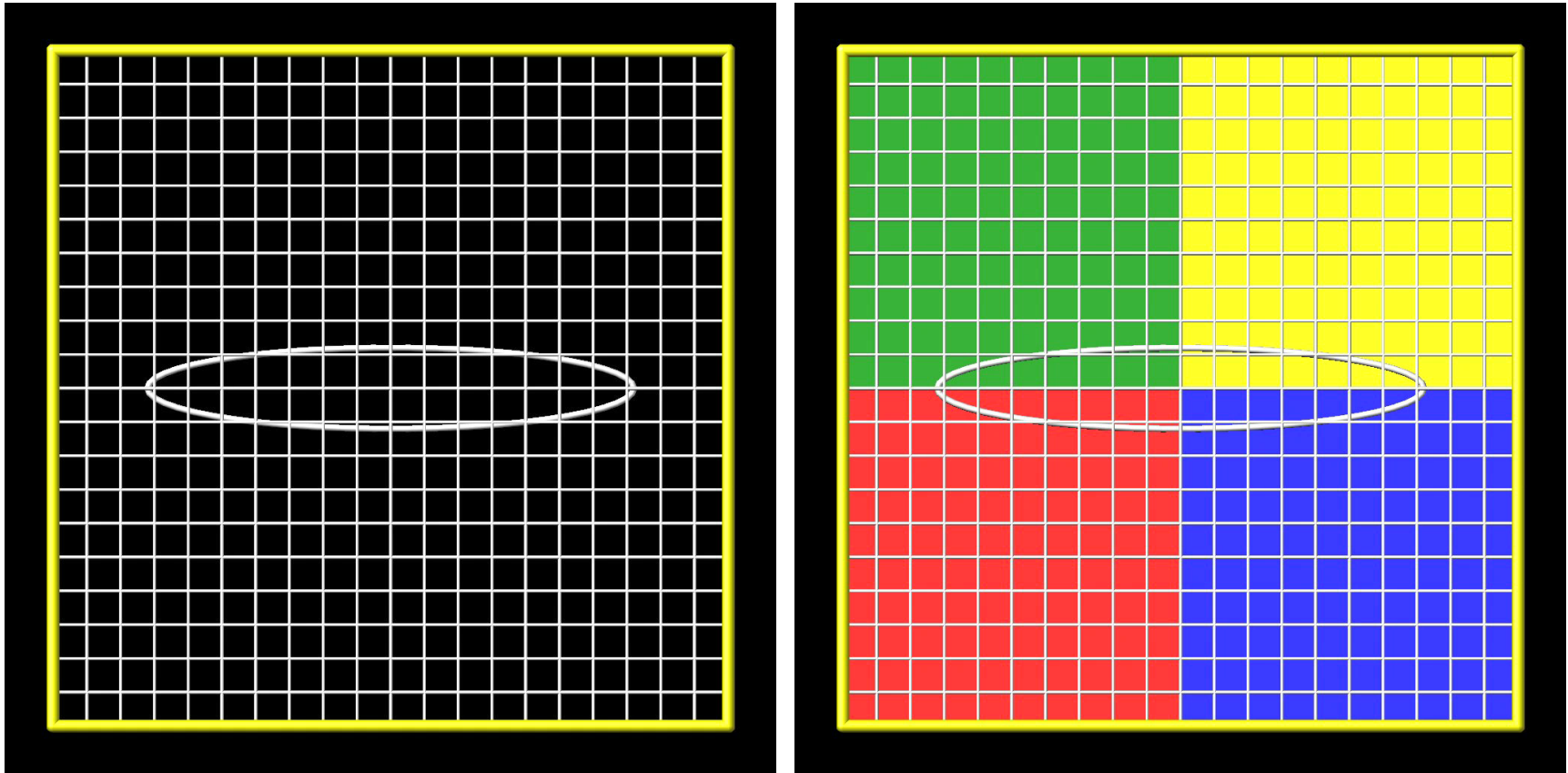
# Simulation of Complicated Shapes



Mir Space Station

Grid generation ( $10^7$  cells) completed in 0.3 seconds on 16 processors  
Geometry comprises multiple “water-tight” bodies

# Efficient Communication & Load Balancing

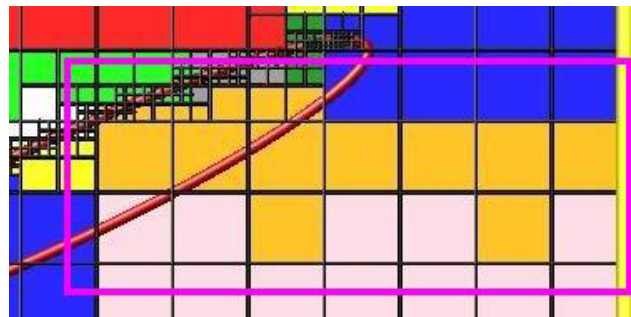
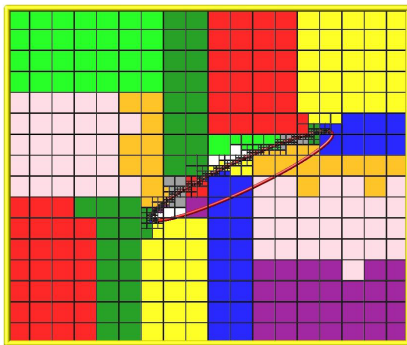


Simulation of a moving object with simultaneous adaptive gridding (left) and load balancing (right)

# Efficient Communication & Load Balancing

To achieve maximum efficiency:

- **One communication per step**
  - Multiple passes if needed (or can bound molecule move)
- Communication with **modest count of neighbor processors**
- One processor = **compact clump of cells via load balancing**
  - Ghost region = nearby cells within **user-defined cutoff**
  - Store surface information for ghost cells to complete move



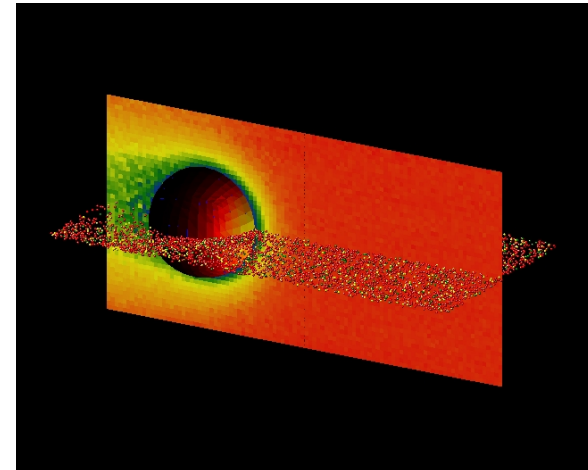
**Example:**

1B cells on 1024 BG/Q node  
Worst case: move all cells  
Balance time = 15 s:  
(RCB=2, move=12, ghosts=1)

- Balance across processors, **static or dynamic**
- Geometric method: recursive coordinate bisection (RCB)
- **Weighted** by cell count or molecules or CPU

# In-Situ Visualization

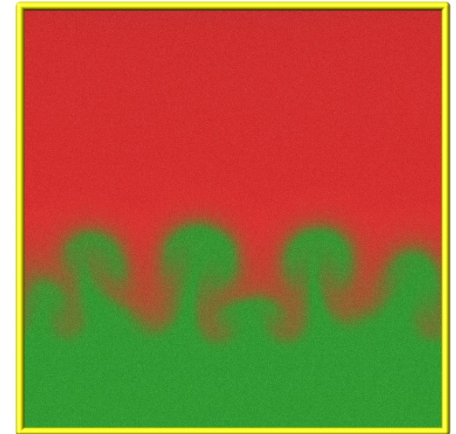
Not a replacement for interactive viz, but ...  
Quite useful for **debugging** & quick analysis  
At end of simulation (or during), instant movie



Render a JPG snapshot every N time steps:

- Each processor starts with blank image (1024x1024)
- Processor draws its cells/surfaces/molecules with depth-per-pixel
- Merge pairs of images, keep the pixel in front, recurse
- Draw is parallel, merge is logarithmic (like MPI Allreduce)

Images are ray-traced quality



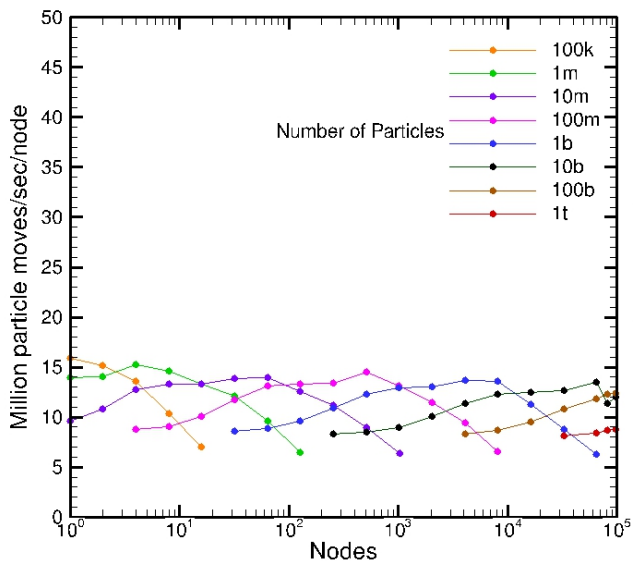
# SPARTA Benchmarking

- Flow in a closed box
  - Stress test for communication
    - No preferred communication direction
  - 3D regular grid,  $10^4$ - $10^{11}$  (0.1 trillion) grid cells
  - 10 molecules/cell,  $10^5$ - $10^{12}$  (1 trillion) molecules
- Effect of threading
  - 2 threads/core = 1.5 speed
  - 4 threads/core = 2x speed

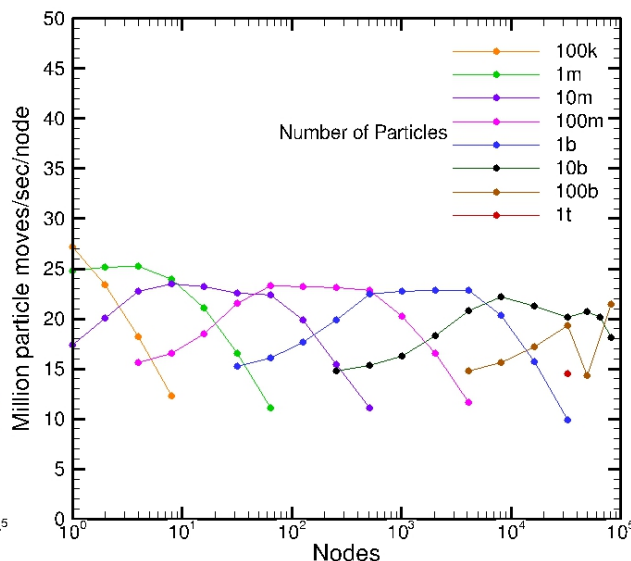


# SPARTA Benchmarking

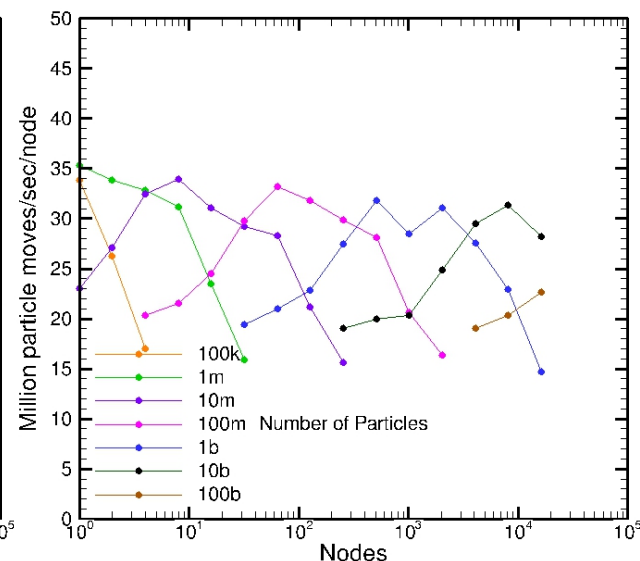
16 cores/node  
1 task/core



16 cores/node  
2 tasks/core



16 cores/node  
4 tasks/core



- Weak scaling indicates, 10% peak performance reduction from 1 to  $10^6$  cores
- 2 tasks/core gives 1.5x speedup, 4 tasks/core gives 2x speedup
- A total of **1 trillion molecules** can be simulated on **one third** of the BG/Q
- Maximum number of tasks is 2.6 million

# Instabilities: When do they occur?



Infinitesimal disturbances amplify spontaneously and ultimately dominate the flows.

The growth of the instability is influenced by viscosity, compressibility, three-dimensionality, density ratio.

It is postulated that the failure to achieve ignition at NIF can be attributed to the **Rayleigh-Taylor instability (RTI)**.



RTI can produce the Kelvin-Helmholtz instability (KHI) and has the Richtmyer-Meshkov instability (RMI) as a limiting case.

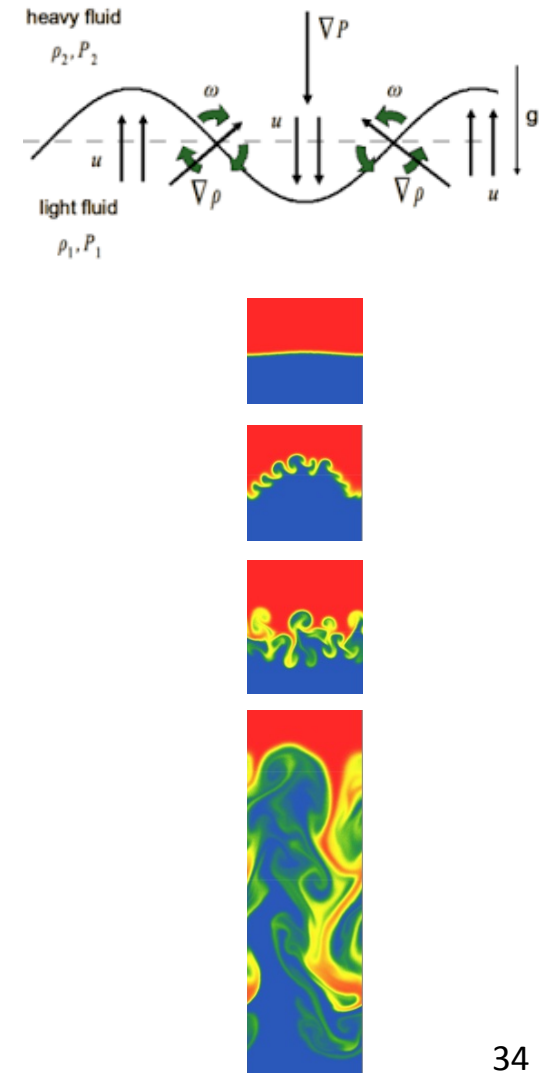
Applications range from Inertial Confinement Fusion (ICF, mm) to the formation of supernova remnants (light-years).

Clark et al. 2013

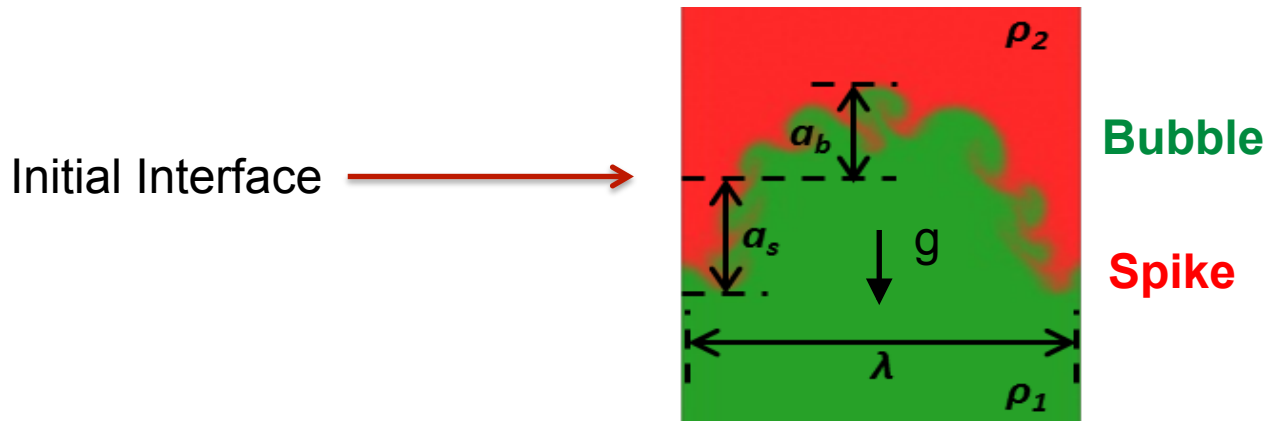
Molecular methods like DSMC are becoming increasingly popular for investigating the effects of viscosity and diffusivity in ICF applications, which are known as “kinetic” or “ion-kinetic” effects. (Larroche *et al.* 2016)

# Rayleigh-Taylor Instability (RTI)

- RTI is an instability of an interface between two fluids of different densities which occurs when the lighter fluid is pushing the heavier fluid.
- Baroclinic torque at the interface creates vorticity and induces a velocity field that increases the amplitude, which in turn increases the baroclinic torque.
- RTI has four main stages:
  - Linear (linear growth of initial perturbations)
  - Nonlinear (mushroom-like structures appear)
  - Structures interact and compete (as in RMI, KHI)
  - Turbulent mixing



# Characteristic & Nondimensional Quantities



$$a = a_b + a_s$$

Amplitude

$$A = \frac{\rho_2 - \rho_1}{\rho_2 + \rho_1}$$

Atwood Number

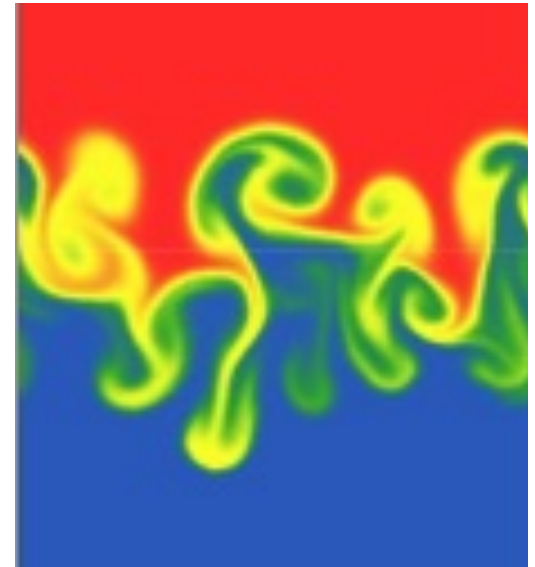
$$\text{Re}_p = \frac{\lambda \sqrt{\frac{A}{1+A}} g \lambda}{\nu}$$

Reynolds Number  
(Wei & Livescu 2012)

# Most Unstable Wavelength

- The initial growth rates of small-amplitude perturbations are influenced by the fluid properties.
- Viscosity and diffusivity inhibit small-wavelength perturbations from growing, allowing a particular wavelength, the **most unstable wavelength**, to emerge, **outpacing** the growth of all other wavelengths:

$$\lambda_m \approx 4\pi(\nu^2 / Ag)^{1/3}$$

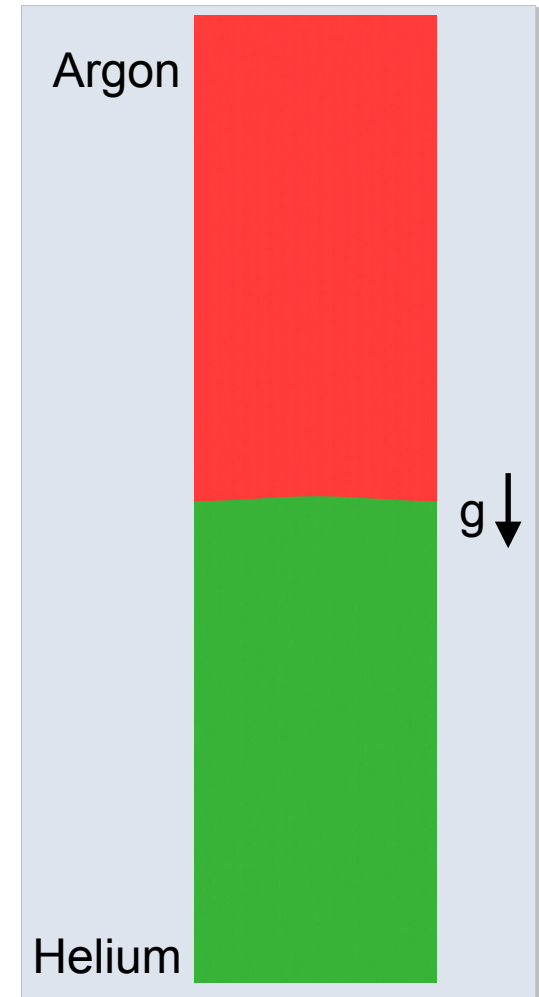


# Why DSMC for Rayleigh-Taylor Instability?

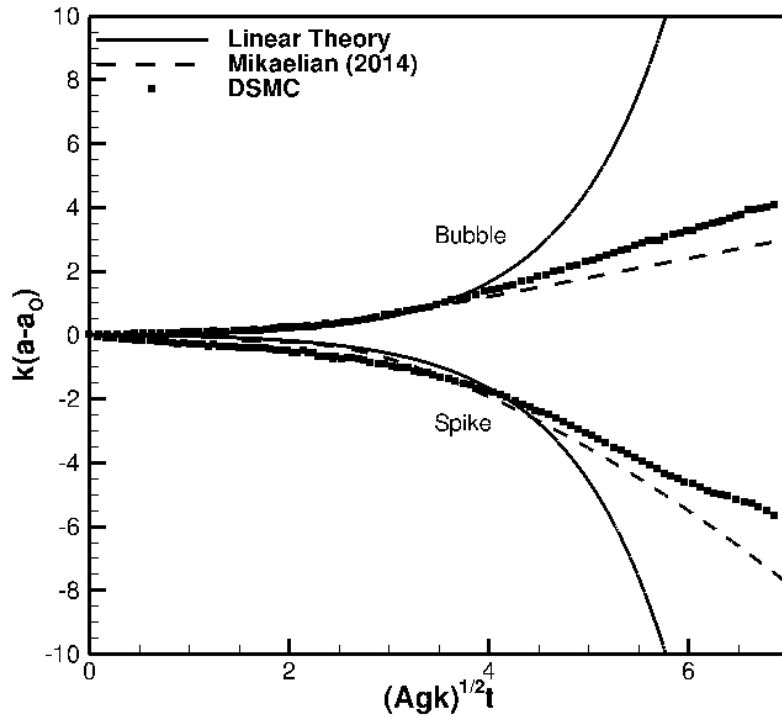
- DSMC provides a molecular-level description of the hydrodynamic processes that may be physically more realistic for **large accelerations and chemically reacting flows and the representation of naturally occurring thermal fluctuations**
- DSMC inherently accounts for transport properties
- The DSMC method offers the potential to identify the impact of molecular level effects (e.g., rotational and vibrational energy exchange, gas-phase chemical reactions, and gas-surface interactions) on hydrodynamic instabilities.
- Typical 2D DSMC simulation characteristics:
  - Physical Domain: 1 mm x 4 mm (ICF-pellet-size domain)
  - # Cells: 4 billion
  - # Particles: 400 billion
  - # Cores: 1/4-1/2 million
  - Run time: 30 hrs (= 900, 1800 CPU years)
  - Time steps:  $200,000 \times 0.1 \text{ ns} = 20 \mu\text{s}$

# DSMC Simulations of the Rayleigh-Taylor Instability in Gases

- The interface between argon (red) and helium (green) gases is slightly perturbed:  
 $\lambda = 0.001m$ ,  $a = 10\mu m$ ,  $A = 0.81$
- Initial state hydrostatic equilibrium
- Acceleration of the system excites the RTI
  - Initially, **thermal fluctuations and diffusion** perturb the interface
  - The initial perturbation amplitude grows exponentially
  - A second growth stage occurs at the most unstable wavelength, which forms “**bubbles**” and “**spikes**”
  - Additional instabilities break up the larger structures, resulting in **turbulent mixing of the gases**

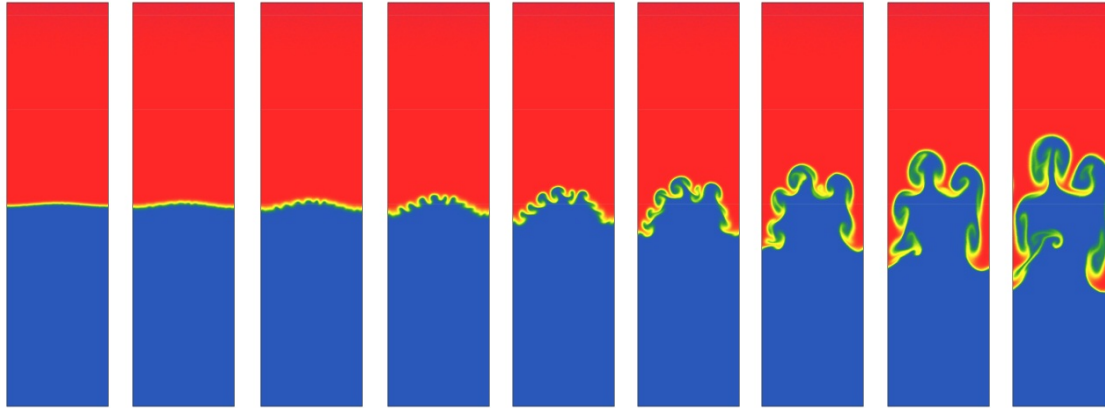


# Development of 1-mm Wavelength Perturbation for Gravity $10^8 \text{ m/s}^2$

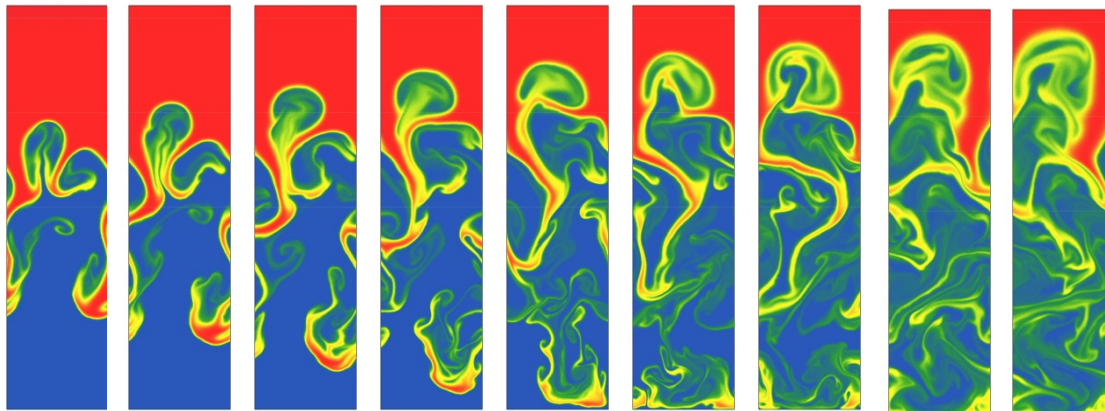


- Initial perturbations of a small wavelength develop and grow exponentially.
- Smaller structures, corresponding to the most unstable wavelength, appear.
  - Their number is independent of the molecular simulation ratio and the random number seed.
- Larger structures emerge as the smaller disturbances interact and combine.

# Density Profiles for 1-mm Wavelength Perturbation for Gravity $10^8 \text{ m/s}^2$

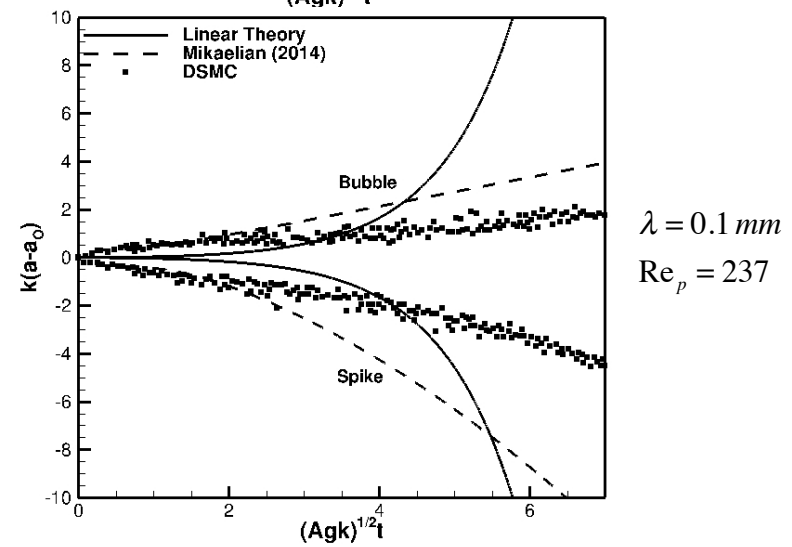
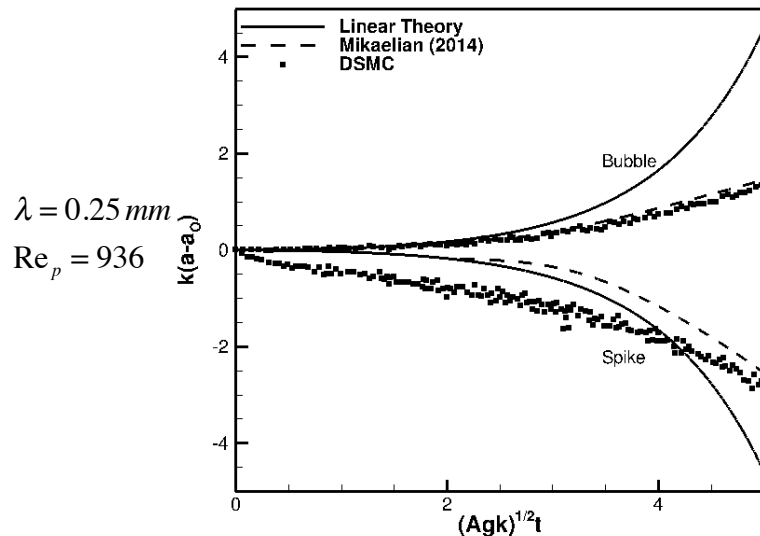
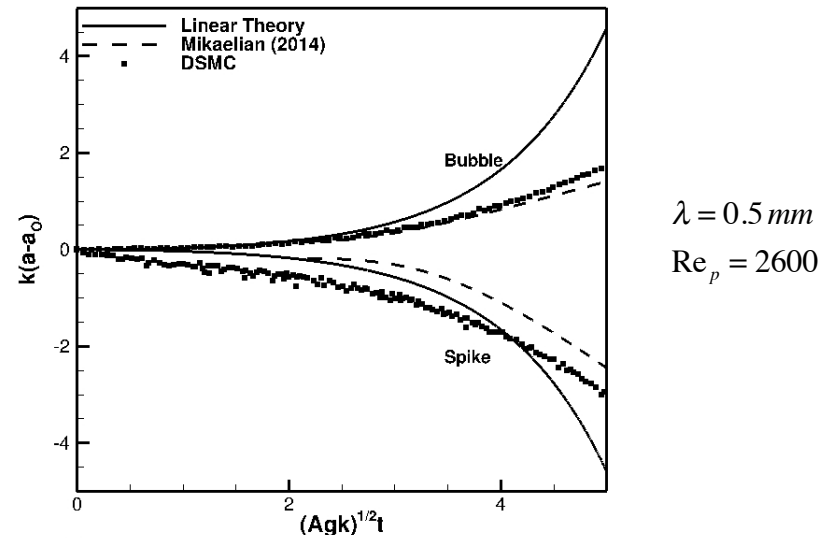
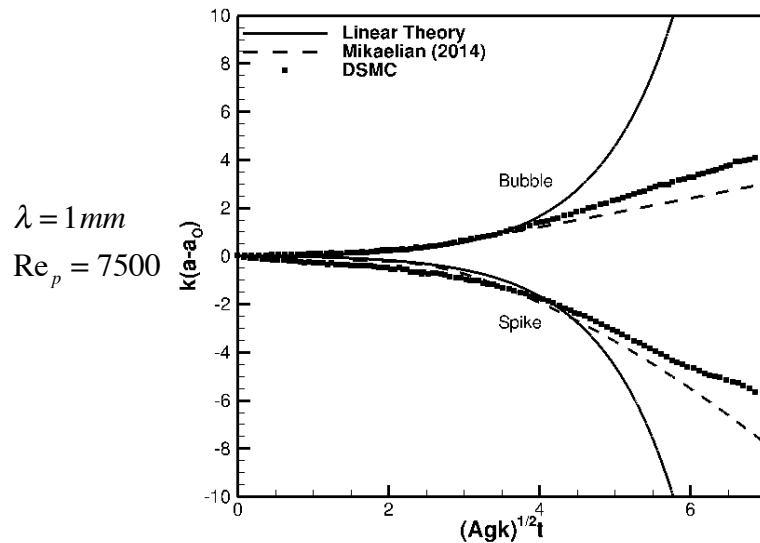


Images progress at 10,000 time step increments



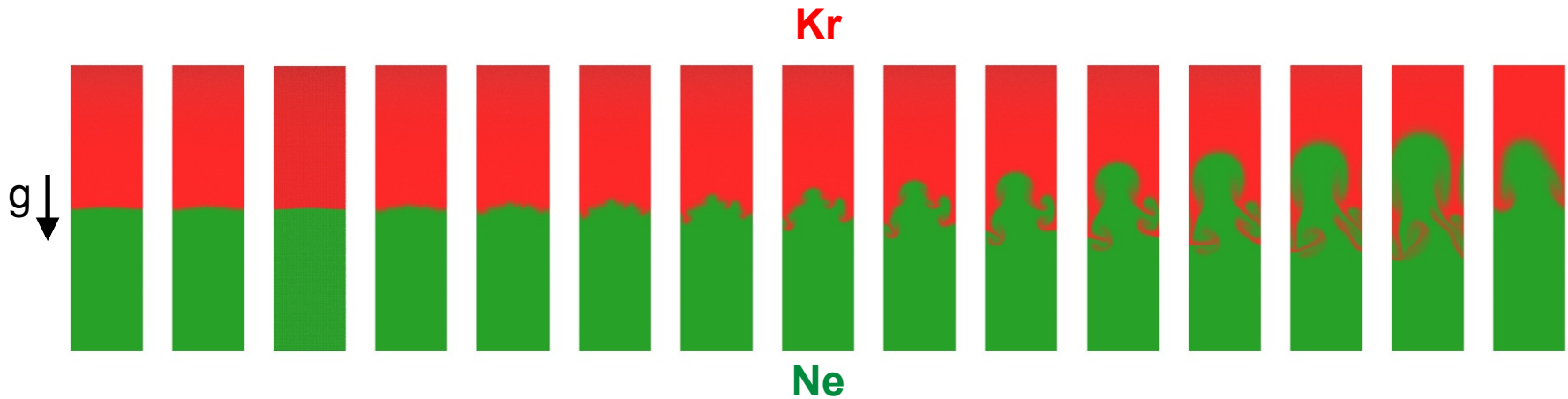
Initially, diffusion thickens the interface. Subsequently, bubbles and spikes appear.

# RTI for Ar/He with Different Wavelengths



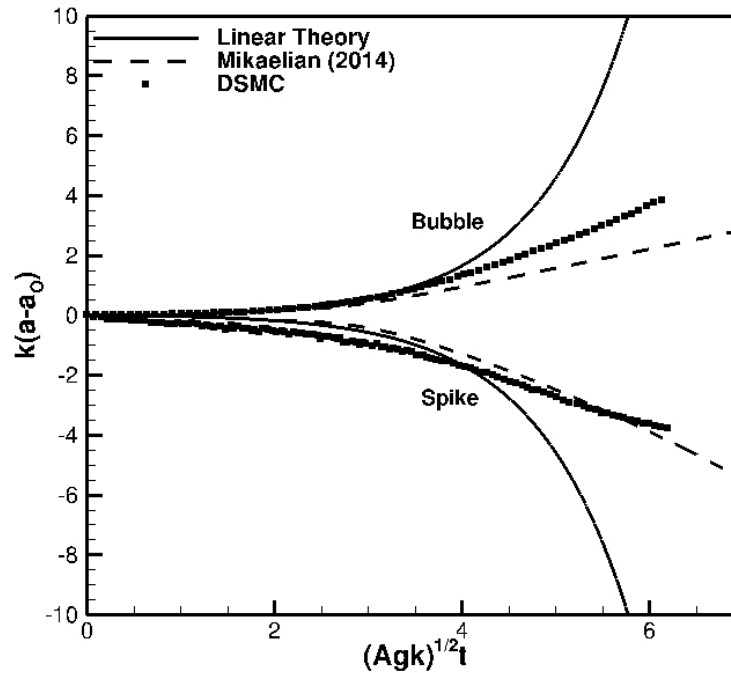
For each simulation, the domain width is one wavelength,  
and the amplitude is 1% of the wavelength.

# DSMC Simulations of the RTI for Kr/Ne

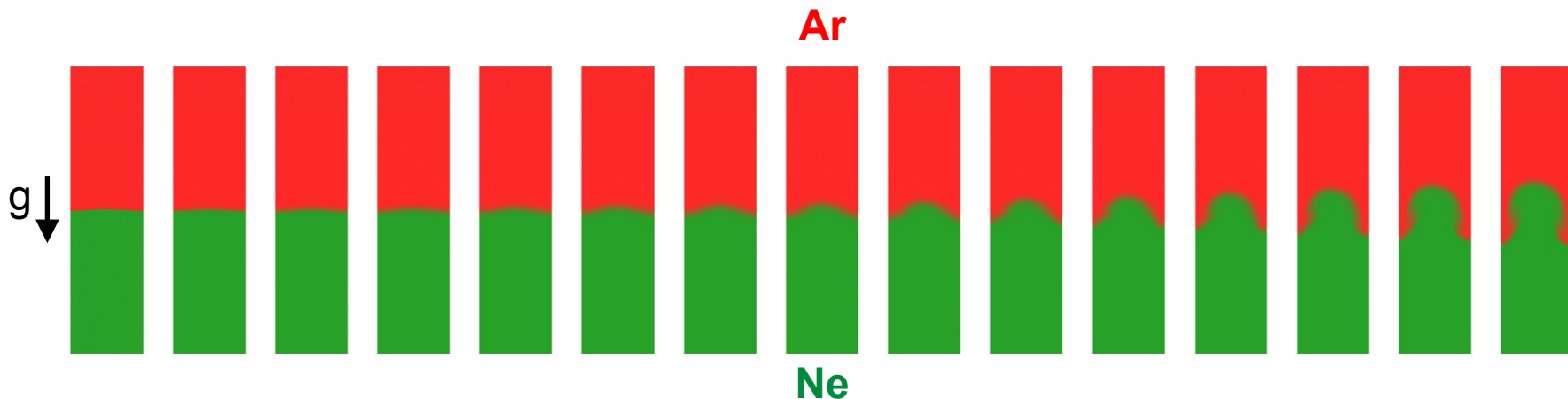


$A = 0.61$   
Gravity =  $10^8 \text{ m/s}^2$

$Re_p = 12800$

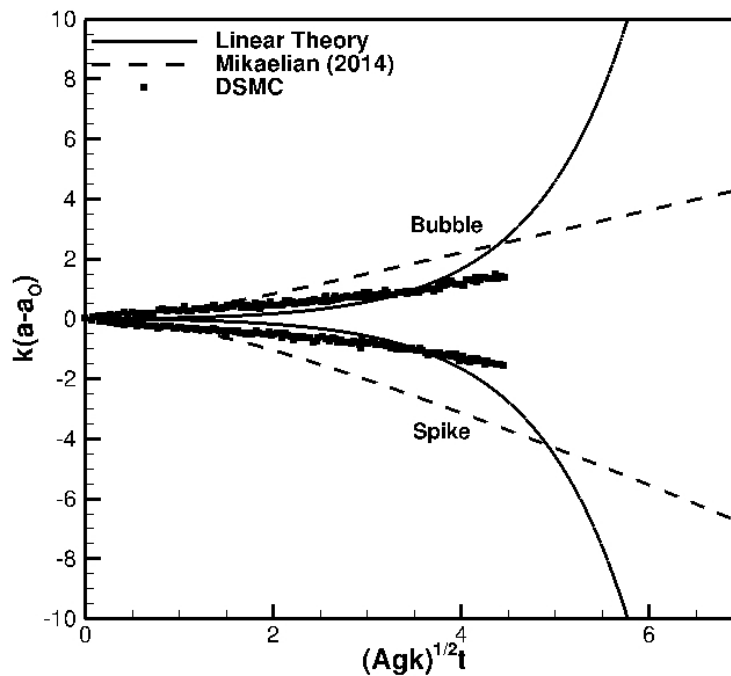


# DSMC Simulations of the RTI for Ar/Ne



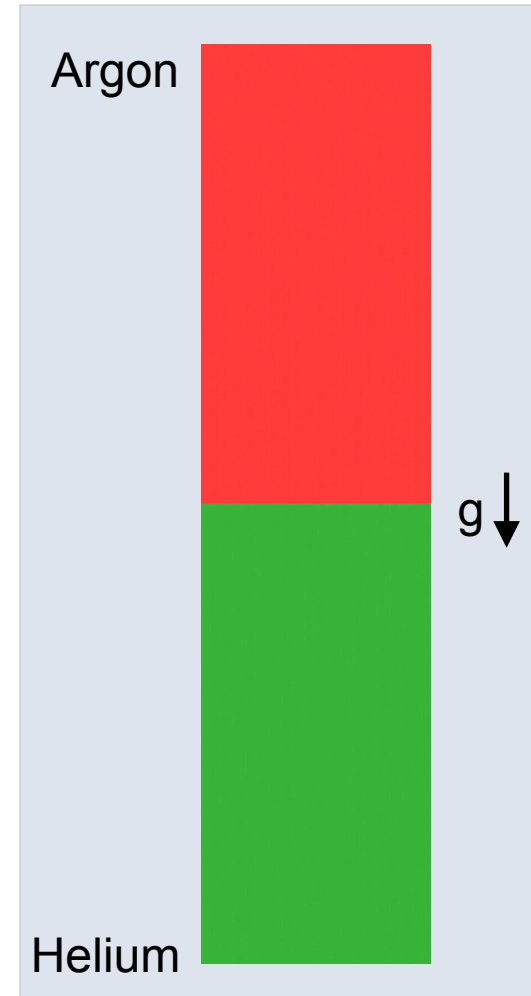
$A = 0.32$   
Gravity =  $10^8 \text{ m/s}^2$

$Re_p = 6000$

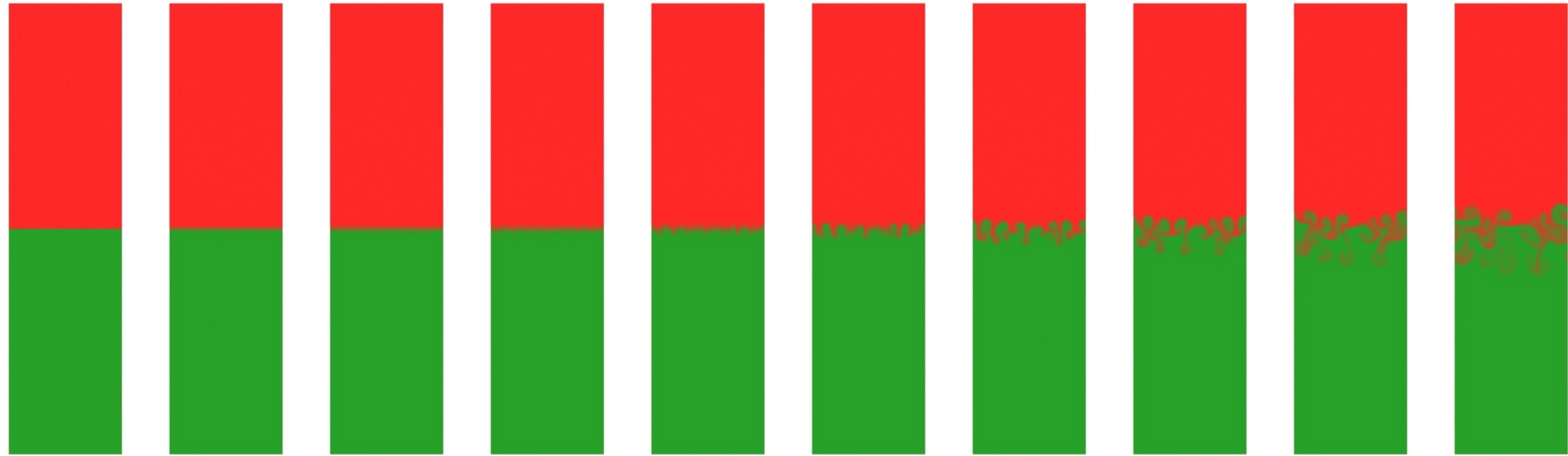


# RTI from an Initially Molecularly Flat Interface

- The interface between argon (red) and helium (green) gases is **initially flat**
- Acceleration of the system excites the RTI
  - **Initially, thermal fluctuations and diffusion perturb the interface**
  - The amplitude of thermal fluctuations grows exponentially
  - Gases penetrate each other differently, forming “**bubbles**” and “**spikes**”
  - Finally, additional instabilities break up the larger structures resulting in turbulent and chaotic mixing of the gases



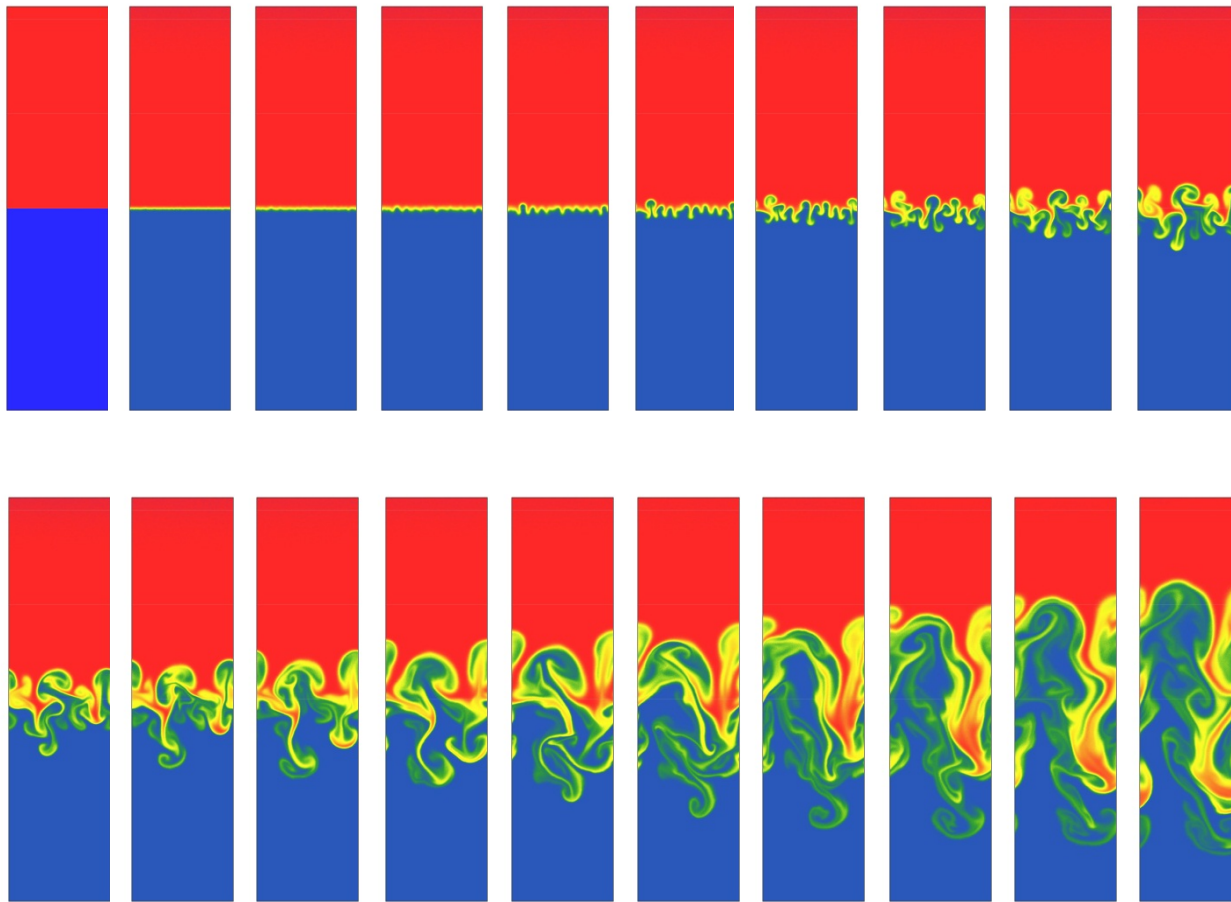
# RTI from an Initially Flat Interface



Images progress at 10,000 time step increments

The numbers of bubbles and spikes correspond to the most unstable wavelength.

# Density Profiles for an Initially Flat Interface

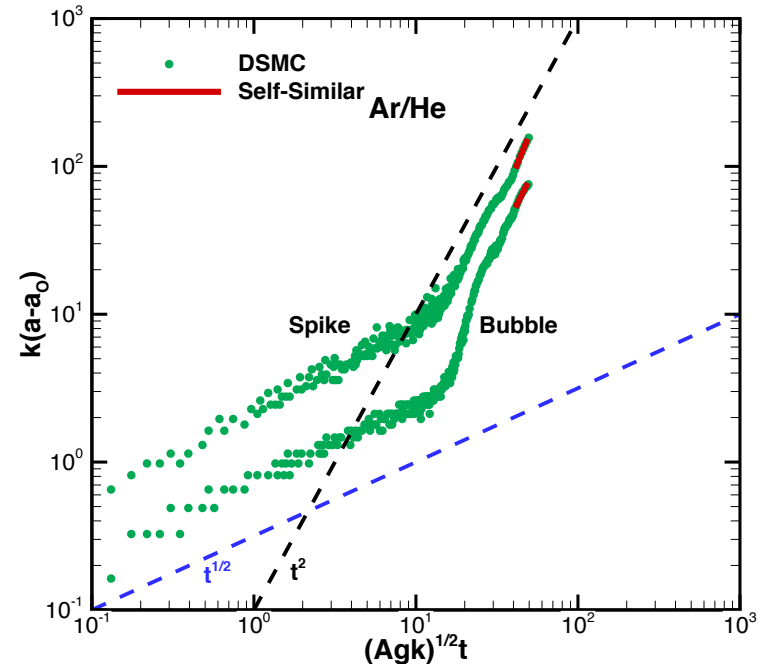
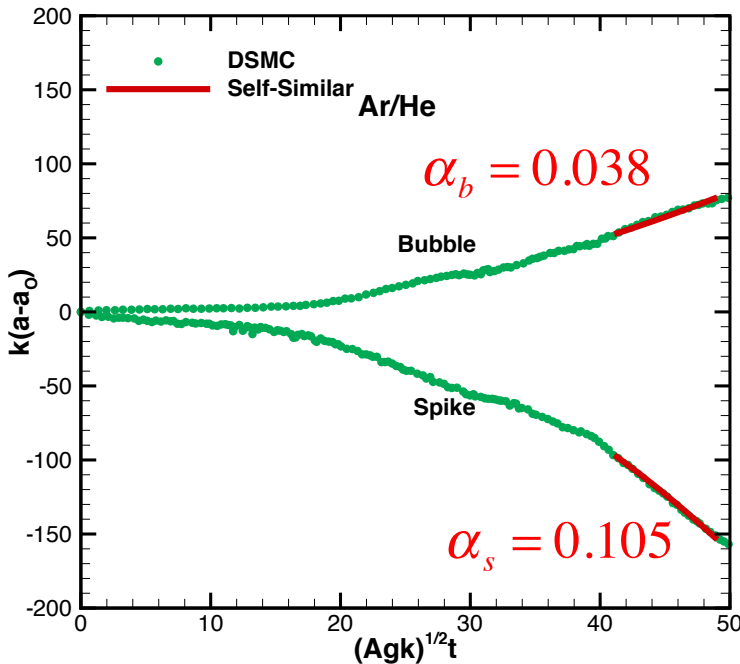


Images progress at 10,000 time step increments

# Late-Time Behavior: Self-Similarity

At late times, under certain idealized conditions, the flow can forget its initial conditions and enter a self-similar growth phase (Fermi and von Neumann 1953) described by the following equation:

$$a_{b,s} = \alpha_{b,s} A g t^2$$



Self-similar behavior is observed for long times.  
Waviness is due to competition between bubbles and spikes.

# RTI in 3D: Density Profile

Typical 3D DSMC simulation characteristics:  
Physical Domain: 1 mm x 1 mm x 4 mm

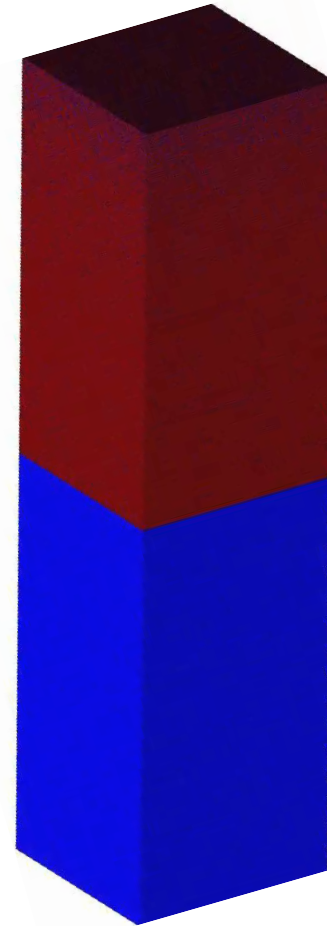
# Cells: 62.5 billion

# Particles: 1.2 trillion

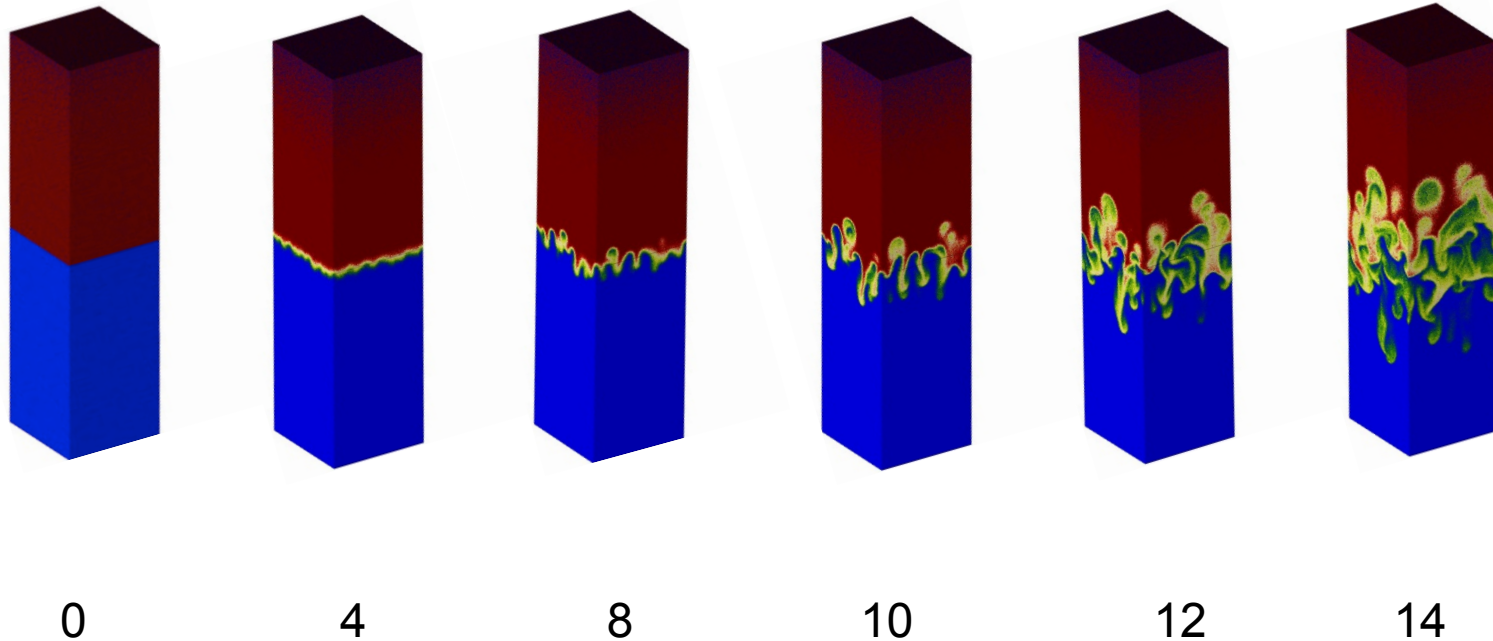
# Cores: ½ million

Run time: 90 hrs (5400 CPU years)

Time steps:  $200,000 \times 0.1 \text{ ns} = 20 \mu\text{s}$



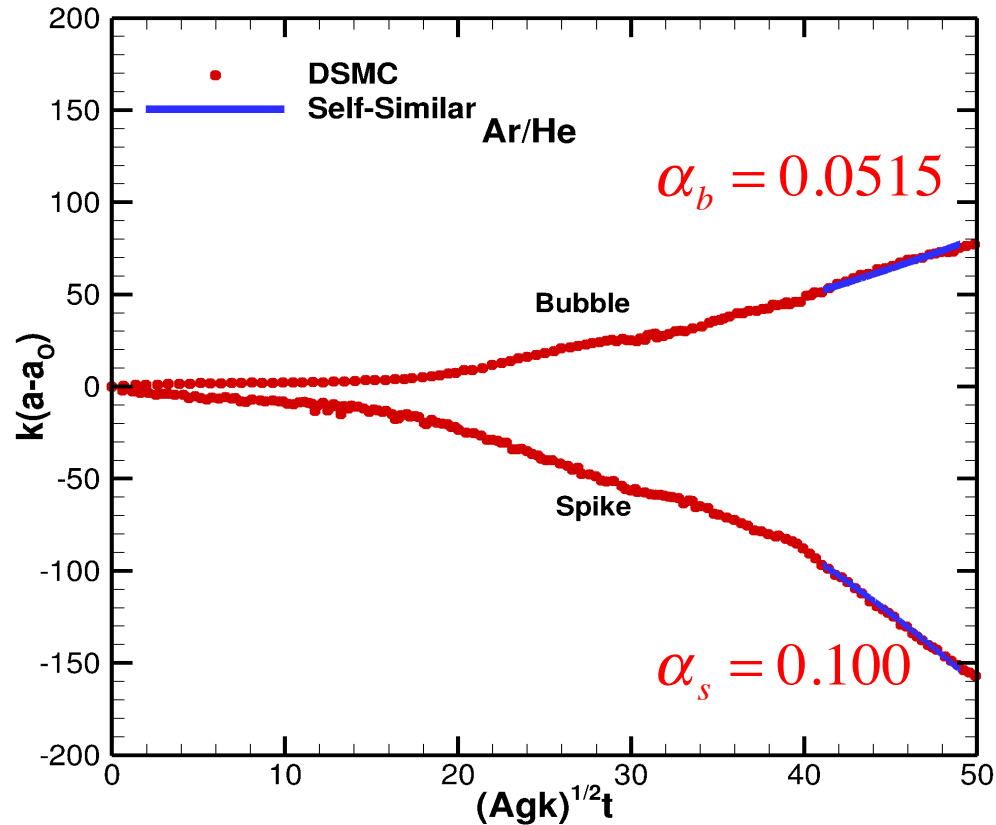
# RTI from a Flat Interface in 3D



Images progress at **multiples** of 10,000 time step increments

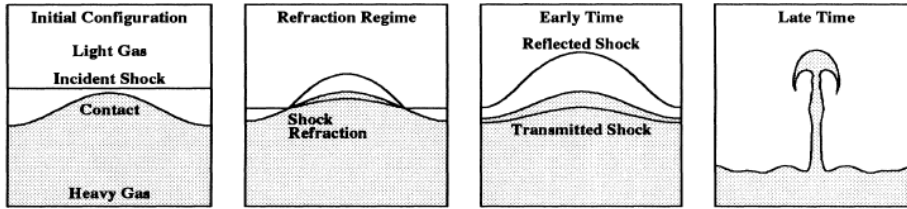
# 3D Late-Time Behavior: Self-Similarity

Condition for Self-Similarity:  $a_{b,s} = \alpha_{b,s} Agt^2$



Self-similar behavior is observed at late times.  
Waviness is due to competition between bubbles and spikes

# RTI Is Related to RMI



Grove et al., Phys. Rev. Lett., 71 (21), 3473 (1993).

## Shock propagation

- Incident shock travels down in upper gas
- Transmitted shock travels down in lower gas
- Reflected shock travels upward in upper gas

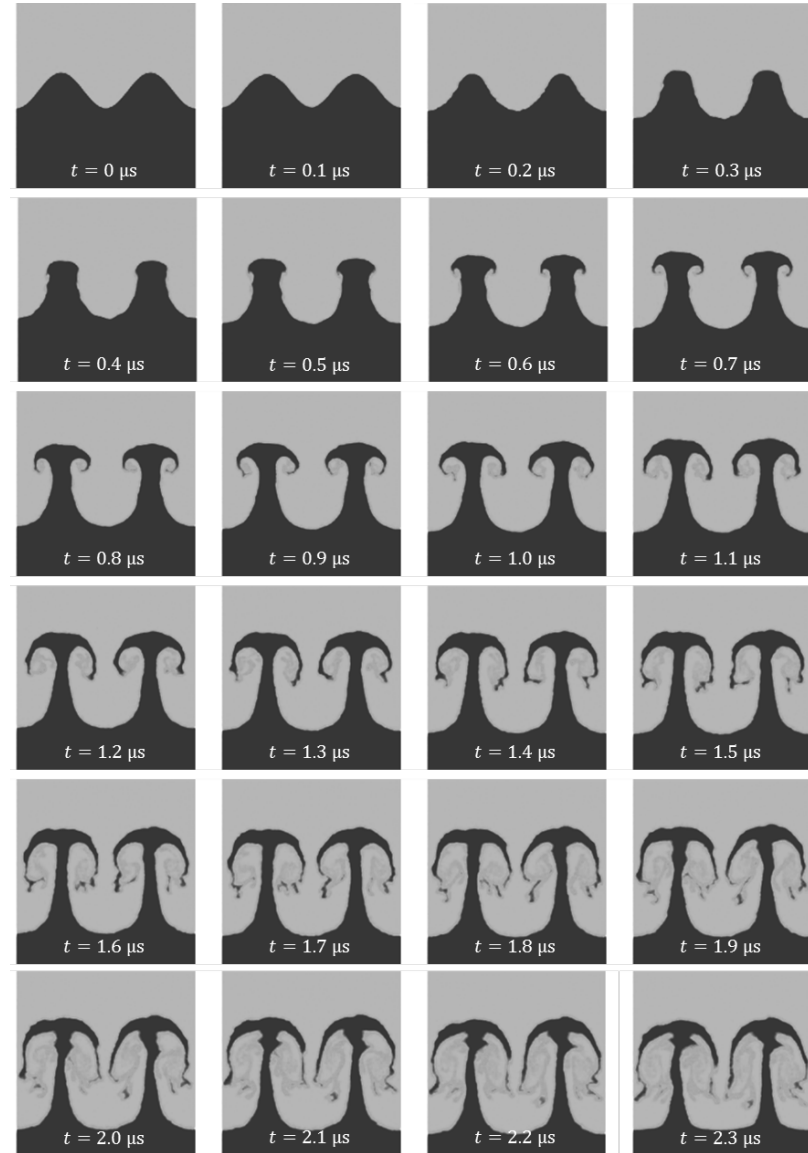
## Interface motion

- Interface is accelerated to constant velocity
  - Travels in same direction as shock
- Vorticity generated baroclinically at interface
  - Density & pressure gradients misaligned

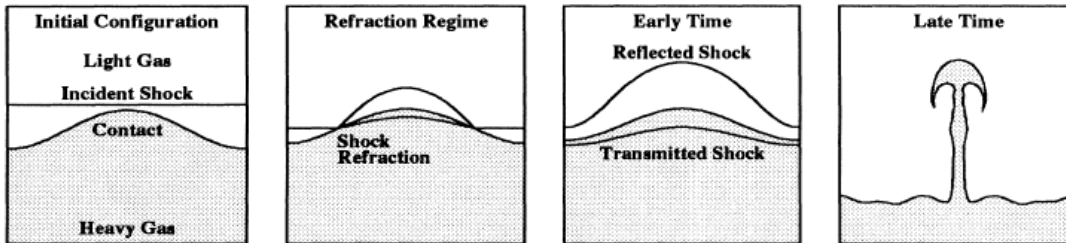
## Perturbation growth

- Initially, amplitude growth is linear with time
- Later, amplitude growth becomes nonlinear
  - When amplitude is similar to wavelength
- Bubbles, spikes, roll-up, more instabilities

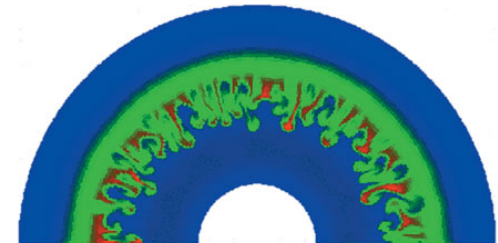
Gallis et al. Physics of Fluids (2015)



# Richtmyer-Meshkov Instability (RMI)



Grove et al., Phys. Rev. Lett., 71(21), 3473 (1993).

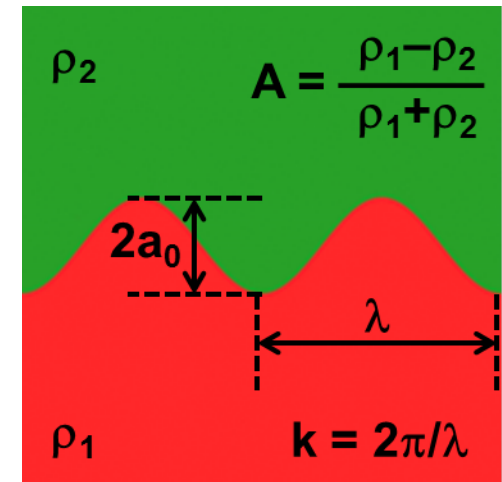


ICF target compression

RMI applications include stellar evolution, inertial confinement fusion, shock-flame interaction

RMI combines multiple fluid-flow phenomena

- Shock transmission and reflection
- Hydrodynamic instabilities
- Linear and nonlinear growth
- Diffusion and turbulent mixing
- Compressibility effects
- Chemical reactions



RMI basic geometry

## ***Simulate RMI using molecular gas dynamics***

- Physical conditions that can be achieved
- Computational software & hardware needed

# RMI in Gas Mixtures

## Physical situation

- Gases: pairs of helium, neon, argon, xenon, air, SF<sub>6</sub>
- STP conditions: both gases at 1 atm and 0 °C
- Two-dimensional domain: 0.1 mm × 0.4 mm
- Wavelength, initial amplitude: 0.05 mm, 0.01-0.1 mm

## Numerical parameters

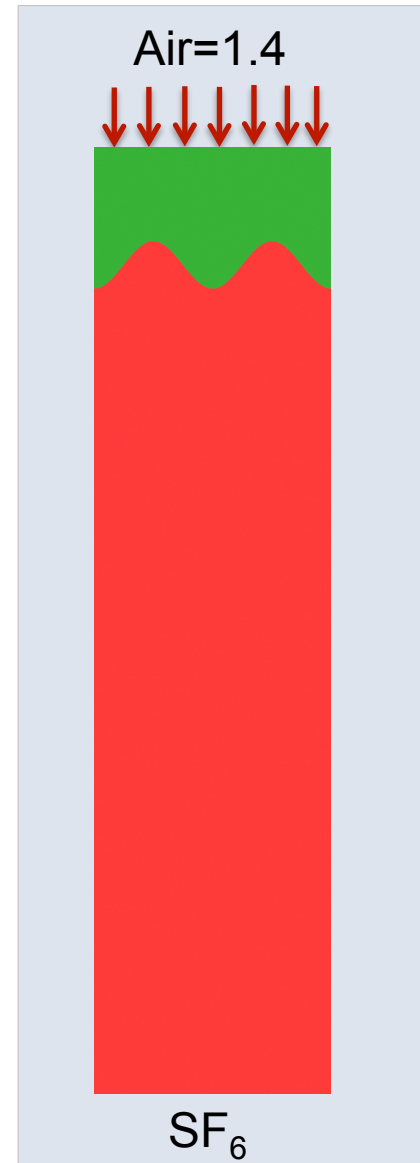
- Mesh: 5 nm, 20,000×80,000 = 1.6 billion cells
- Molecules: 800 billion molecules (500 per cell)
- Time steps: 200,000×0.01 ns = 2 μs

## Computational aspects

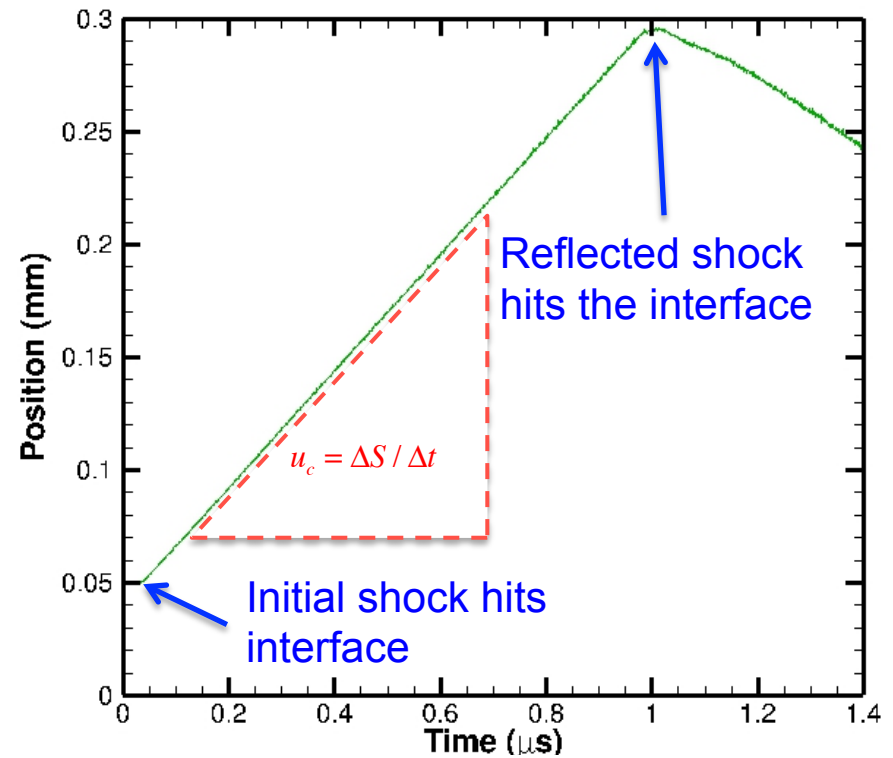
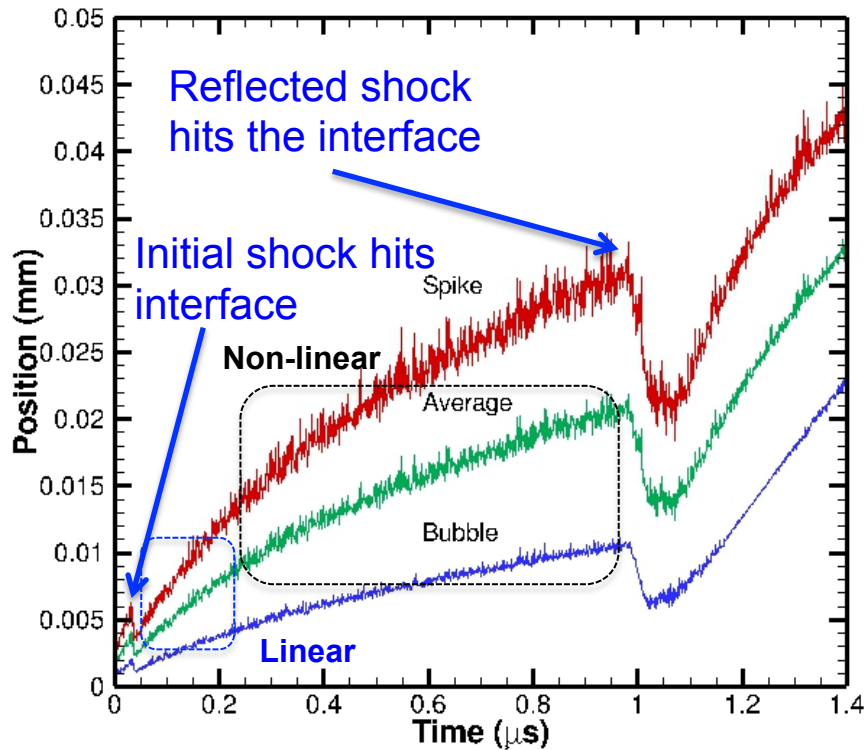
- Platform: Sequoia, 30 hours
- Processors: ~¼ million cores (16k nodes) (900 years CPU time)

## Flow phenomena

- Flow at top is impulsively started and maintained
- Shock wave propagates down and hits interface
- Transmitted and reflected shock waves depart
- Interface moves down and grows thicker



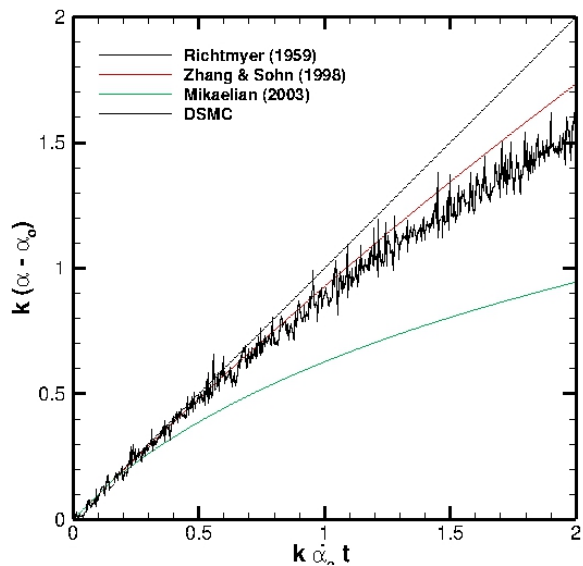
# Development of Bubbles and Spikes in RMI



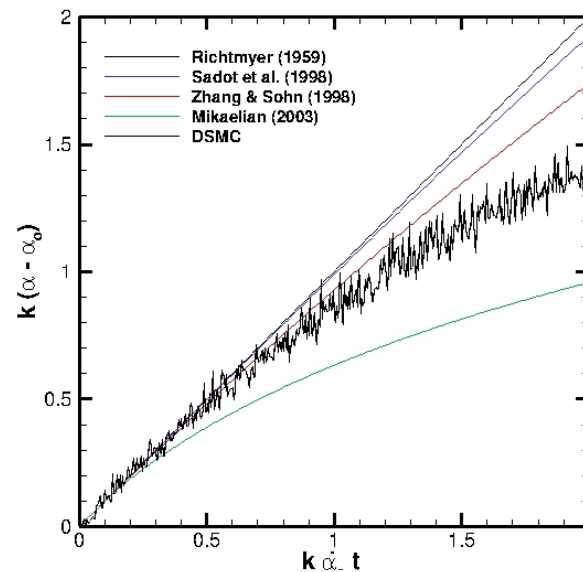
Interface moves with constant speed until the interface gets re-shocked  
The development of bubbles and spikes can be tracked independently

# DSMC-RMI Comparison to Theory

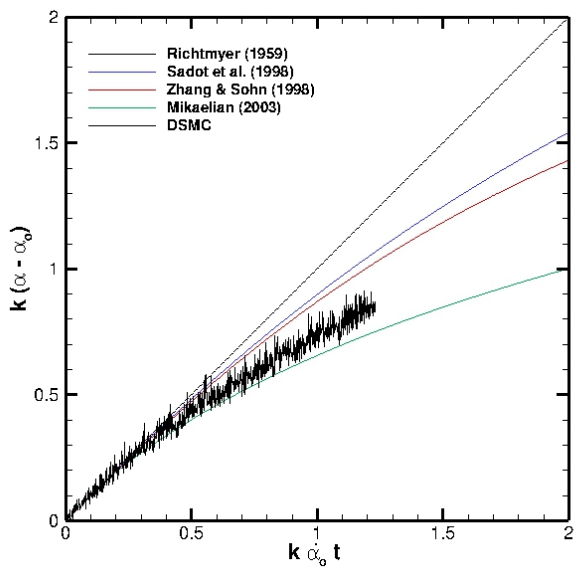
He/Xe  
A=0.94



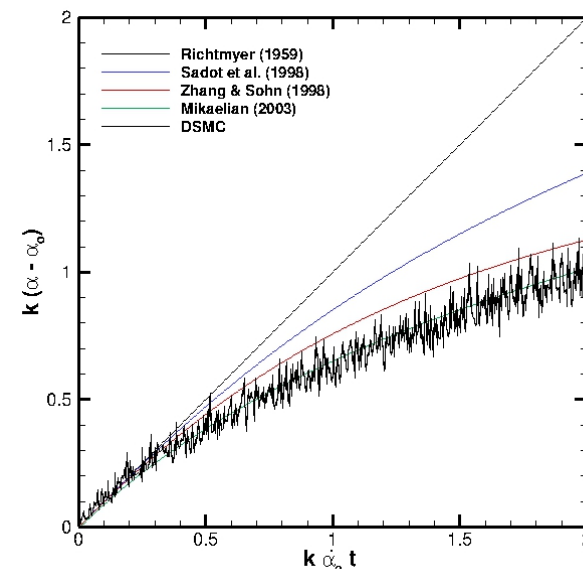
He/Ar  
A=0.61



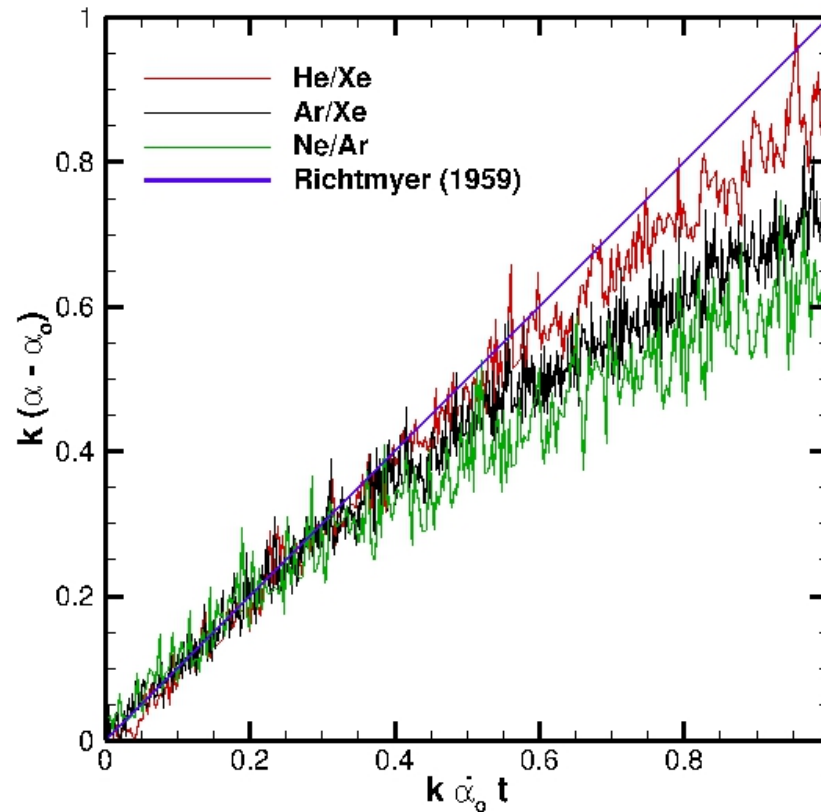
Ar/Xe  
A=0.53



Ne/Ar  
A=0.33

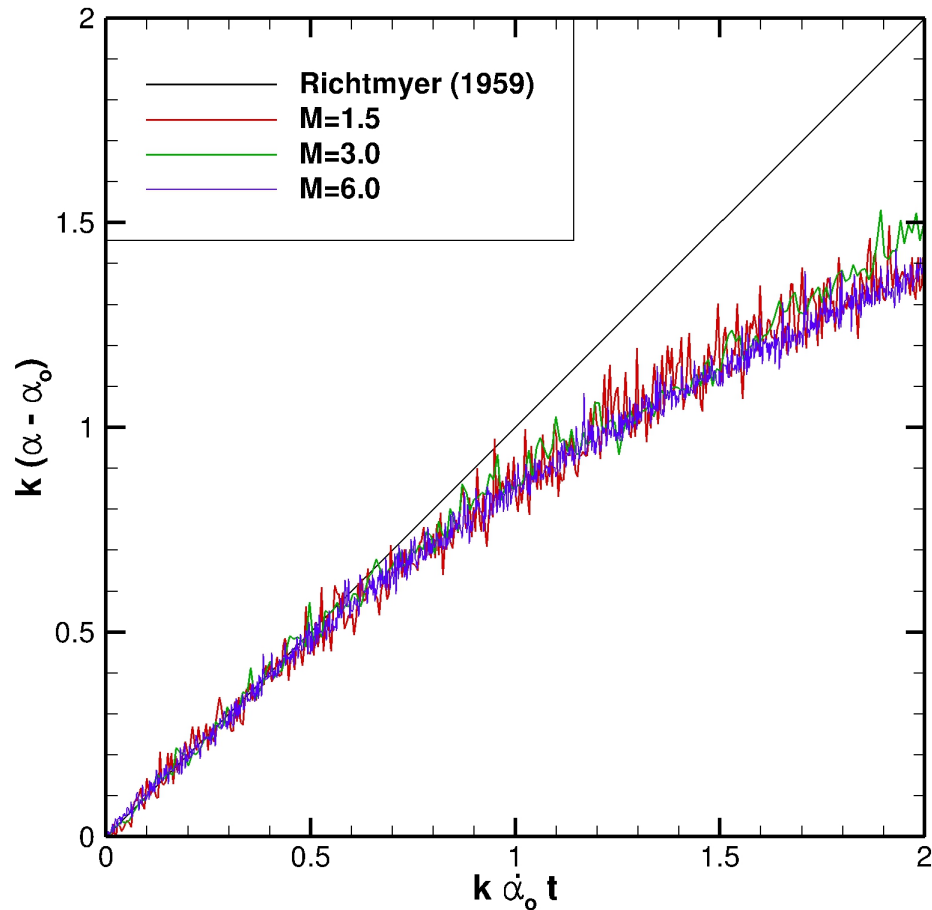


# RMI: Effect of Atwood Number



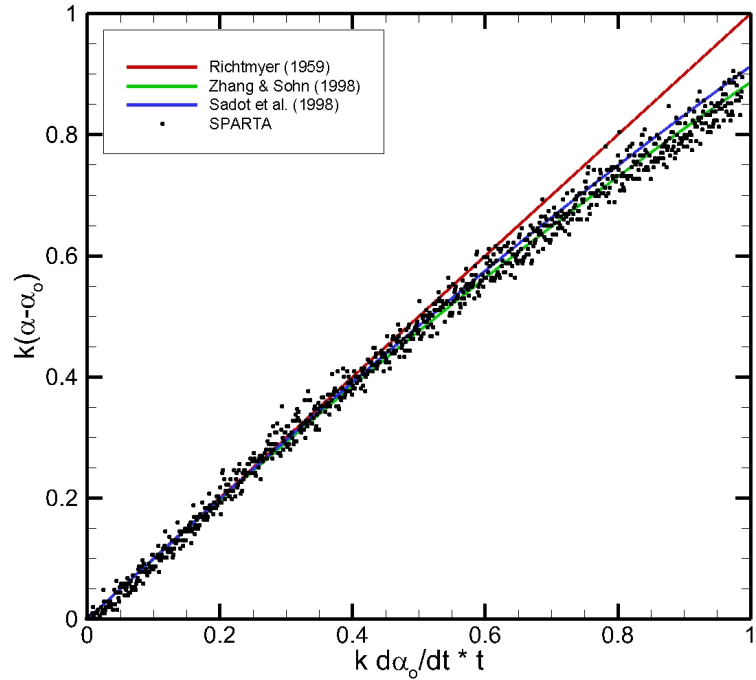
- Different gas pairs give different Atwood numbers in the range 0.33-0.94
- Modest differences are seen over the range examined

# RMI: Effect of Mach Number

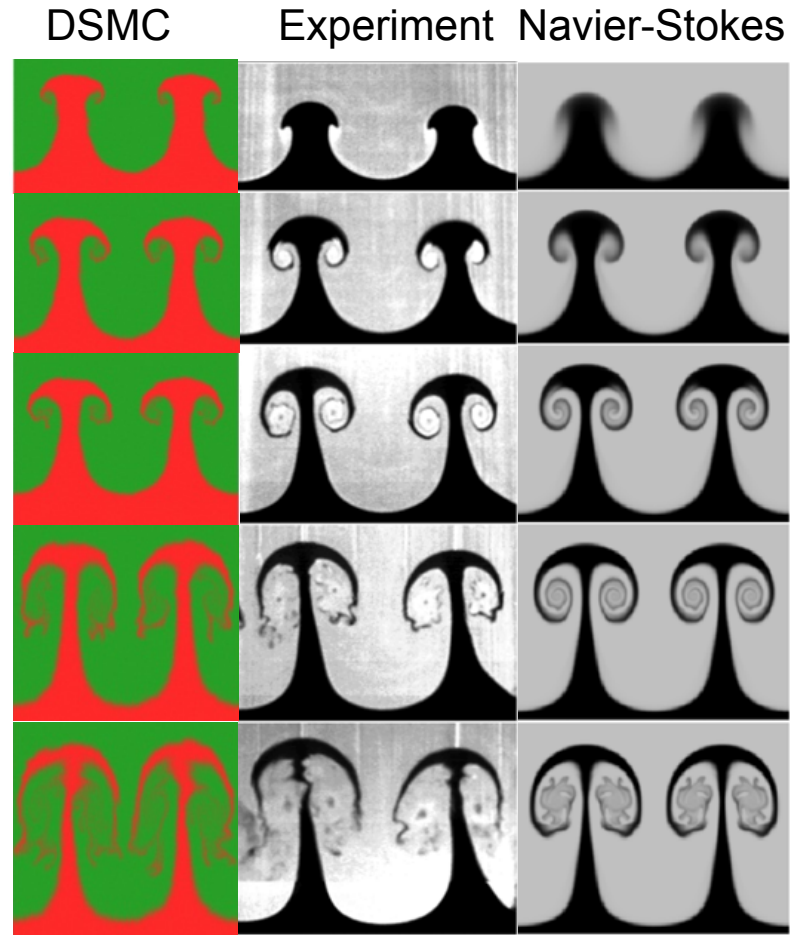


Normalization indicates that Mach number plays a small role  
None of the theoretical models accounts for Mach number

# RMI in Air-SF<sub>6</sub> Mixture: Mach = 1.4 Shock



Non-dimensional amplitude for an initially small amplitude perturbation compared to theoretical/empirical models

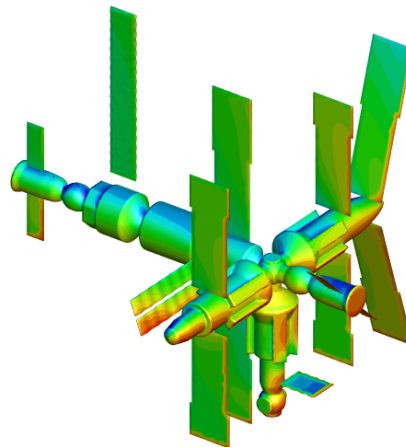
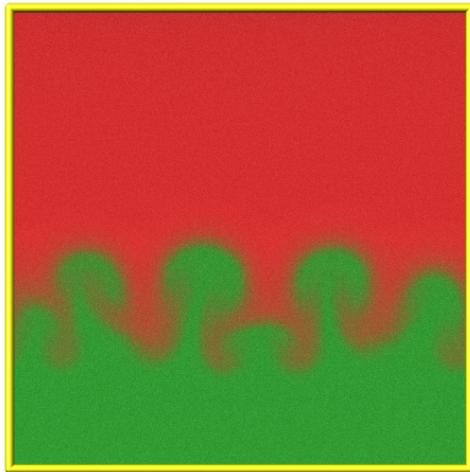
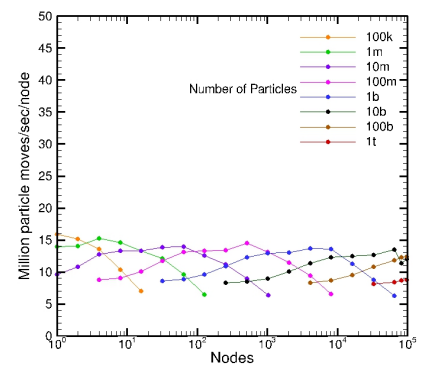
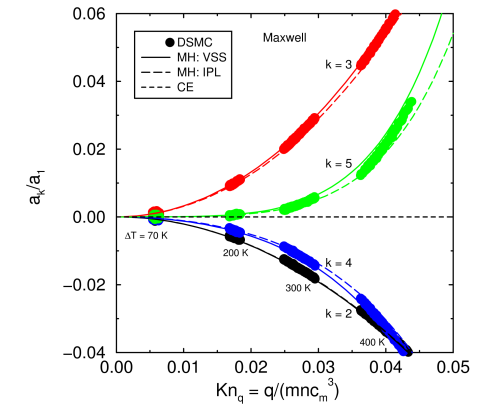
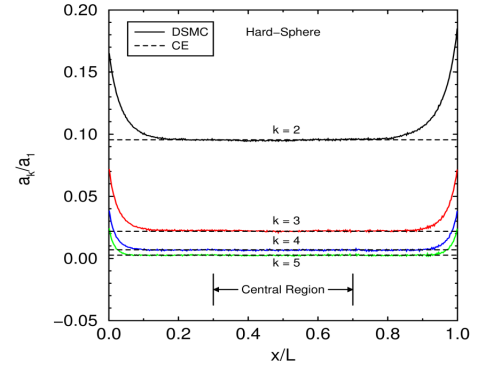


Morgan *et al.* JFM 2012

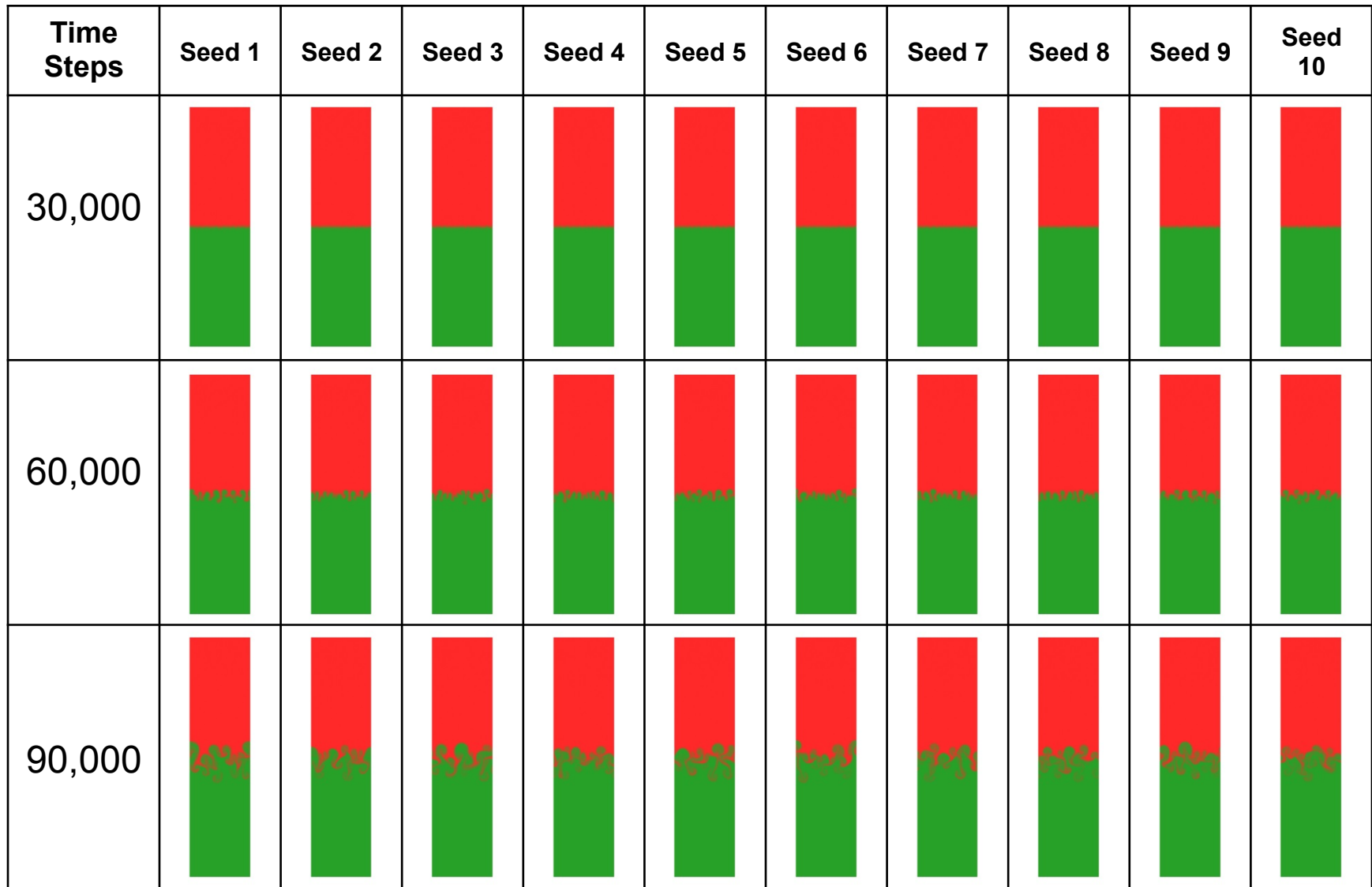
# Conclusions

DSMC yields exquisite agreement with analytical results, where available

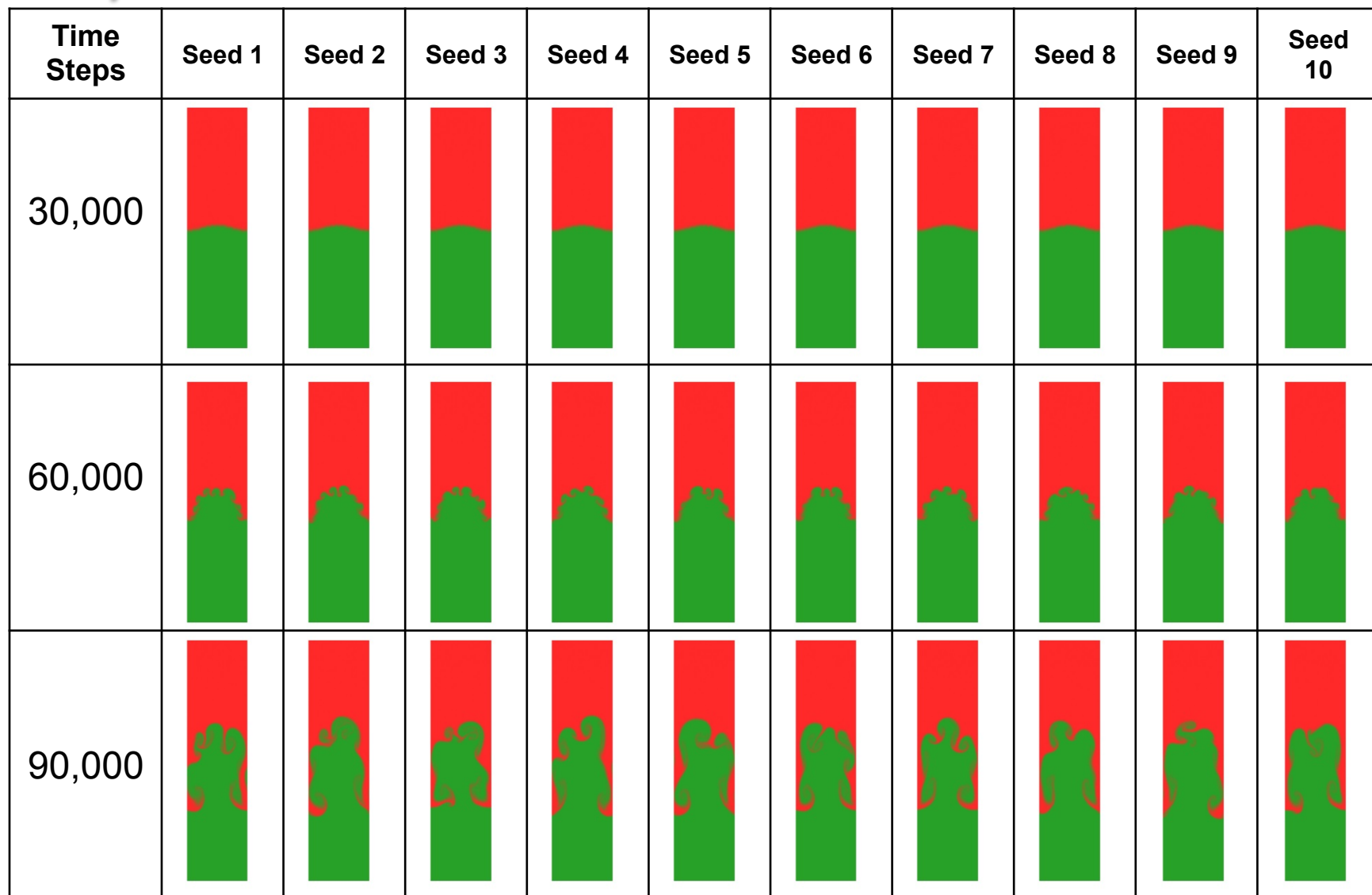
- Chapman-Enskog, Moment-Hierarchy theory
- DSMC scales extremely well & can take full advantage of massively parallel platforms
- Can simulate unprecedented flow regimes
  - Hydrodynamic instabilities, lower altitudes



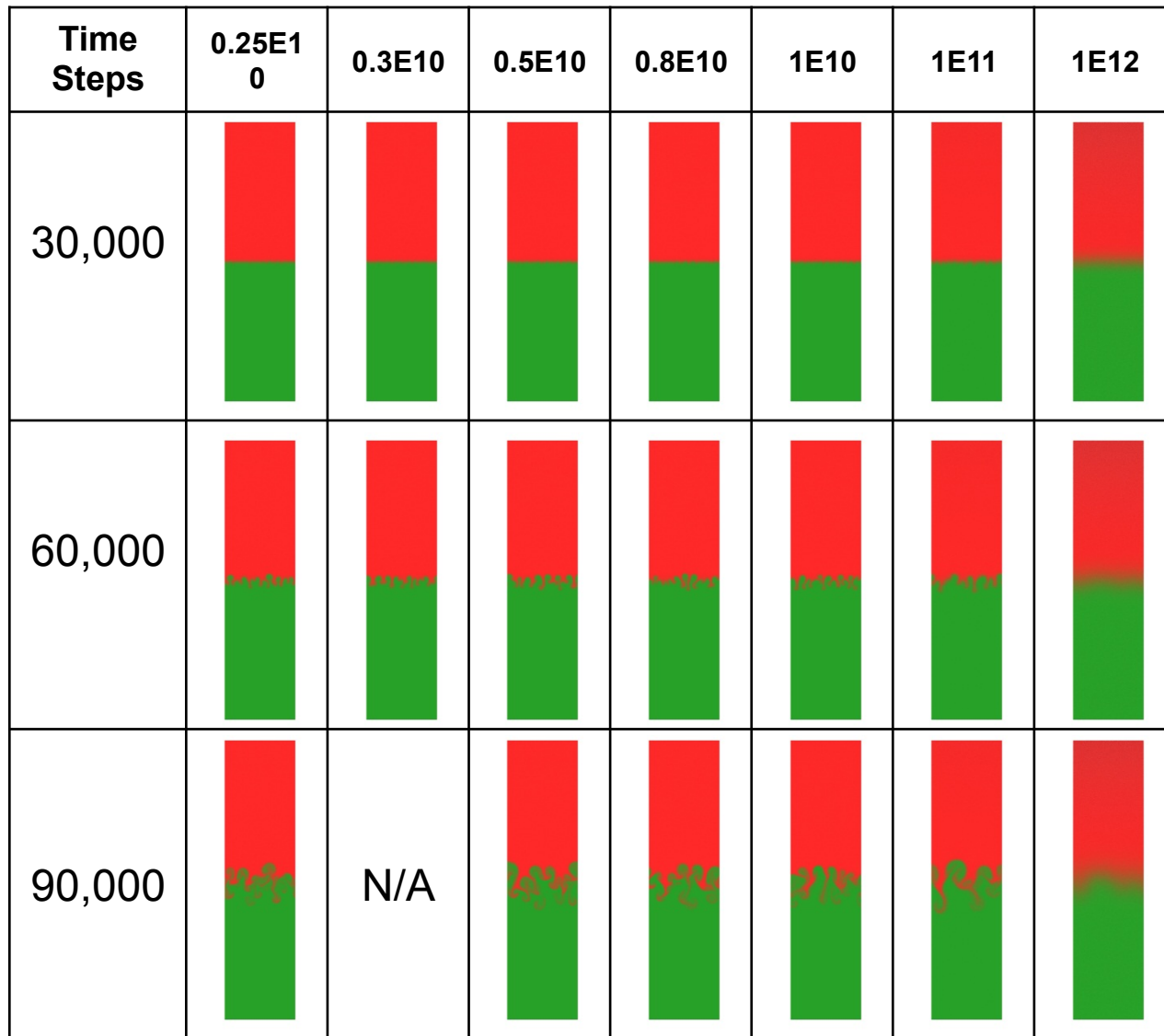
# Seed Comparisons: Hard Sphere Ar/He Flat Interface



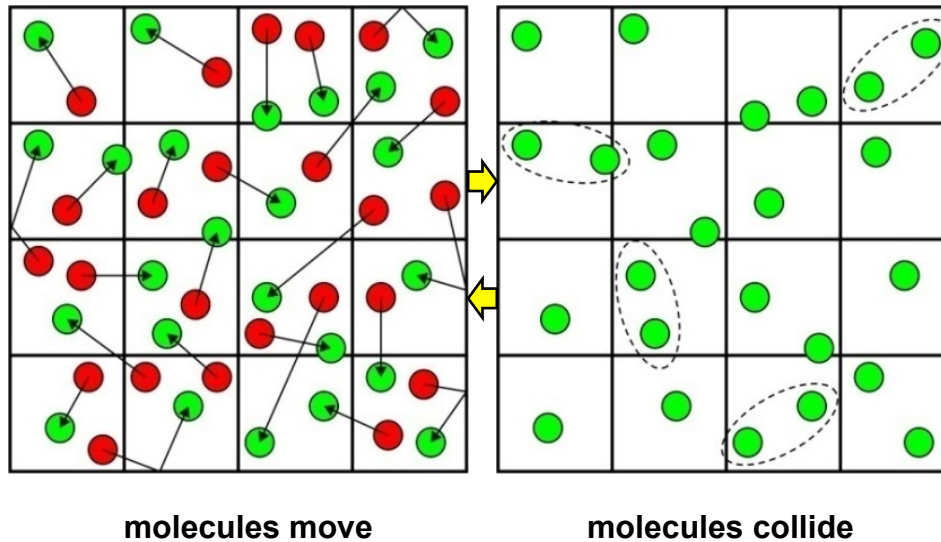
# Seed Comparisons: Hard Sphere Ar/He Perturbed Interface



# Simulation Ratio Comparisons: Ar/He Flat Interface



# DSMC Numerical Error



Four parameters control DSMC error:

*Statistical error (1)*

Samples per cell ( $S_c$ )

*Discretization error (3)*

- Particles per cell ( $N_c$ )
- Cell size ( $\Delta x$ )
- Time step ( $\Delta t$ )

# Statistical and Particle-Number Errors

## Error related to sample size

- Statistical error
- Cell sample size  $S_c = N_c \times N_t$
- $N_c$  = particles per cell;  $N_t$  = time steps

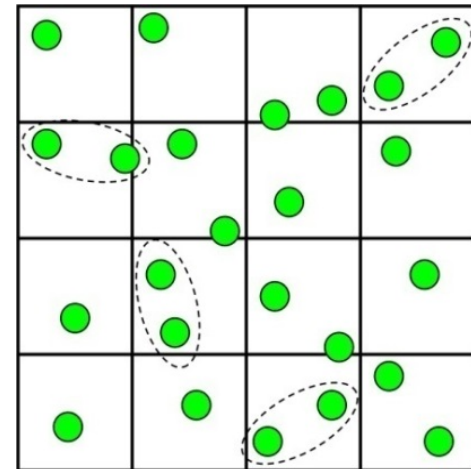
## Strategies for overcoming statistical error

- Use large number of samples
- For steady flows, use time and/or ensemble averaging
- Computational expense  $\sim S_c$

## Error related to local number of particles

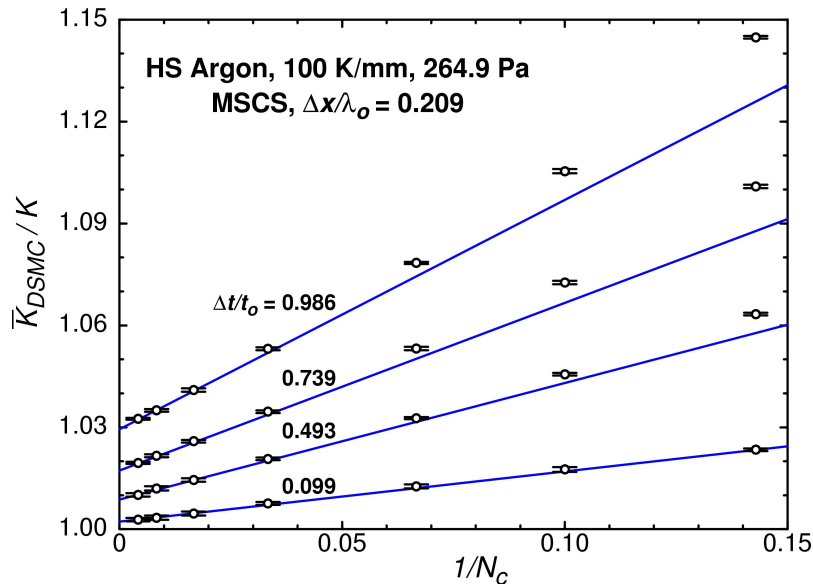
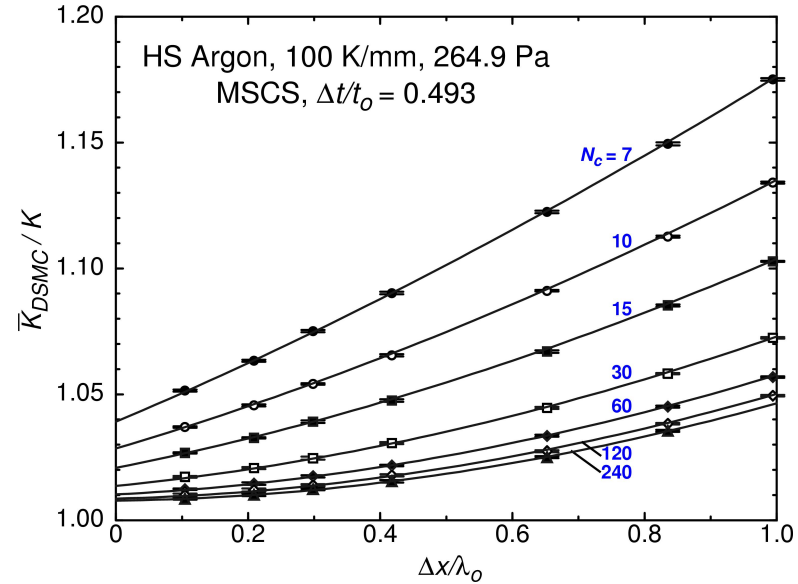
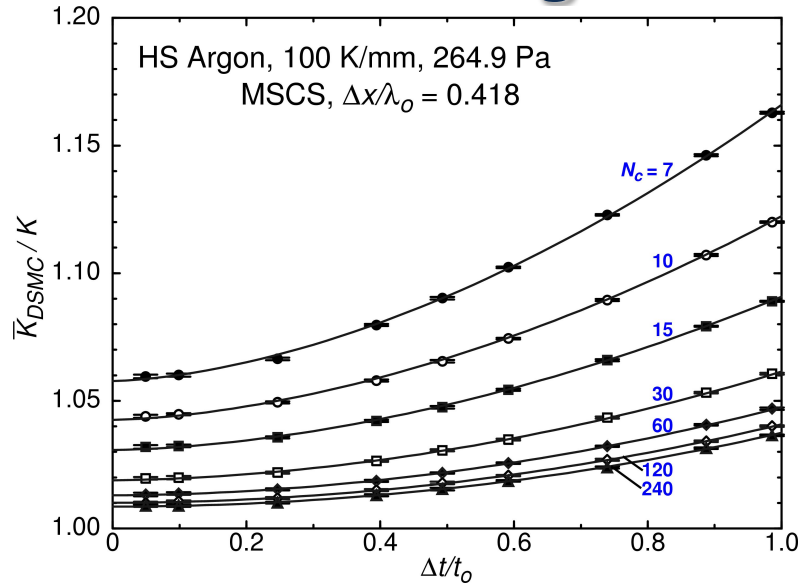
- Error  $\sim 1 / N_c$
- Systematic – persists even as  $S_c \rightarrow \infty$

## Limited number of samples per time step



Not enough particles to capture physics

# DSMC Convergence



- Curves are best fits
- Error bars represent 95% confidence intervals
- Quadratic convergence for  $\Delta x$ ,  $\Delta t$
- **First-order convergence**  $O(1/N_c)$ , as  $N_c \rightarrow \infty$
- Higher-order for long time steps
- For  $N_c = 7$  and  $Dt/t_o = 0.493$ , convergence rate **appears linear** in  $Dx/\lambda_o$

# Functional Form of Error

*Functional form that represents DSMC data*

- Ad hoc series expansion in  $Dx$ ,  $Dt$ , and  $1/N_c$
- Perform least-squares fitting of entire data set

$$\frac{K_{DSMC}}{K} = 1.0000 + 0.0286\Delta\tilde{t}^2 + 0.0411\Delta\tilde{x}^2 - 0.0016\Delta\tilde{x}^3 - 0.023\Delta\tilde{t}^2\Delta\tilde{x}^2 +$$

$$-\frac{0.111}{N_c} + \frac{1}{N_c} \left[ 1.22\Delta\tilde{x} - 0.26\Delta\tilde{x}^2 + 0.97\Delta\tilde{t}^{3/2} + \dots \right] + 0.95\frac{\Delta\tilde{t}^2}{N_c^2} + \dots$$

*Cross terms show convergence behavior is complex*

Rader D. J., Gallis M. A., Torczynski J. R., Wagner W., "DSMC Convergence Behavior of the Hard-Sphere-Gas Thermal Conductivity for Fourier Heat Flow", *Phys. Fluids*, 18, 077102, 2006.

# DSMC Numerical Error

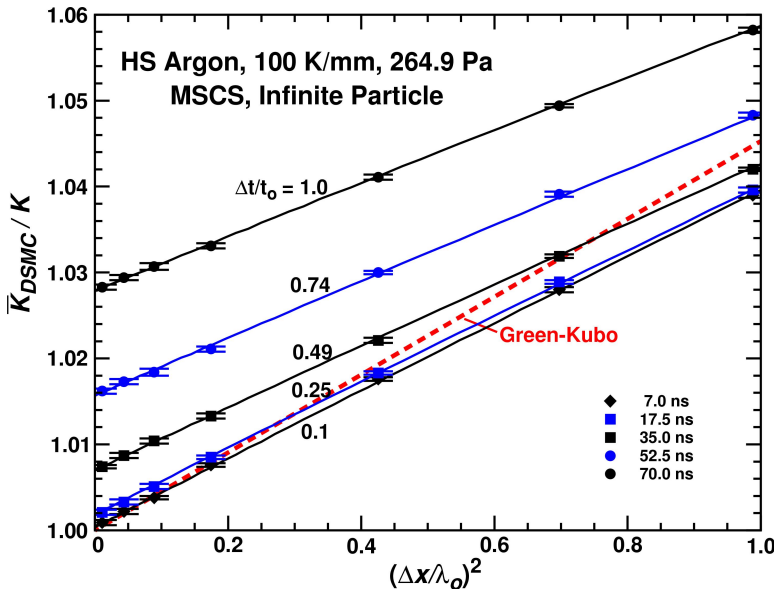
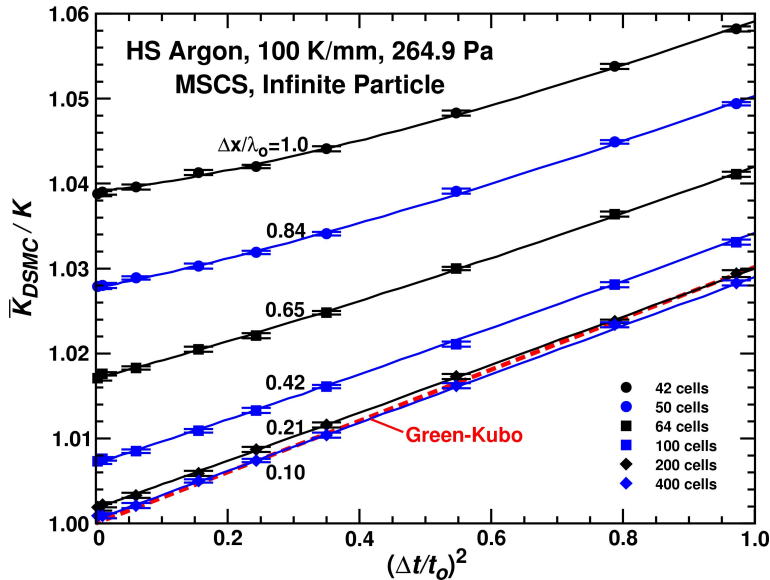
## Traditional DSMC rule-of-thumb guidelines:

- Take enough samples to drive statistical error down to “acceptable” level
- Keep time step smaller than  $\sim 1/4$  mean collision time
- Keep cell size smaller than  $\sim 1/3$  mean free path
- Use a minimum of  $\sim 20$  particles per cell

*These guidelines give 2% error, which is similar to the uncertainty in measured transport properties for most gases*

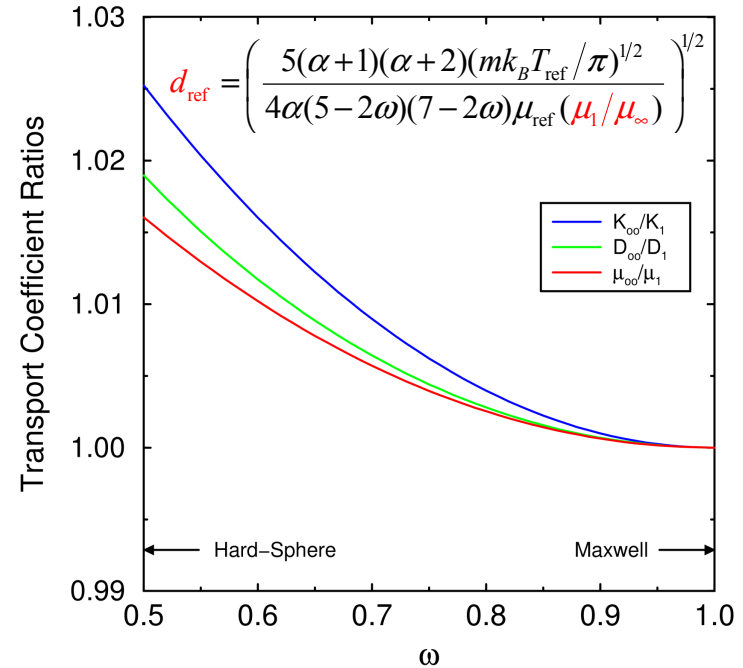
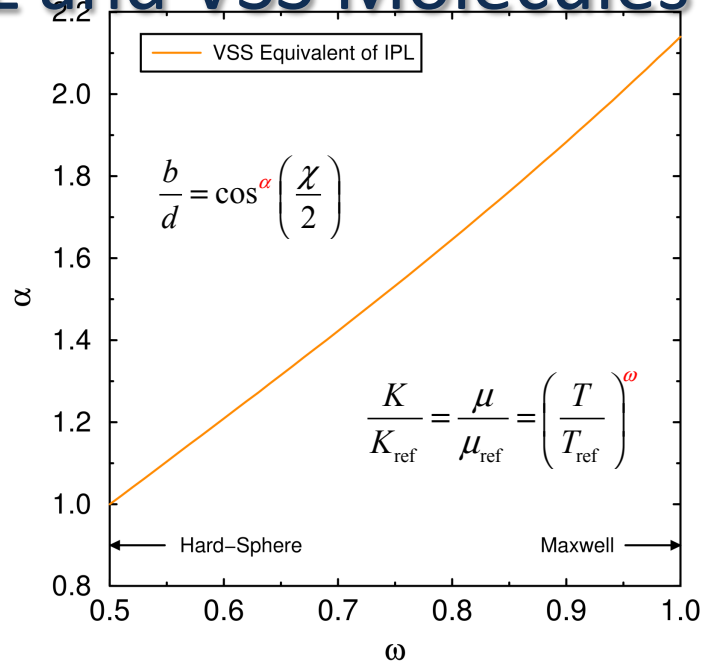
- DSMC is subject to the same constraints as other numerical methods.
- DSMC is correct to the limit of vanishing discretization.

# Infinite-Particle Convergence



- Finite-particle error removed: values “extrapolated” to  $N_c \rightarrow \infty$
- 63 extrapolated data points
- Error bars: fitting uncertainty
- Quadratic convergence in time step and cell size
- Qualitative agreement with *Green-Kubo* theory, but slopes are different
- Lines are best fits of data

# IPL and VSS Molecules



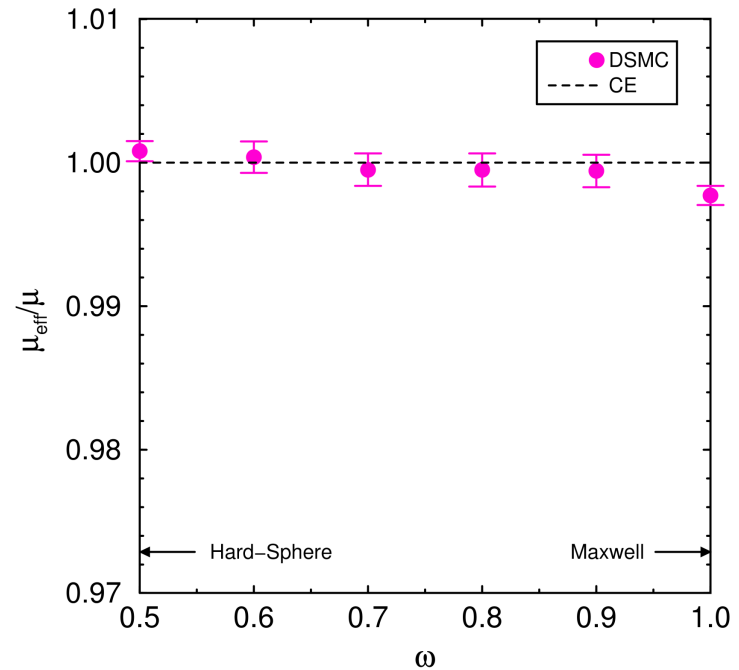
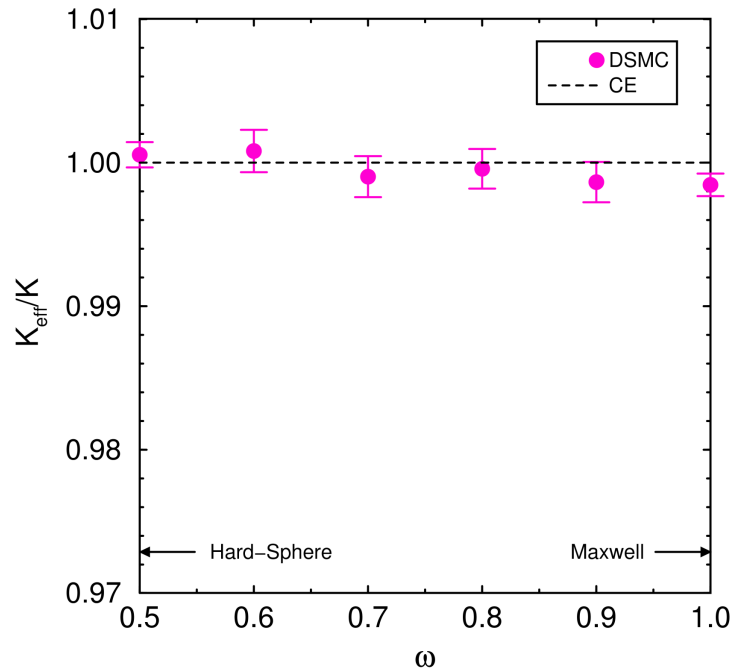
## Best VSS $w$ , $a$ to match IPL $w$ by equating diffusivities

- Identical match only for hard-sphere
- VSS-Maxwell  $\neq$  IPL-Maxwell (they are very similar)

## Infinite-approximation CE changes $K$ and $m$ by $O(0.03)$

- Affects reference diameter  $d_{\text{ref}}$  very slightly

# Transport Coefficients

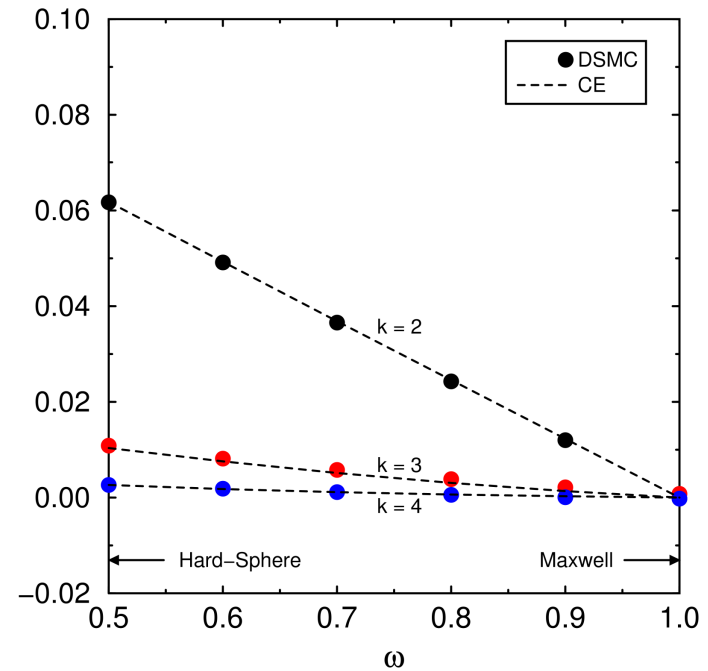
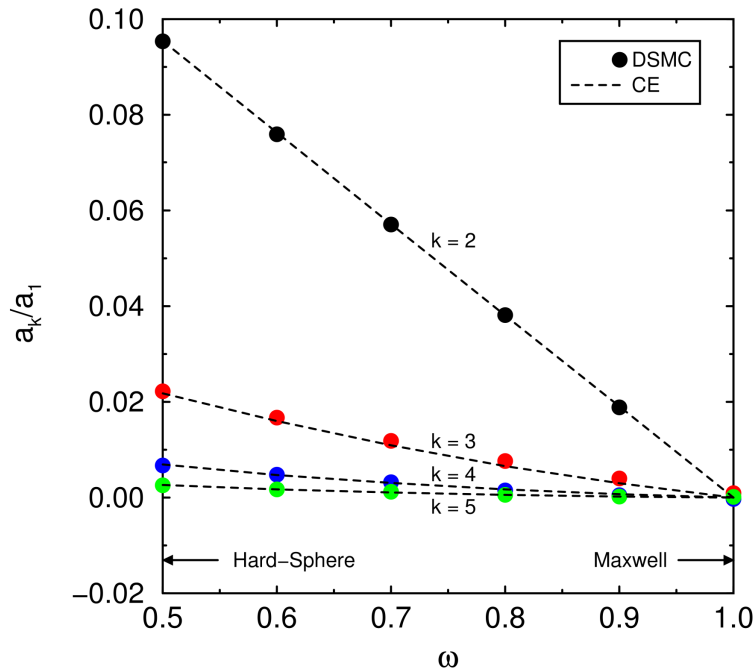


## Thermal conductivity and viscosity for IPL molecules

- Intermolecular force: hard-sphere through Maxwell
- Stochastic and discretization errors:  $\pm 0.002$  each
- CE infinite-to-first-approximation difference:  $O(0.03)$

Excellent agreement between DSMC and CE

# Sonine Coefficients



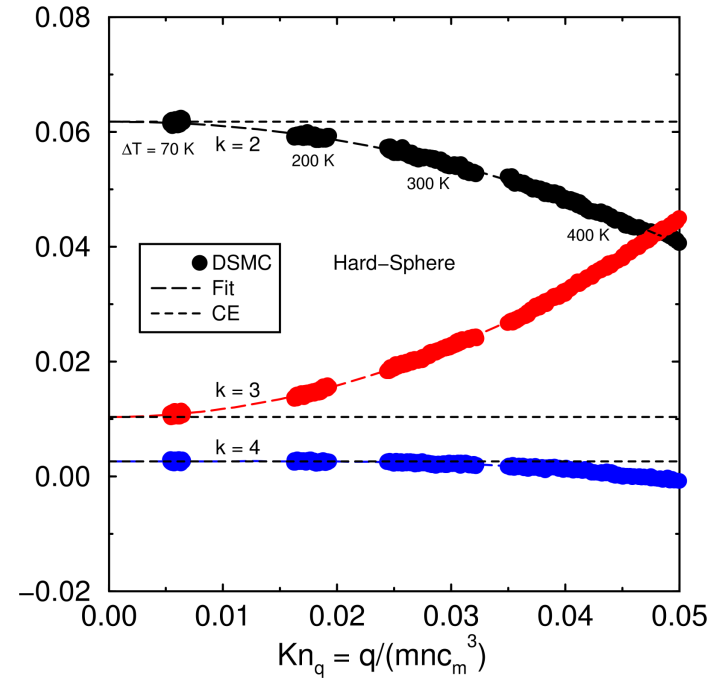
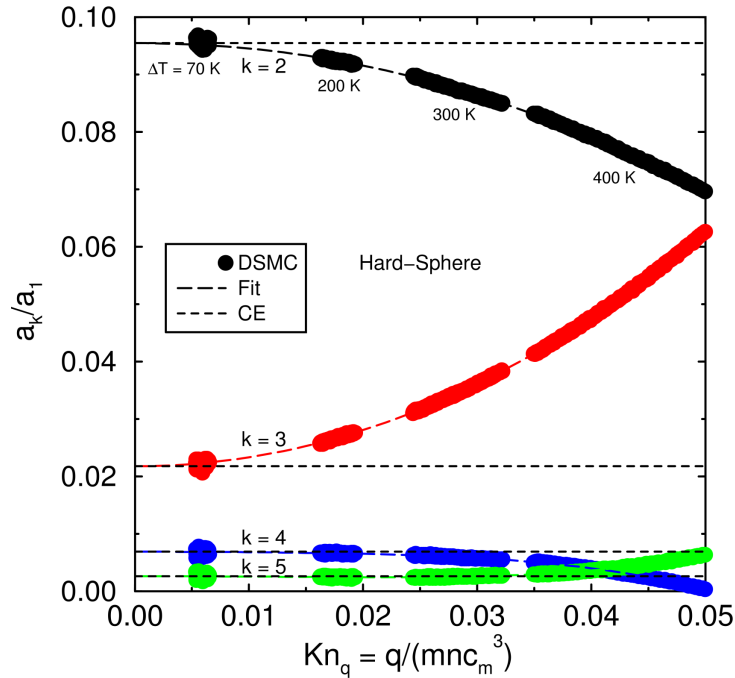
## Sonine coefficients $a_k/a_1$ and $b_k/b_1$ for IPL molecules

- Intermolecular force: hard-sphere through Maxwell
- Stochastic, discretization errors: smaller than symbols

## Good agreement between DSMC and CE

- Higher- $k$  coefficients have similar agreement
- Slight difference for  $k=3$ ,  $Kn_q$  not small enough

# Hard-Sphere Sonine Coefficients

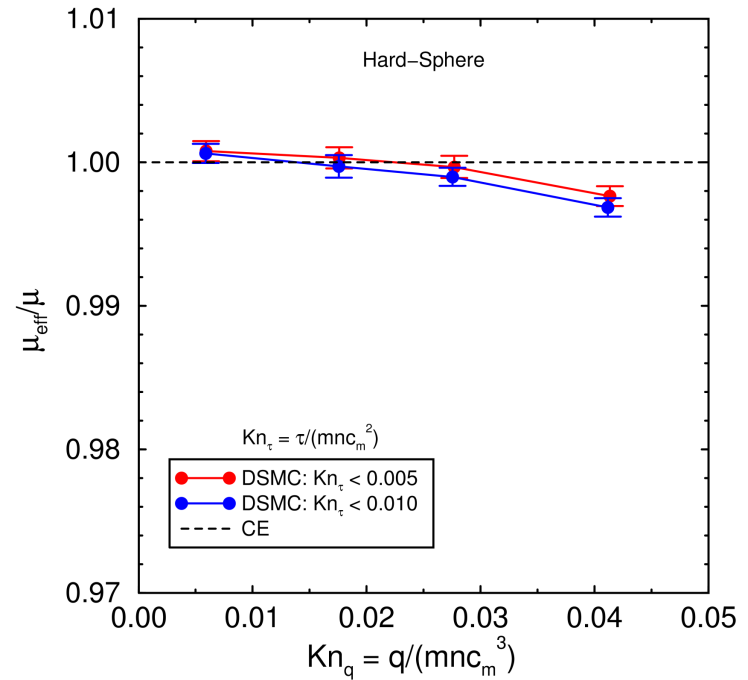
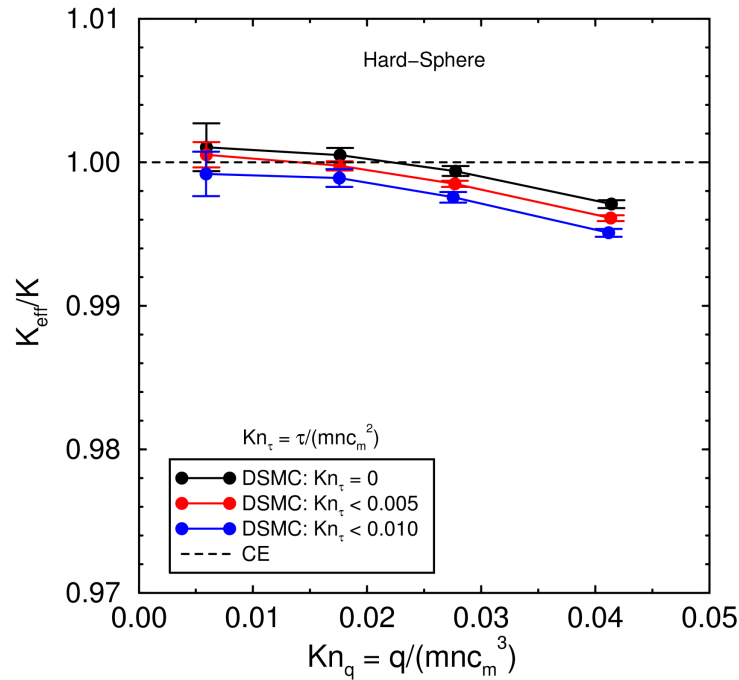


Hard-sphere normal solutions for  $a_k/a_1$  and  $b_k/b_1$

DSMC hard-sphere and VSS-Maxwell have same trends

- Four DSMC simulations at same conditions as Maxwell
- No exact results available: MH does not apply
- Even- $k$  terms decrease, odd- $k$  terms increase

# Hard-Sphere Normal Transport Coefficients

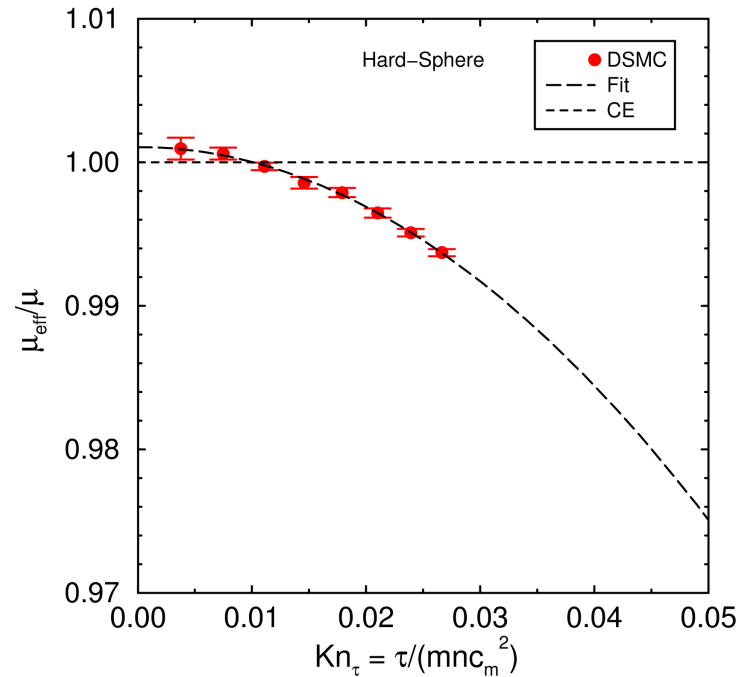
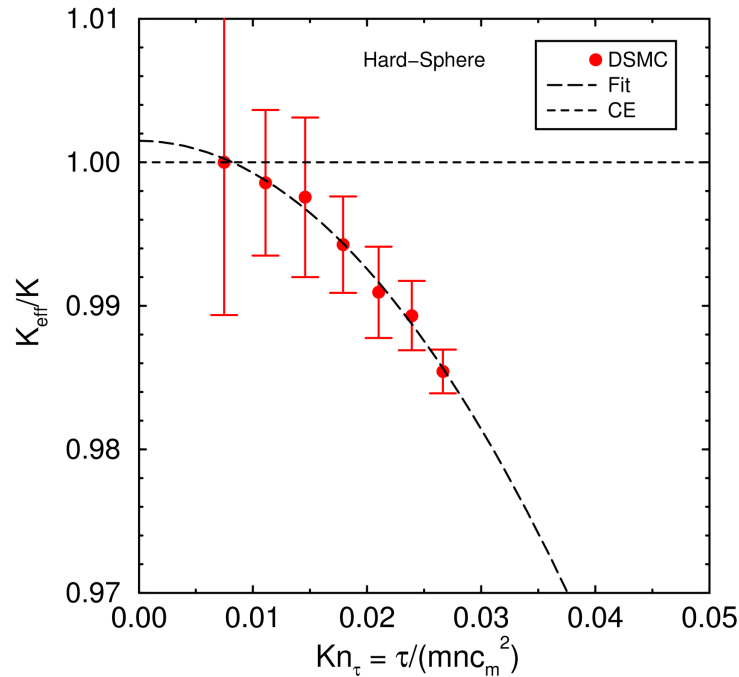


## DSMC hard-sphere normal solution for K and $\mu$

- No theoretical results available: MH does not apply
- DSMC values decrease slightly with  $Kn_q$
- Difference apparently greater than discretization error

Hard-sphere gas: “flux-insulating” and “flux-thinning”

# Hard-Sphere Normal Transport Coefficients

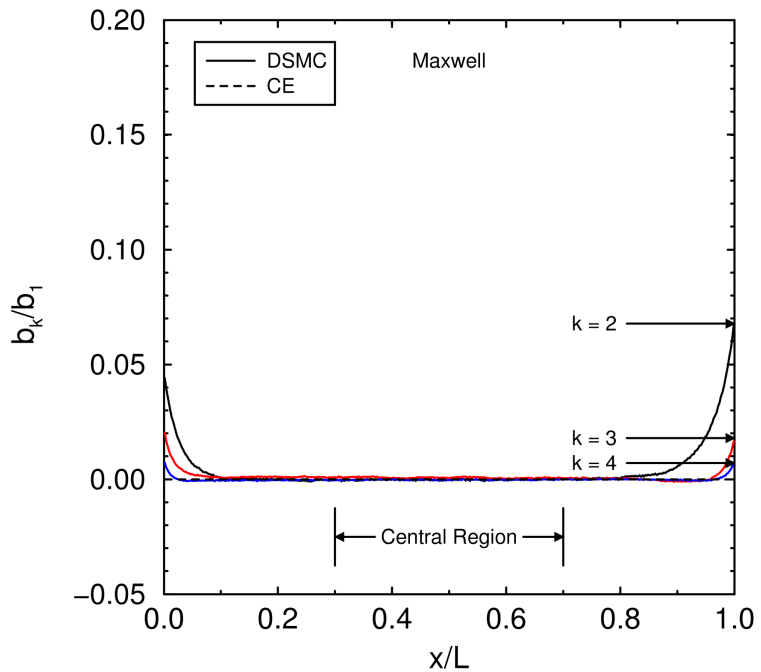
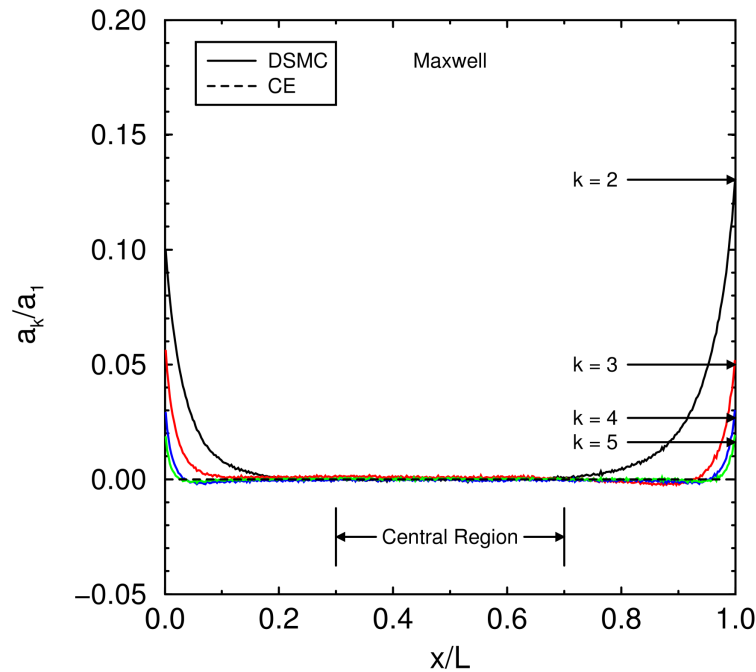


## DSMC hard-sphere normal solution for K and $\mu$

- Finite  $Kn_{\tau}$  (shear stress), low  $Kn_q$  (heat flux)
- No theoretical results available: MH does not apply
- DSMC values decrease with  $Kn_{\tau}$  (like Maxwell)

Hard-sphere gas: “shear-insulating” and “shear-thinning”

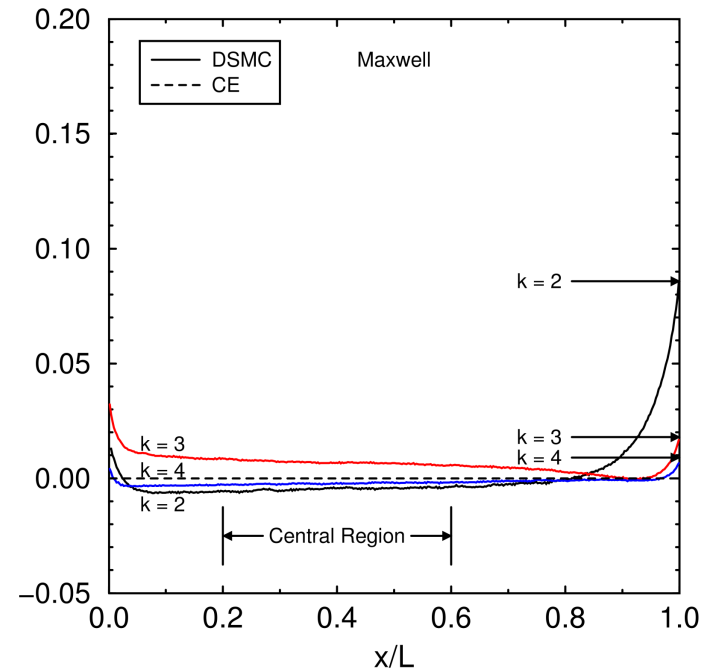
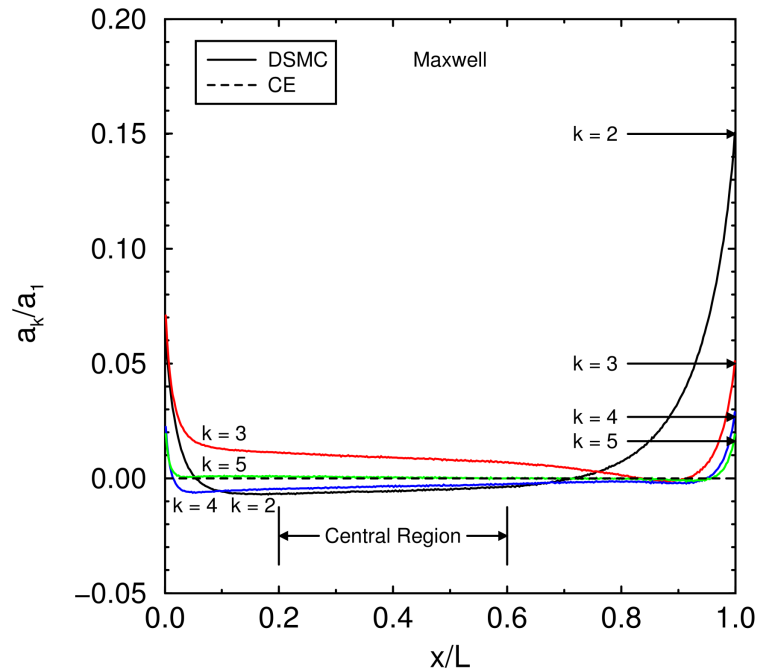
# Maxwell Sonine-Coefficient Profiles



## DSMC and CE Maxwell coefficients $a_k/a_1$ and $b_k/b_1$

- Low heat flux, low shear stress:  $Kn_q = 0.006$ ,  $Kn_\tau = 0.003$
- Good agreement in central region: normal solution
- Knudsen layers easily observed:  $\sim 10\%$  of domain

# Maxwell Sonine-Coefficient Profiles



Finite heat flux, low shear stress:  $Kn_q \sim 0.017$ ,  $Kn_\tau = 0.003$

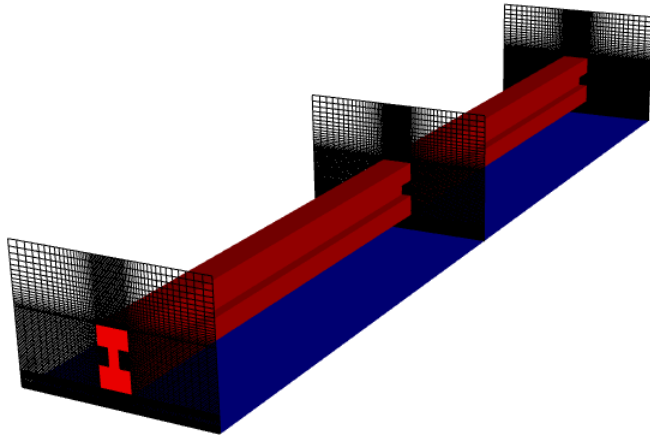
Maxwell Sonine-polynomial coefficients  $a_k/a_1$ ,  $b_k/b_1$

- CE and DSMC differ in central region:  $Kn_q$  not small
- Normal solution is non-uniform:  $Kn_q \sim T^{-1/2}$  and  $T = T[x]$

Plot DSMC values vs.  $Kn_q$  from central region

# Continuum but Non-equilibrium in MEMS Heated Microbeam Near Substrate

Non-equilibrium may be observed in continuum conditions



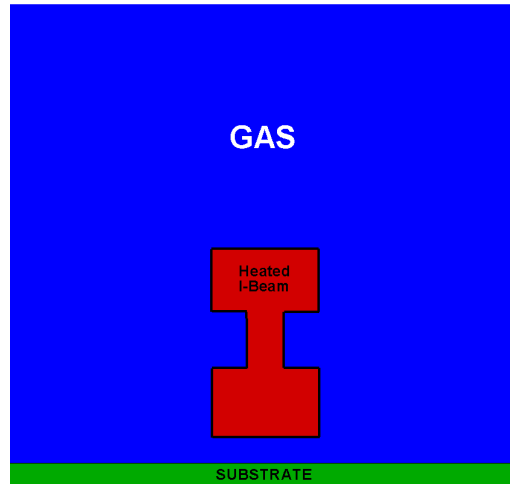
## Solid regions: silicon

- Geometry: 2-micron gap
- Beam temperature:  $\sim 900$  K
- Substrate temperature:  $\sim 300$  K

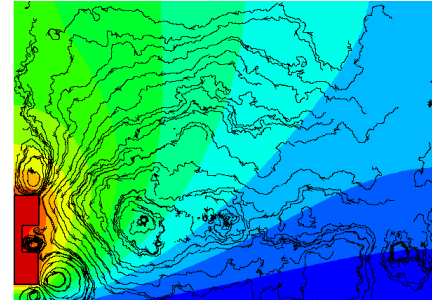
## Gas region: nitrogen

- Pressure: atmospheric
- Initial temperature:  $\sim 300$  K
- **Mean free path: 70 nm**

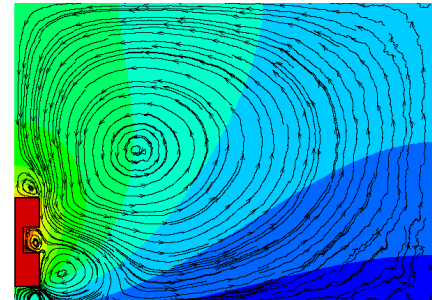
# Heated Microbeam Makes Gas Move



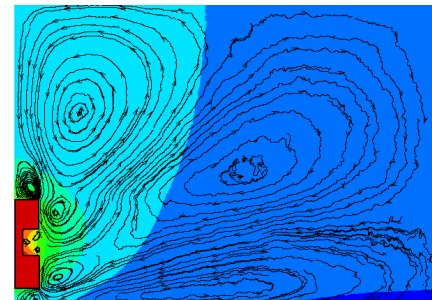
1 atm  
~0.1 m/s



0.1 atm  
~2 m/s



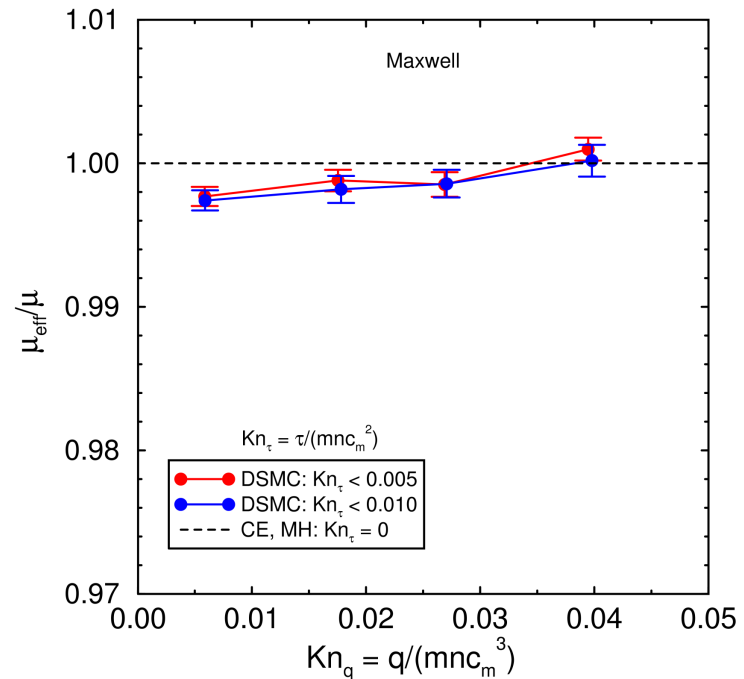
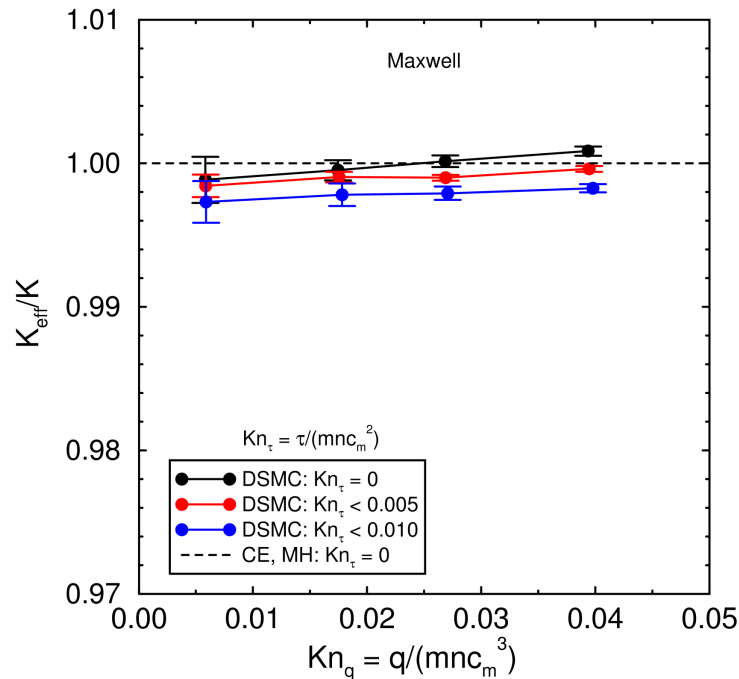
0.01 atm  
~1 m/s



## DSMC microbeam simulations

- **Steady gas motion** is induced by temperature differences  
*Not buoyancy, not transient*
- **Noncontinuum effects** cause motion  
*Not seen in NSSJ simulations*

# Maxwell Normal Transport Coefficients



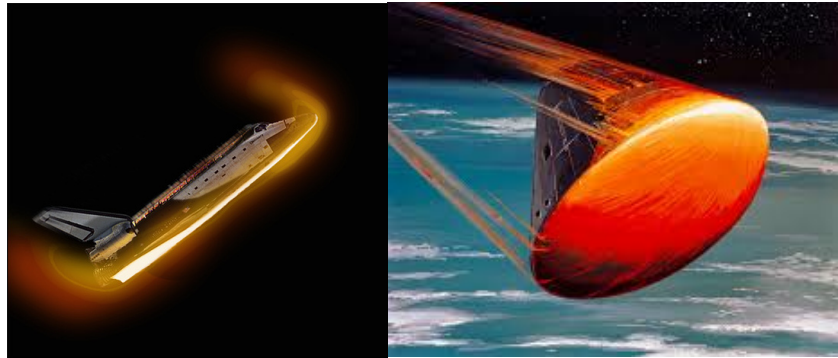
## DSMC and MH Maxwell normal solutions for $K$ and $\mu$

- DSMC profiles look like low- $Kn_q$  profiles
- MH values for  $Kn_\tau = 0$  are independent of  $Kn_q$
- DSMC values approach MH values as  $Kn_\tau \rightarrow 0$
- DSMC values increase very slightly with  $Kn_q$

Agree to within DSMC discretization error

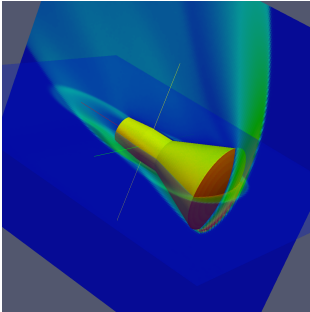
# Rarefied Gas Dynamics Regime

- High Mach number flight is more easily achieved in rarefied conditions (low-density, low-friction)
- When low-density/non-continuum conditions prevail, flows are out of thermodynamic equilibrium
  - Not enough molecular collisions to maintain LTE
- This flight regime results in high temperatures (more than 10,000 K), chemically reacting, ionizing, radiating flows pushing the flow further away from equilibrium
- In the rarefied, hypersonic regime the NS equations are usually not applicable

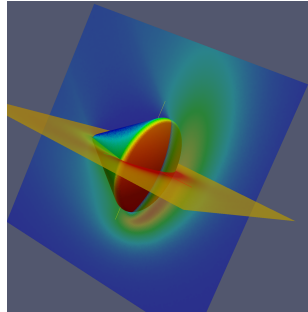


# Diffusing energy through re-entry

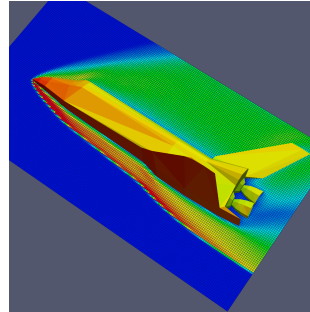
Gemini  
1961-1966



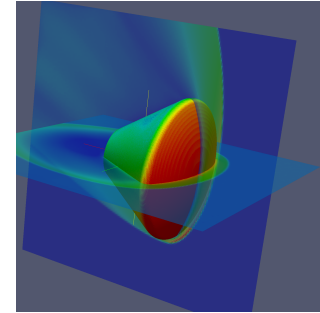
Apollo  
1963-1972



Space Shuttle  
1981-2011



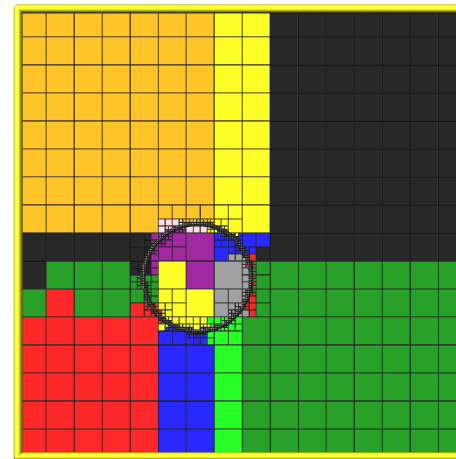
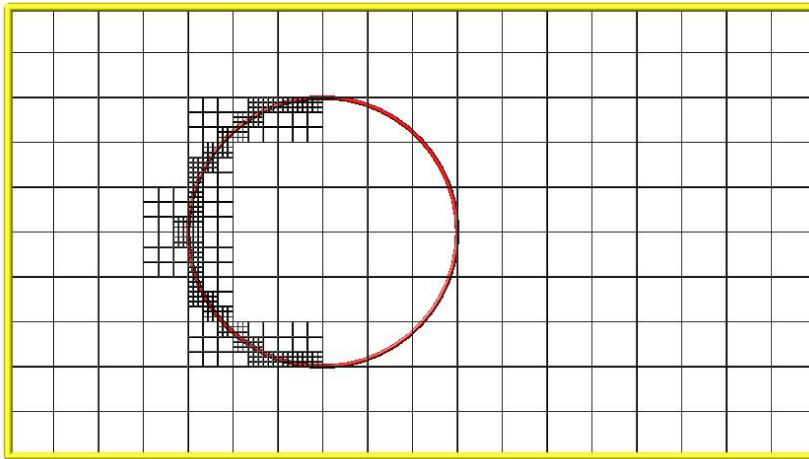
Orion  
2014-?



- Atmospheric entry system must provide **controlled dissipation of kinetic and potential energy** of the vehicle.
- Dynamic and thermal loads **must be kept with certain range**

# Adaptive Gridding

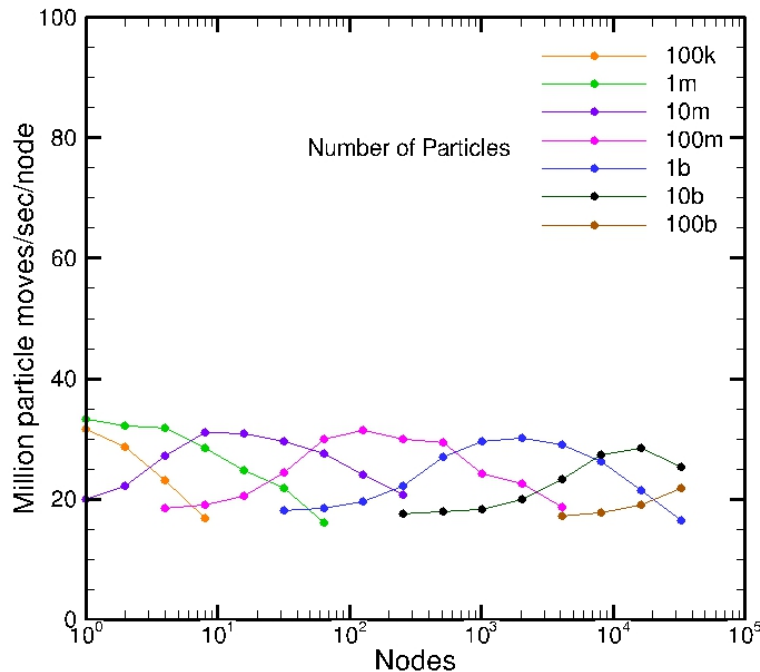
- Create/adapt grid in situ, rather than pre-process & read in
- Examples: Generate around surface to user-specified resolution, adapt grid based on flow properties
- Algorithms should be efficient if they require only local communications



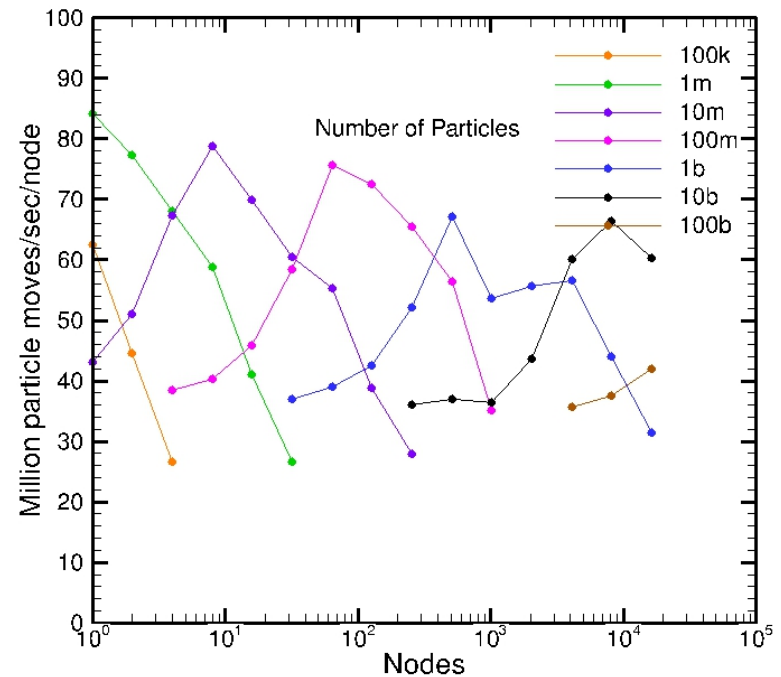
- Another setup task: label cells as outside/inside
- Simple if pre-processing, in situ easier for large problems

# SPARTA Benchmarking (FM)

16 cores/node, 1 task/core



16 cores/node, 4 tasks/core



- Free-molecular (FM) calculations stress-test for communications
- 2x speedup compared to collisional

# Aiming for MPI+X via Kokkos

- What is Kokkos:
  - Programming model in development at Sandia
  - C++ template library
  - Open-source
  - Stand-alone
- **Goal: write application kernels only once, and run them efficiently on a wide variety of hardware platforms**
- Two major components:
  - Data access abstraction via Kokkos arrays optimal layout & access pattern for each device: GPU, Xeon Phi, etc.
  - Parallel dispatch of small chunks of work auto-mapped onto back-end languages: CUDA, OpenMP, etc.

# The Mars Reconnaissance Orbiter mission

- Launch Date : August 12 2005
- Mars Orbit insertion : March 10 2006
- Final Orbit reached : August 30 2006

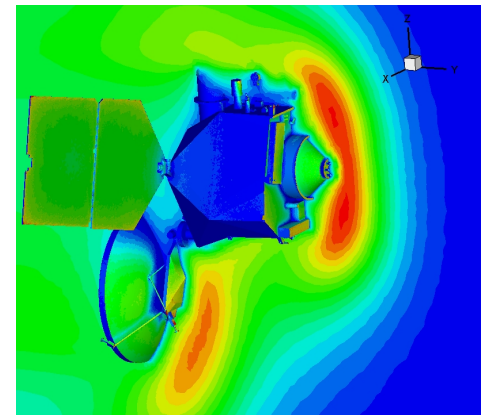
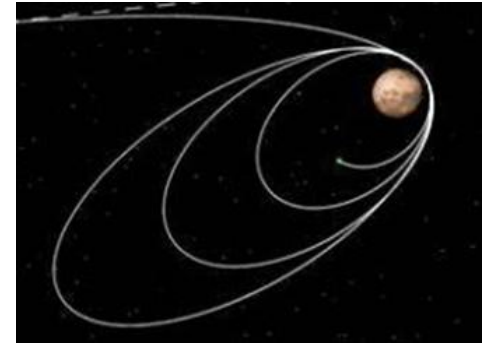


# Scope of MRO DSMC analysis

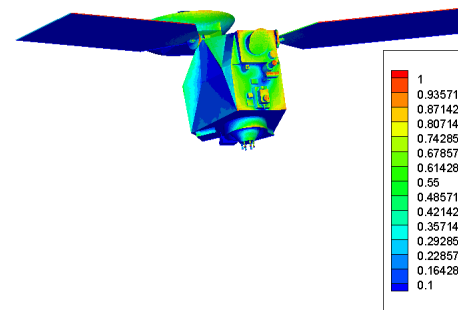
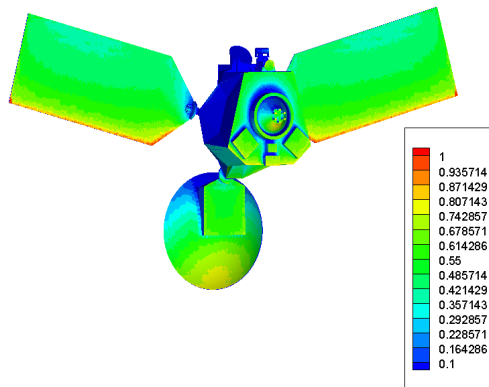
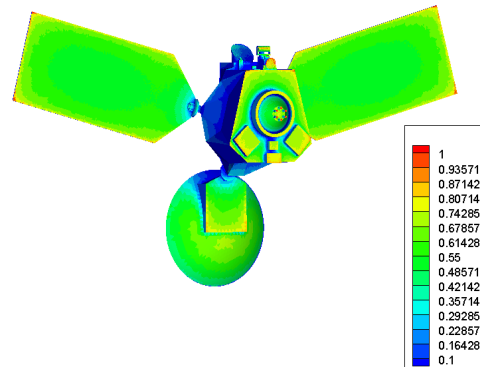
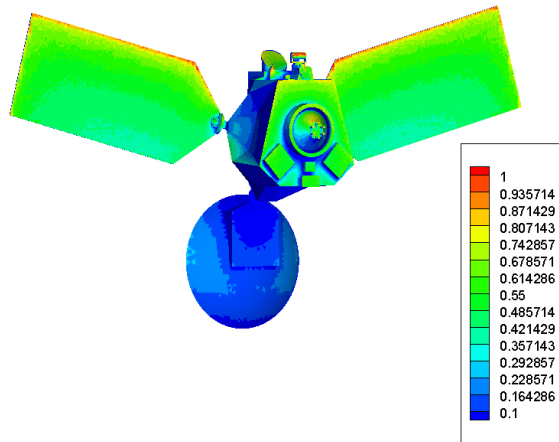
- Aerobraking was used to reduce fuel requirements during orbit placing maneuvers
- From a highly elliptic orbit the spacecraft was brought down to a near circular science orbit (255-320 km)
- During the maneuvers the vehicle had to be aerodynamically stable and the heat load could not exceed maximum values

Scope of the following calculations:

- Determine the heat transfer to the vehicle for a number of angles of attack at nominal aerobraking altitude and velocity
- Determine drag for a number of altitudes

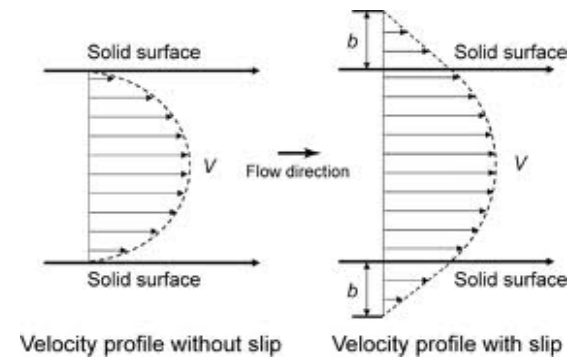


# Heat flux for nominal aerobraking conditions

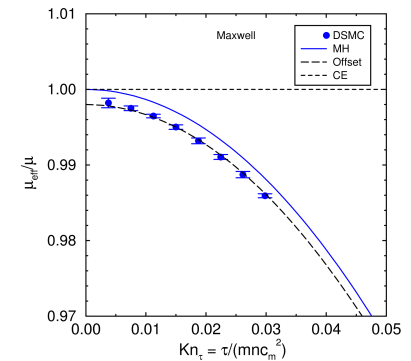


# Could the N-S Equations be extended ?

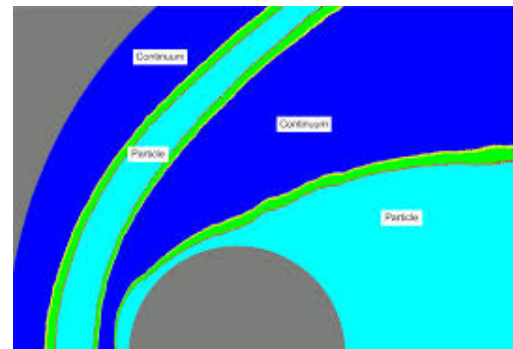
- Velocity-slip and Temperature jump



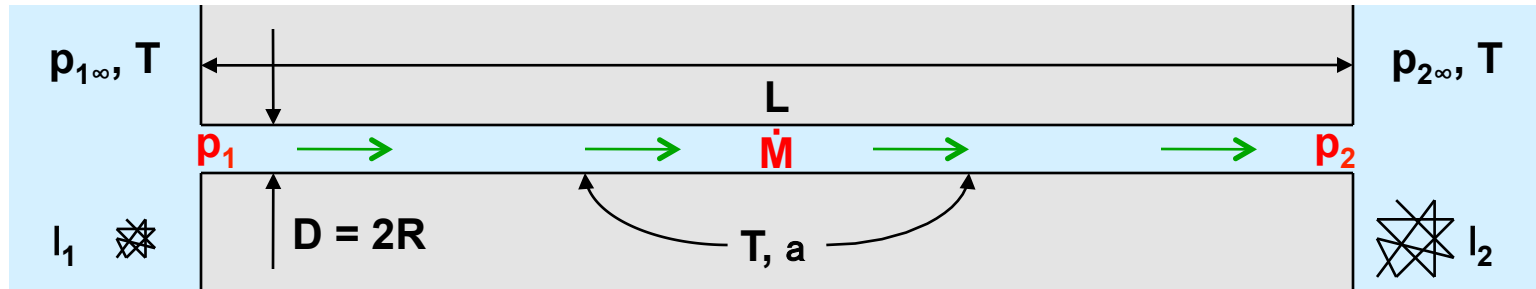
- Modified transport coefficients (viscosity, conductivity, diffusivity)



- Hybrid Schemes (NS-DSMC)



# Gas Flow in a Microscale Tube



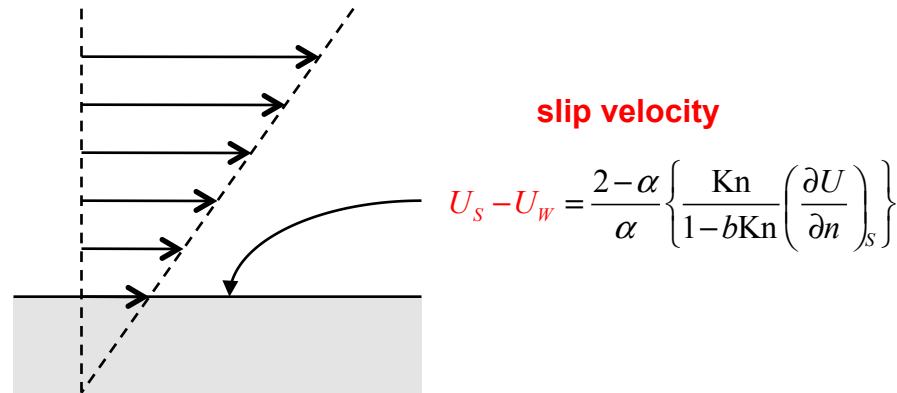
## Investigate steady isothermal gas flow in microscale tube

- Tube is long and thin ( $L \gg D$ ) with circular cross section
- Tube joins gas reservoirs at different pressures ( $p_{1\infty} \geq p_{2\infty}$ )
- Tube and reservoirs have same temperature ( $T$ )
- Molecules partially accommodate ( $a \leq 1$ ) when reflecting
- Flow speed  $\ll$  molecule speed, laminar, no turbulence

## Determine the mass flow rate and the pressure profile

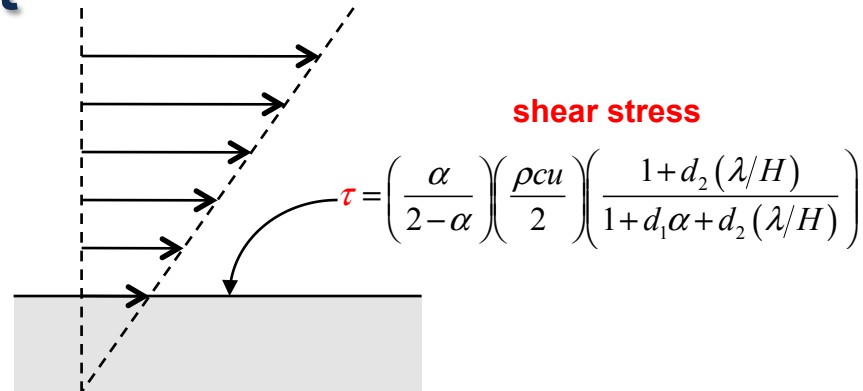
- General physics-based closed-form expressions
- Free-molecular to continuum (arbitrary mean free path  $l$ )
- Theory and molecular-gas-dynamics simulations

# Extending the Navier-Stokes equations



- Mean free path at STP is 0.06 mm, large enough to matter
- Silicon channels of <math><10 \mu\text{m}</math> height and <math>>10 \mu\text{m}</math> length
- Accurate mass flow rate needs accurate velocity profile
- Slip boundary condition improves prediction by Navier-Stokes equations

# Boundary Conditions for Accurate Transport



- Transport rates are of primary importance
  - Mass, momentum, energy
- Fields are of secondary importance
  - Concentration, velocity, temperature

## Construct boundary conditions to give accurate transport

- When used with Navier-Stokes equations
- For free-molecular, transition, slip, continuum

## Resulting fields are only qualitatively correct

- Fields are accurate in continuum limit

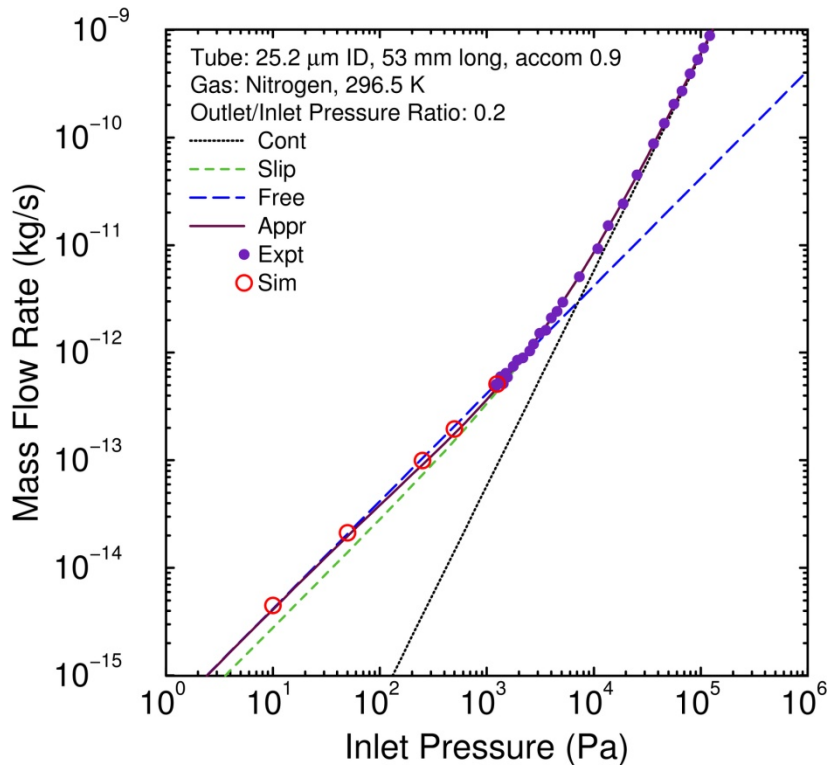
# Mass Flow Rate Has Correct Limits

<b>Approximate Closed-Form Expression</b> $\dot{M} = \dot{M}_C \left( 1 + \frac{8p_\lambda}{p_m} \varpi[p_1, p_2] \right), \quad \varpi[p_A, p_B] = \frac{2-\alpha}{\alpha} \left\{ 1 + b_1\alpha + (\epsilon b_0 - 1 - b_1\alpha) \frac{b_2 p_\lambda}{p_A - p_B} \ln \left[ \frac{p_A + b_2 p_\lambda}{p_B + b_2 p_\lambda} \right] \right\}$		
<b>Continuum</b> $\dot{M}_C = \frac{D^4 p_m (p_1 - p_2)}{16\mu c^2 L}$	<b>Slip</b> $\dot{M}_S = \dot{M}_C \left( 1 + \frac{8p_\lambda}{p_m} \varpi_S \right), \quad \varpi_S = \frac{2-\alpha}{\alpha} (1 + b_1\alpha)$	<b>Free-Molecular</b> $\dot{M}_F = \dot{M}_C \left( \frac{8p_\lambda}{p_m} \varpi_F \right), \quad \varpi_F = \frac{2-\alpha}{\alpha} \epsilon b_0$
<b>Continuum Orifice</b> $\dot{M}_{OC} = \frac{R^3 \rho_{m\infty}}{3\mu} (p_{1\infty} - p_{2\infty})$	<b>Free-Molecular Orifice</b> $\dot{M}_{OF} = \pi R^2 \frac{mc}{4} (n_{1\infty} - n_{2\infty})$	<b>Free-Molecular Short Tube</b> $\dot{M}_{TF} = \dot{M}_{OF} / (1 + (\alpha L/D)), \quad \alpha L/D \ll 1$

## Expression reproduces known limits correctly

Continuum	Not affected by $\epsilon$ , $b_0$ , $b_1$ , $b_2$
Slip	Determined by $b_1$
Free-Molecular	Determined by $\epsilon$ , $b_0$
Orifice/Short-Tube	Determined by $\epsilon$ , $b_0$

# Ewart et al. (2006) Tube Experiments



## Tube Mass Flow Rate

$$\dot{M} = \dot{M}_C \left( 1 + \frac{8p_\lambda}{p_m} \varpi[p_1, p_2] \right), \quad \dot{M}_C = \frac{D^4}{16} \frac{p_m (p_1 - p_2)}{\mu c^2 L}$$

$$\varpi[p_A, p_B] = \frac{2 - \alpha}{\alpha} \left\{ 1 + b_1 \alpha + (\varepsilon b_0 - 1 - b_1 \alpha) \frac{b_2 p_\lambda}{p_A - p_B} \ln \left[ \frac{p_A + b_2 p_\lambda}{p_B + b_2 p_\lambda} \right] \right\}$$

$$\rho = \frac{mp}{k_B T}, \quad \mu = \mu[T], \quad c = \sqrt{\frac{8k_B T}{\pi m}}, \quad \lambda = \frac{2\mu}{\rho c}, \quad p_\lambda = \frac{p\lambda}{D}, \quad p_m = \frac{p_1 + p_2}{2}, \quad \text{Kn}_m = \frac{p_\lambda}{p_m}$$

$$\frac{\alpha L}{D} > 10^3, \quad \varepsilon \rightarrow 1, \quad p_1 \rightarrow p_{1\infty}, \quad p_2 \rightarrow p_{2\infty}; \quad b_0 = \frac{16}{3\pi}, \quad b_1 = 0.15, \quad b_2 = \frac{0.7\alpha}{2 - \alpha}$$

Same values of  $\varepsilon$ ,  $b_0$ ,  $b_1$ ,  $b_2$  used for all circular tubes

Values are unchanged from previous cases (no adjusting)  
 Relative to diameter, this tube length is essentially infinite

## Mass flow rate measured for silica microscale tube

- $D = 25.2 \text{ mm}$ ,  $L = 53 \text{ mm}$ ,  $a = 0.9$ ,  $\text{N}_2$ ,  $T = 296.5 \text{ K}$ ,  $p_2/p_1 = 0.2$

## Expression and simulations agree well with experiment

- Lowest experiment pressure is above Knudsen minimum
- Highest simulation pressure reaches experiment